

1 Robust Tensor Completion: Equivalent Surrogates, Error Bounds and Algorithms*

2 Xueying Zhao[†], Minru Bai[‡], Defeng Sun[§], and Libin Zheng[¶]

3
4 **Abstract.** Robust Low-Rank Tensor Completion (RTC) problems have received considerable attention in recent
5 years such as signal processing and computer vision. In this paper, we focus on the bound constrained
6 RTC problem for third-order tensors which recovers a low-rank tensor from partial observations
7 corrupted by impulse noise. A widely used convex relaxation of this problem is to minimize the tensor
8 nuclear norm for low rank and the ℓ_1 -norm for sparsity. However, it may result in biased solutions.
9 To handle this issue, we propose a nonconvex model with a novel nonconvex tensor rank surrogate
10 function and a novel nonconvex sparsity measure for RTC problems under limited sample constraints
11 and two bound constraints, where these two nonconvex terms have a difference of convex functions
12 (DC) structure. Then, a proximal majorization-minimization (PMM) algorithm is developed to solve
13 the proposed model and this algorithm consists of solving a series of convex subproblems with an
14 initial estimator to generate a new estimator which is used for the next subproblem. Theoretically, for
15 this new estimator, we establish a recovery error bound for its recoverability and give the theoretical
16 guarantee that lower error bounds can be obtained when a reasonable initial estimator is available.
17 Then, by using the Kurdyka-Lojasiewicz property exhibited in the resulting problem, we show that
18 the sequence generated by the PMM algorithm globally converges to a critical point of the problem.
19 Extensive numerical experiments including color images and multispectral images show the high
20 efficiency of the proposed model.

21 **Key words.** robust low-rank tensor completion, DC equivalent surrogates, proximal majorization-minimization,
22 error bounds, impulse noise

23 **AMS subject classifications.** 15A69, 68U10, 90C26

24 **1. Introduction.** Multi-dimensional data is becoming prevalent in many areas such as
25 computer vision [27, 44], data mining [32], signal processing [10], and machine learning [39].
26 Tensor-based modeling has the capability of capturing these underlying multi-dimensional
27 structures. However, the tensor data observed may suffer from information loss and be per-
28 turbed by different kinds of noise originating from human errors or signal interference. The
29 purpose of this paper is to study Robust Low-Rank Tensor Completion (RTC) problems for
30 third-order tensors, in which few available entries are defiled by impulse noise.

31 The original model of RTC problems is to minimize an optimization problem which con-
32 sists of the tensor rank function plus the ℓ_0 -norm under limited sample constraints, which
33 is a generalization of Robust Matrix Completion (RMC) [8, 22]. As the rank function is

*Submitted to the editors DATE.

Funding: The work of the second author was supported in part by the National Natural Science Foundation of China under grant 11971159, Hunan Provincial Key Laboratory of Intelligent information processing and Applied Mathematics, Changsha 410082, PR China. The work of the third author was supported in part by the Hong Kong Research Grant Council under grant 15304019 .

[†]School of Mathematics, Hunan University, Changsha, Hunan 410082, China (xueying_zhao@hnu.edu.cn).

[‡]School of Mathematics, Hunan University, Changsha, Hunan 410082, China (minru-bai@hnu.edu.cn).

[§]Department of Applied Mathematics, The Hong Kong Polytechnic University, Hung Hom, Hong Kong (defeng.sun@polyu.edu.hk).

[¶]School of Mathematics, Hunan University, Changsha, Hunan 410082, China (lszt301@163.com).

nonconvex, the nuclear norm is widely used to approximate the rank function. Candès et al. [8] studied the RMC problem by solving a convex optimization problem that minimizes a weighted combination of the nuclear norm and the ℓ_1 -norm under limited sample constraints, and theoretical conditions to ensure the perfect recovery in the probabilistic sense have been analyzed. Although the nuclear norm is a convex relaxation of the rank function, this kind of surrogate may make the solution seriously deviate from the solution of rank minimization. To improve the recovery quality of the solution for matrix completion with fixed basis coefficient, Miao et al. [31] proposed a rank-corrected procedure to generate an estimator with a pre-estimator and established a non-asymptotic recovery error bound. Liu et al. [28] recently reformulated the rank regularized problem as a family of nonconvex equivalent surrogates by establishing its global exact penalty.

Compared with RMC, RTC is more difficult to solve due to the fact that the rank of a tensor is not unique. The two commonly used tensor ranks are the CANDECOMP/PARAFAC (CP) rank [9] and the Tucker rank [43]. However, computing the CP rank of a given tensor is known to be NP-hard [16]. Liu et al. [27] proposed the sum of nuclear norms of unfolding matrices (SNN) of a tensor to approximate the Tucker rank to solve the low-rank tensor completion problem, which has since appeared frequently in practical settings. Although the SNN is easy to compute, Romera-Paredes et al. [36] showed that it is not the tightest convex envelope of the sum of entries of the Tucker rank. Recently, Huang et al. [17] proposed a tensor ring (TR) decomposition that factorizes a high-order tensor into a sequence of three-order tensors and used a number of TR unfoldings for RTC problems. However, the matricization of a tensor may break the intrinsic structures and correlations in the tensor data, hence the rank defined by the unfolding matrices cannot accurately describe the low-rank property of the tensor. Different from the rank based matricization above, Kilmer et al. [19] proposed the tensor multi-rank and tubal rank definitions based on a tensor singular value decomposition (t-SVD) framework [20] and Semerci et al. [37] developed a new tubal nuclear norm (TNN), which is a convex surrogate of the multi-rank [57]. In recent years, the tubal rank and the TNN have been widely studied for tensor recovery problems [18, 29, 45, 55]. Jiang et al. [18] showed that one can recover a low tubal rank tensor exactly with overwhelming probability by solving a convex program, where the objective function is a weighted combination of the TNN and the ℓ_1 -norm. However, as pointed out in [38], the low-rank property of most natural images is mainly affected by a few large singular values, which present a heavy-tailed distribution. It means that the larger singular values are expected to be penalized mildly while the smaller ones are penalized severely. Nevertheless, the TNN treats the singular values with the same penalty, which will over-penalize large singular values and hence get the suboptimal performance. To address this issue, Zhang et al. [55] proposed a corrected TNN (CTNN) model for third-order tensor recovery from partial observations corrupted by Gaussian noise based on the rank-corrected procedure [31] and provided a non-asymptotic error bound of the CTNN model. However, [55] is not able to address the observations with impulse noise and the outer loop convergence of the adaptive correction procedure is unknown.

On the other hand, it is challenging to solve the ℓ_0 regularization problem since it is NP-hard [33]. As a convex relaxation of the ℓ_0 -norm, the ℓ_1 -norm has been widely used for sparsity in statistics. The least absolute shrinkage and selection operator (lasso) problem is the ℓ_1 -norm penalized least squares method, which was proposed in [42] and has been used extensively in

78 high-dimensional statistics and machine learning. However, as indicated by [12], the ℓ_1 -norm
79 has long been known by statisticians to yield biased estimators and cannot achieve the best
80 estimation performance, and might not be statistically optimal in more challenging scenarios.
81 Hence, to solve the above mentioned problems, some nonconvex penalties have been proposed
82 to substitute sparsity measures [13, 14, 41, 50, 51, 58]. In [41], a sparse semismooth Newton
83 based proximal majorization-minimization (PMM) algorithm for nonconvex square-root-loss
84 regression problems was introduced where the nonconvex regularizer has the difference of
85 convex functions (DC) structure. Ahn et al. [1] gave a unified DC representation for a
86 family of surrogate sparsity functions that are employed as approximations of the ℓ_0 -norm
87 in statistical learning and established some sparsity properties of the directional stationary
88 points. Yang et al. [51] proposed nonconvex models for RTC by the regularizing redescending
89 M-estimators as sparsity measures and developed the linearized and proximal block coordinate
90 methods to solve the nonconvex problems. Zhao et al. [58] studied a nonconvex model,
91 consisting of the data-fitting term combined with the TNN and the nonconvex data fidelity
92 term, for RTC problems and presented a Gauss-Seidel DC algorithm (GS-DCA) to solve
93 the resulting optimization. By numerical experiments, [51] and [58] all showed that these
94 nonconvex penalties outperformed the ℓ_1 -norm penalty. Actually, the TNN is the sum of
95 nuclear norms of all frontal slices of the tensor in the Fourier domain, which is the ℓ_1 -norm
96 of all singular vectors. In other words, the TNN results in a biased estimator as well as the
97 ℓ_1 -norm does. Therefore, some works [26, 49, 50, 54] proposed nonconvex penalties to replace
98 the ℓ_1 -norm in TNN. For example, Li et al. [26] established a nonconvex ℓ_p -norm relaxation
99 model for low Tucker rank tensor recovery problem, which can recover the data in lower
100 sampling ratios compared to the convex nuclear norm relaxation model, and the alternating
101 direction method of multipliers (ADMM) was used to solve the resulting model. Xu et al.
102 [49] proposed a novel nonconvex surrogate for the tensor multi-rank based on the Laplace
103 function, which can more tightly approximate to the ℓ_0 -norm than the tensor nuclear norm.
104 However, there are few works on the mechanism to produce equivalent surrogates for the
105 rank and the zero-norm optimization problems, although much research has been considering
106 the nonconvex surrogates. What's more, prior studies mentioned above only focused on the
107 algorithm and its convergence analysis, but statistical error bounds of obtained solutions were
108 rarely discussed.

109 With an eye toward statistical performance, some researchers have studied the error bound
110 for various models. Wu [48] proposed a two-stage rank-sparsity-correction procedure to deal
111 with the problem of noisy low-rank and sparse matrix decomposition by adding adaptive rank-
112 correction terms designed in [31], and examined its recovery performance by developing an
113 error bound. However, [48] did not establish any theoretical guarantee that the recovery error
114 bound obtained by the corrected model is smaller than that of the model without correction
115 terms. Furthermore, it is difficult to generalize the error bound to tensor cases directly. In
116 the tensor algebra framework, Bai et al. [4] proposed an adaptive correction approach for
117 higher-order tensor completion and showed that the correction term with a suitable estimator
118 could reduce the error bound of the corrected model, while the corrected model mainly deals
119 with data missing problems without noises. In order to derive solutions with higher accuracy,
120 zhang et al. [55] presented the CTNN model for low-rank tensor recovery and provided a
121 non-asymptotic error bound, but this model could not address the sparse outliers.

122 To address the above problems, in this paper, we not only pay attention to nonconvex
 123 surrogates of the rank function and the ℓ_0 -norm to overcome biased estimators yielded by the
 124 ℓ_1 -norm penalty and the TNN penalty, but also study the statistical performance analysis
 125 of our method by establishing the recovery error bounds. We propose a bound constrained
 126 Nonconvex Robust Tensor Completion (BCNRTC) model which aims to recover a third-order
 127 tensor corrupted by impulse noise with partial observations. The proposed model consists
 128 of two nonconvex regularization terms with the DC structure for low-rank and sparsity un-
 129 der limited sample constraints and two bound constraints. These two nonconvex penalties
 130 can be chosen as the minimax concave penalty (MCP) function, the smoothly clipped abso-
 131 lute deviation (SCAD) function since such functions are continuous, sparsity promoting, and
 132 nearly unbiased [12, 52]. In addition, we prove the equivalence of global solutions between the
 133 bound constrained RTC problems and our proposed nonconvex model in theory. Recently,
 134 some works [6, 15, 40, 46] have been proposed to solve nonconvex and nonsmooth problems.
 135 Unfortunately, these works could not be applied to solve our proposed model directly. For
 136 example, Bolte et al. [6] proposed a proximal alternating linearized minimization (PALM) al-
 137 gorithm to solve the nonconvex and nonsmooth problems, but no constraints were considered.
 138 Guo et al. [15] studied the convergence of ADMM for minimizing the sum of two nonconvex
 139 functions with linear constraints, however, one of the nonconvex functions was required to be
 140 differentiable. [46] analyzed the convergence of ADMM for minimizing a nonconvex problem
 141 with coupled linear equality constraints, but the objective functions also needed to be Lips-
 142 chitz differentiable. Therefore, for the proposed nonconvex and nonsmooth model, we design
 143 a proximal majorization-minimization (PMM) algorithm similar to [24, 41, 53] to solve it.
 144 The key idea of the PMM algorithm is to solve a series of convex subproblems with an initial
 145 estimator to generate a new estimator which is used for the next subproblem. Specifically,
 146 each subproblem solves a convex program which is to minimize a weighted combination of the
 147 TNN and the ℓ_1 -norm minus two linear terms, where the linear terms can be seen as the rank-
 148 correction term and sparsity-correction term constructed on the initial estimator. Meanwhile,
 149 we establish the recovery error bound between new estimators and initial estimators and also
 150 discuss the impact of the correction term on recovery error. Compared with the one obtained
 151 without these two linear terms, the error bound has a certain degree of reduction. Finally,
 152 the convergence of the PMM algorithm is established by using the Kurdyka-Łojasiewicz prop-
 153 erty and extensive numerical experiments are presented to demonstrate the efficiency of the
 154 proposed BCNRTC model. Therefore, our work not only improves the tensor rank surrogate
 155 function but also modifies the tensor sparsity measure.

156 The main contributions of this paper are four aspects.

- 157 • We produce and prove equivalent nonconvex surrogates with DC structures in the
 158 sense that they have the same global optimal solution set as RTC problems with the
 159 tensor average rank and the ℓ_0 -norm do. We also show that these equivalent surrogates
 160 include the popular MCP function and SCAD function in statistics as special cases.
- 161 • A proximal majorization-minimization (PMM) algorithm with convergence analysis
 162 is presented to solve the BCNRTC model, which is a nonconvex optimization prob-
 163 lem with linear constraints and bound constraints. Each subproblem of the PMM
 164 algorithm is to solve a convex program, where the two linear terms obtained by ma-
 165 jorization can be seen as the tensor rank-correction term and the sparsity-correction

term constructed on the initial estimator.

- We establish a non-asymptotic recovery error bound for the subproblem of the PMM algorithm, which gives the theoretical guarantee that under the mild condition the subproblem of the PMM algorithm can reduce recovery error bounds. Our results of recovery error bounds also suggest a criterion for constructing a suitable rank-correction function and a sparsity-correction function. We show that rank-correction functions and sparsity-correction functions constructed by the MCP function and SCAD function satisfy the above criterion.
- Numerically, we confirm that the error bounds decrease as the number of outer iterations increases. Moreover, extensive numerical experiments on color images and multispectral images demonstrate the superiority of the proposed model over several existing methods.

The rest of this paper is organized as follows. Some notations used throughout this paper are introduced in Section 2. The bound constrained Nonconvex Robust Tensor Completion (BCNRTC) model is proposed in Section 3. The PMM algorithm is presented to solve the resulting model and its global convergence is also established in Section 4. In Section 5, we establish a recovery error bound for the estimator generated from the PMM algorithm. Finally, we report numerical results to validate the efficiency of our proposed model in Section 6 and draw conclusions in Section 7.

2. Preliminaries. Throughout this paper, tensors are denoted by Euler script letters, e.g., \mathcal{X} . Matrices are denoted by boldface capital letters, e.g., \mathbf{X} . Vectors are denoted by bold lowercase letters, e.g., \mathbf{x} , and scalars are denoted by ordinary letters, e.g., x . The fields of real numbers and complex numbers are denoted as \mathbb{R} and \mathbb{C} , respectively. For a third-order tensor $\mathcal{X} \in \mathbb{C}^{n_1 \times n_2 \times n_3}$, we denote its (i, j, k) -th entry as \mathcal{X}_{ijk} . A slice of a tensor \mathcal{X} is a matrix defined by fixing all indices but two. We use the notation $\mathcal{X}(i, :, :)$, $\mathcal{X}(:, i, :)$ and $\mathcal{X}(:, :, i)$ to denote the i -th horizontal, lateral and frontal slice, respectively. Specifically, the front slice $\mathcal{X}(:, :, i)$ is also denoted by $\mathbf{X}^{(i)}$. A fiber of a tensor \mathcal{X} is a vector defined by fixing all indices but one. The fiber along the third dimension $\mathcal{X}(i, j, :)$ is also called as the (i, j) -th tube of \mathcal{X} . We denote $\lfloor t \rfloor$ as the nearest integer less than or equal to t and $\lceil t \rceil$ as the one greater than or equal to t .

For $\mathcal{X} \in \mathbb{R}^{n_1 \times n_2 \times n_3}$, $\pi(\mathcal{X}) \in \mathbb{R}^{n_1 n_2 n_3}$ means the vector obtained by arranging the entries of $|\mathcal{X}|$ in a non-increasing order, where $|\mathcal{X}|$ means the tensor whose (i, j, k) -th component is $|\mathcal{X}_{ijk}|$; and $\pi_i(\cdot)$ denotes the i -th entry of $\pi(\cdot)$. For $\mathbf{X} \in \mathbb{C}^{n_1 \times n_2}$, $\sigma(\mathbf{X})$ means the singular value vector of \mathbf{X} with entries arranged in a non-increasing order; and $\sigma_i(\cdot)$ denotes the i -th entry of $\sigma(\cdot)$. For any given vector \mathbf{x} , $\text{Diag}(\mathbf{x})$ denotes a rectangular diagonal matrix of suitable size with the i -th diagonal entry being x_i . For any matrix \mathbf{X} , $\text{diag}(\mathbf{X})$ denotes a vector of suitable size with the i -th diagonal entry being x_{ii} . Denote the function $\text{sign} : \mathbb{R} \rightarrow \mathbb{R}$ by $\text{sign}(t) = 1$ if $t > 0$, $\text{sign}(t) = -1$ if $t < 0$, and $\text{sign}(t) = 0$ if $t = 0$, for $t \in \mathbb{R}$. For any $\mathcal{X} \in \mathbb{R}^{n_1 \times n_2 \times n_3}$, let $\text{sign}(\mathcal{X})$ be the sign tensor of \mathcal{X} where $[\text{sign}(\mathcal{X})]_{ijk} = \text{sign}(\mathcal{X}_{ijk})$.

The inner product of two matrices \mathbf{X} and \mathbf{Y} in $\mathbb{C}^{n_1 \times n_2}$ is defined as $\langle \mathbf{X}, \mathbf{Y} \rangle := \text{Tr}(\mathbf{X}^H \mathbf{Y})$, where \mathbf{X}^H denotes the conjugate transpose of \mathbf{X} , and $\text{Tr}(\cdot)$ denotes the matrix trace. The inner product of two tensors $\mathcal{X}, \mathcal{Y} \in \mathbb{C}^{n_1 \times n_2 \times n_3}$ is defined as $\langle \mathcal{X}, \mathcal{Y} \rangle := \sum_{i=1}^{n_3} \langle \mathbf{X}^{(i)}, \mathbf{Y}^{(i)} \rangle$. The Frobenius norm of a tensor \mathcal{X} is defined as $\|\mathcal{X}\|_F = \sqrt{\langle \mathcal{X}, \mathcal{X} \rangle}$. And the infinity norm and the

209 l_1 -norm of a tensor are defined as $\|\mathcal{X}\|_\infty = \max_{ijk} |\mathcal{X}_{ijk}|$ and $\|\mathcal{X}\|_1 = \sum_{i=1}^{n_1} \sum_{j=1}^{n_2} \sum_{k=1}^{n_3} |\mathcal{X}_{ijk}|$,
 210 respectively. For any $\mathcal{X} \in \mathbb{C}^{n_1 \times n_2 \times n_3}$, the complex conjugate of \mathcal{X} is denoted as $\text{conj}(\mathcal{X})$ which
 211 takes the complex conjugate of each entry of \mathcal{X} .

212 For any tensor $\mathcal{X} \in \mathbb{R}^{n_1 \times n_2 \times n_3}$, we denote $\widehat{\mathcal{X}} \in \mathbb{C}^{n_1 \times n_2 \times n_3}$ as the results of the Fast
 213 Fourier Transform (FFT) of all tubes along the third dimension. Using MATLAB command
 214 `fft`, $\widehat{\mathcal{X}} = \text{fft}(\mathcal{X}, [], 3)$. One can also compute \mathcal{X} from $\widehat{\mathcal{X}}$ by using the inverse FFT operation
 215 along the third-dimension, i.e., $\mathcal{X} = \text{ifft}(\widehat{\mathcal{X}}, [], 3)$. Let $\overline{\mathbf{X}}$ denote the block diagonal matrix
 216 of the tensor $\widehat{\mathcal{X}}$, where the i -th diagonal block of $\overline{\mathbf{X}}$ is the i -th frontal slice $\widehat{\mathbf{X}}^{(i)}$ of $\widehat{\mathcal{X}}$, i.e.,

$$217 \quad \overline{\mathbf{X}} := \text{bdiag}(\widehat{\mathcal{X}}) = \begin{bmatrix} \widehat{\mathbf{X}}^{(1)} & & & \\ & \widehat{\mathbf{X}}^{(2)} & & \\ & & \ddots & \\ & & & \widehat{\mathbf{X}}^{(n_3)} \end{bmatrix}.$$

218 We define a block circular matrix from the frontal slices $\mathbf{X}^{(i)}$ of \mathcal{X} as

$$219 \quad \text{bcirc}(\mathcal{X}) := \begin{bmatrix} \mathbf{X}^{(1)} & \mathbf{X}^{(n_3)} & \dots & \mathbf{X}^{(2)} \\ \mathbf{X}^{(2)} & \mathbf{X}^{(1)} & \dots & \mathbf{X}^{(3)} \\ \vdots & \vdots & \ddots & \vdots \\ \mathbf{X}^{(n_3)} & \mathbf{X}^{(n_3-1)} & \dots & \mathbf{X}^{(1)} \end{bmatrix}.$$

220 It can be block diagonalized by using the FFT, i.e., $(\mathbf{F}_{n_3} \otimes \mathbf{I}_{n_1}) \cdot \text{bcirc}(\mathcal{X}) \cdot (\mathbf{F}_{n_3}^{-1} \otimes \mathbf{I}_{n_2}) = \overline{\mathbf{X}}$,
 221 where \mathbf{F}_n is the $n \times n$ discrete Fourier matrix, \mathbf{I}_n is the $n \times n$ identity matrix, \otimes denotes the
 222 Kronecker product, and $(\mathbf{F}_{n_3} \otimes \mathbf{I}_{n_1})/\sqrt{n_3}$ is unitary. The command `unfold`(\mathcal{X}) takes \mathcal{X} into
 223 a block $n_1 n_3 \times n_2$ matrix:

$$224 \quad \text{unfold}(\mathcal{X}) := \begin{bmatrix} \mathbf{X}^{(1)} \\ \mathbf{X}^{(2)} \\ \vdots \\ \mathbf{X}^{(n_3)} \end{bmatrix}.$$

225 The inverse operator `fold` takes `unfold`(\mathcal{X}) into a tensor form: `fold`(`unfold`(\mathcal{X})) = \mathcal{X} . It is
 226 showed in [29] that

$$227 \quad \text{conj}(\widehat{\mathbf{X}}^{(i)}) = \widehat{\mathbf{X}}^{(n_3-i+2)} \quad \forall i = 2, \dots, \left\lfloor \frac{n_3+1}{2} \right\rfloor.$$

228 The tensor spectral norm of \mathcal{X} is defined as $\|\mathcal{X}\| := \|\overline{\mathbf{X}}\|$, i.e., the spectral norm of the block
 229 diagonal matrix $\overline{\mathbf{X}}$ in the Fourier domain. The following properties will be used frequently:
 230 $\langle \mathcal{X}, \mathcal{Y} \rangle = \frac{1}{n_3} \langle \overline{\mathbf{X}}, \overline{\mathbf{Y}} \rangle$, $\|\mathcal{X}\|_F = \frac{1}{\sqrt{n_3}} \|\overline{\mathbf{X}}\|_F$.

231 Now we give some basic definitions about tensors, which serve as the foundation for our
 232 further analysis.

233 **Definition 2.1 (T-product [20]).** The t -product $\mathcal{X} * \mathcal{Y}$ of $\mathcal{X} \in \mathbb{C}^{n_1 \times n_2 \times n_3}$ and $\mathcal{Y} \in \mathbb{C}^{n_2 \times n_4 \times n_3}$
 234 is a tensor $\mathcal{Z} \in \mathbb{C}^{n_1 \times n_4 \times n_3}$ given by $\mathcal{Z} = \text{fold}(\text{bcirc}(\mathcal{X}) \cdot \text{unfold}(\mathcal{Y}))$. Moreover, we have the
 235 following equivalence: $\mathcal{X} * \mathcal{Y} = \mathcal{Z} \Leftrightarrow \overline{\mathbf{X}} \overline{\mathbf{Y}} = \overline{\mathbf{Z}}$.

236 **Definition 2.2 (Tensor transpose [20]).** The conjugate transpose of a tensor $\mathcal{X} \in \mathbb{C}^{n_1 \times n_2 \times n_3}$
 237 is the tensor $\mathcal{X}^H \in \mathbb{C}^{n_2 \times n_1 \times n_3}$ obtained by conjugate transposing each of the frontal slice and
 238 then reversing the order of transposed frontal slices 2 through n_3 .

239 **Definition 2.3 (F-diagonal tensor [20]).** A tensor \mathcal{X} is called *f-diagonal* if each frontal slice
 240 $\mathbf{X}^{(i)}$ is a diagonal matrix.

241 **Definition 2.4 (Tensor Singular Value Decomposition: t-SVD [20]).** For $\mathcal{X} \in \mathbb{R}^{n_1 \times n_2 \times n_3}$, the
 242 t-SVD of \mathcal{X} is given by $\mathcal{X} = \mathcal{U} * \mathcal{S} * \mathcal{V}^H$, where $\mathcal{U} \in \mathbb{R}^{n_1 \times n_1 \times n_3}$ and $\mathcal{V} \in \mathbb{R}^{n_2 \times n_2 \times n_3}$ are
 243 orthogonal tensors, and $\mathcal{S} \in \mathbb{R}^{n_1 \times n_2 \times n_3}$ is a *f-diagonal* tensor, respectively. The entries in \mathcal{S}
 244 are called the singular fibers of \mathcal{X} .

245 **Definition 2.5 (Tubal multi-rank [19, 57]).** The multi-rank of a tensor $\mathcal{X} \in \mathbb{R}^{n_1 \times n_2 \times n_3}$ is
 246 a vector $\mathbf{r} \in \mathbb{R}^{n_3}$ with its i -th entry as the rank of the i -th frontal slice $\widehat{\mathbf{X}}^{(i)}$ of $\widehat{\mathcal{X}}$, i.e.,
 247 $r_i = \text{rank}(\widehat{\mathbf{X}}^{(i)})$.

248 **Definition 2.6 (Tensor average rank [29]).** For $\mathcal{X} \in \mathbb{R}^{n_1 \times n_2 \times n_3}$, the tensor average rank,
 249 denoted as $\text{rank}_a(\mathcal{X})$, is defined as $\text{rank}_a(\mathcal{X}) = \frac{1}{n_3} \sum_{i=1}^{n_3} \text{rank}(\widehat{\mathbf{X}}^{(i)})$.

250 **Definition 2.7 (Tubal nuclear norm [29]).** The tubal nuclear norm of $\mathcal{X} \in \mathbb{R}^{n_1 \times n_2 \times n_3}$, de-
 251 noted as $\|\mathcal{X}\|_{\text{TNN}}$, is the average of the nuclear norm of all the frontal slices of $\widehat{\mathcal{X}}$, i.e.,
 252 $\|\mathcal{X}\|_{\text{TNN}} = \frac{1}{n_3} \sum_{i=1}^{n_3} \|\widehat{\mathbf{X}}^{(i)}\|_*$, where $\|\cdot\|_*$ denote the nuclear norm of matrix, i.e., the sum of
 253 all singular values of matrix.

254 **Definition 2.8 (Tensor basis [56]).** The column basis, denoted by \vec{e}_i is a tensor of size $n_1 \times$
 255 $1 \times n_3$ with the $(i, 1, 1)$ -th entry equaling to 1 and the rest equaling to 0. The row basis is the
 256 transpose of \vec{e}_i , i.e., \vec{e}_i^T . The tube basis, denoted by \hat{e}_i , is a tensor of size $1 \times 1 \times n_3$ with the
 257 $(1, 1, k)$ -th entry equaling to 1 and the rest equaling to 0. Hence, one can obtain a unit tensor
 258 $\Theta_{ijk} \in \mathbb{R}^{n_1 \times n_2 \times n_3}$ with the (i, j, k) -th nonzero entry equaling 1 via $\Theta_{ijk} = \vec{e}_i * \hat{e}_k * \vec{e}_j^T$. Now
 259 for any tensor $\mathcal{X} \in \mathbb{R}^{n_1 \times n_2 \times n_3}$, its description based on the basis form can be given as follows:
 260 $\mathcal{X} = \sum_{i=1}^{n_1} \sum_{j=1}^{n_2} \sum_{k=1}^{n_3} \langle \Theta_{ijk}, \mathcal{X} \rangle \Theta_{ijk}$.

261 Other notations will be defined in appropriate sections if necessary.

262 **3. The Equivalent Surrogates for Robust Tensor Completion Model.** Since the tensor is
 263 bounded in many practical applications, such as an 8-byte image with elements ranging from
 264 0 to 255, in this section, we introduce a nonconvex optimization model for bound constrained
 265 robust low-rank tensor completion problems.

266 **3.1. Robust Tensor Completion Model.** Given the noisy data tensor $\mathcal{X} \in \mathbb{R}^{n_1 \times n_2 \times n_3}$,
 267 only partial entries of \mathcal{X} are observed, and the noisy data tensor \mathcal{X} is an unknown low-rank
 268 tensor $\mathcal{L}^* \in \mathbb{R}^{n_1 \times n_2 \times n_3}$ corrupted by an unknown sparse noise $\mathcal{M}^* \in \mathbb{R}^{n_1 \times n_2 \times n_3}$. Then, we
 269 can recover the low-rank tensor \mathcal{L}^* by solving the following bound constrained Robust Tensor
 270 Completion model:

$$\begin{aligned}
 & \min_{\mathcal{L}, \mathcal{M}} \text{rank}_a(\mathcal{L}) + \lambda \|\mathcal{M}\|_0 \\
 & \text{s.t. } \mathcal{P}_\Omega(\mathcal{L} + \mathcal{M}) = \mathcal{P}_\Omega(\mathcal{X}), \quad \|\mathcal{M}\|_\infty \leq b_m, \quad \|\mathcal{L}\| \leq b_l,
 \end{aligned}
 \tag{3.1}$$

where $b_l, b_m > 0$ are given constants, $\lambda > 0$ is a regularization parameter, $\|\cdot\|_0$ denotes the number of non-zero elements, $\text{rank}_a(\mathcal{L})$ is the tensor average rank, $\|\cdot\|_\infty$ denotes the infinity norm, $\|\cdot\|$ is the tensor spectral norm, Ω is an index set, and \mathcal{P}_Ω is the orthogonal projection operator on Ω , i.e.,

$$\mathcal{P}_\Omega(\mathcal{X}) := \begin{cases} \mathcal{X}_{ijk}, & (i, j, k) \in \Omega, \\ 0, & \text{otherwise.} \end{cases}$$

It is well known that the rank and zero-norm optimization problems are in general NP-hard. Next, in terms of the variational characterization of the rank function and the zero-norm, we give its equivalent surrogates of (3.1) and prove that they have the same global optimal solution set as (3.1).

3.2. Equivalent Surrogates . Let Φ denote the family of closed proper convex functions $\phi : \mathbb{R} \rightarrow (-\infty, +\infty]$ satisfying $[0, 1] \subseteq \text{int}(\text{dom}\phi)$, $\phi(1) = 1$ and $\phi(t_\phi^*) = 0$ where t_ϕ^* is the unique minimizer of ϕ over $[0, 1]$. Let \mathbf{e} be the vector of all ones. Then

$$\|\mathbf{z}\|_0 = \min_{\mathbf{w}} \{\sum_{i=1}^p \phi(w_i) \text{ s.t. } \langle \mathbf{e} - \mathbf{w}, |\mathbf{z}| \rangle = 0, 0 \leq \mathbf{w} \leq \mathbf{e}\}$$

and

$$\text{rank}(\mathbf{X}) = \min_{\mathbf{W}} \{\sum_{i=1}^n \phi(\sigma_i(\mathbf{W})) \text{ s.t. } \|\mathbf{X}\|_* - \langle \mathbf{W}, \mathbf{X} \rangle = 0, \|\mathbf{W}\| \leq 1\},$$

which are introduced in [28]. By the variational characterization of the zero-norm and the rank function in (3.2) and (3.3), the rank plus zero-norm minimization problem (3.1) is equivalent to the problem

$$\begin{aligned} \min_{\mathcal{L}, \mathcal{M}, \mathcal{B}, \mathcal{S}} & \frac{1}{n_3} \sum_{i=1}^{n_3} \sum_{j=1}^{\tilde{n}} \phi(\sigma_j(\widehat{\mathbf{S}}^{(i)})) + \lambda \sum_{i=1}^{n_1} \sum_{j=1}^{n_2} \sum_{k=1}^{n_3} \phi(\mathcal{B}_{ijk}) \\ \text{s.t.} & \frac{1}{n_3} \sum_{i=1}^{n_3} (\|\widehat{\mathbf{L}}^{(i)}\|_* - \langle \widehat{\mathbf{S}}^{(i)}, \widehat{\mathbf{L}}^{(i)} \rangle) + \lambda \langle \mathcal{E} - \mathcal{B}, |\mathcal{M}| \rangle = 0, \quad 0 \leq \mathcal{B} \leq \mathcal{E}, \quad \|\widehat{\mathbf{S}}^{(i)}\| \leq 1, \\ & \mathcal{P}_\Omega(\mathcal{L} + \mathcal{M}) = \mathcal{P}_\Omega(\mathcal{X}), \quad \|\mathcal{M}\|_\infty \leq b_m, \quad \|\mathcal{L}\| \leq b_l, \end{aligned}$$

where $\tilde{n} = \min\{n_1, n_2\}$ and \mathcal{E} is the tensor of all ones. Notice that $\frac{1}{n_3} \sum_{i=1}^{n_3} (\|\widehat{\mathbf{L}}^{(i)}\|_* - \langle \widehat{\mathbf{S}}^{(i)}, \widehat{\mathbf{L}}^{(i)} \rangle) + \lambda \langle \mathcal{E} - \mathcal{B}, |\mathcal{M}| \rangle = 0$, $0 \leq \mathcal{B} \leq \mathcal{E}$, and $\|\widehat{\mathbf{S}}^{(i)}\| \leq 1$ if and only if $\|\widehat{\mathbf{L}}^{(i)}\|_* - \langle \widehat{\mathbf{S}}^{(i)}, \widehat{\mathbf{L}}^{(i)} \rangle = 0$, $\langle \mathcal{E} - \mathcal{B}, |\mathcal{M}| \rangle = 0$, $0 \leq \mathcal{B} \leq \mathcal{E}$, and $\|\widehat{\mathbf{S}}^{(i)}\| \leq 1$, which can be obtained by the definition of the dual norm.

For brevity, we denote $J := \{(i, j, k)\}$. Now we consider the following penalty problem:

$$\begin{aligned} \min_{\mathcal{L}, \mathcal{M}, \mathcal{B}, \mathcal{S}} & \frac{1}{n_3} \sum_{i=1}^{n_3} \sum_{j=1}^{\tilde{n}} \phi(\sigma_j(\widehat{\mathbf{S}}^{(i)})) + \lambda \sum_J^{(n_1, n_2, n_3)} \phi(\mathcal{B}_J) + \frac{\rho}{n_3} \sum_{i=1}^{n_3} (\|\widehat{\mathbf{L}}^{(i)}\|_* - \langle \widehat{\mathbf{S}}^{(i)}, \widehat{\mathbf{L}}^{(i)} \rangle) \\ \text{s.t.} & 0 \leq \mathcal{B} \leq \mathcal{E}, \quad \|\widehat{\mathbf{S}}^{(i)}\| \leq 1, \quad \mathcal{P}_\Omega(\mathcal{L} + \mathcal{M}) = \mathcal{P}_\Omega(\mathcal{X}), \quad \|\mathcal{M}\|_\infty \leq b_m, \quad \|\mathcal{L}\| \leq b_l, \end{aligned}$$

where $\rho > 0$ is the penalty factor. Next, we show that the penalty problem (3.5) is a global exact penalty for (3.4) in the sense that it has the same global optimal solution set as (3.4)

299 does. The proof follows the line of [28, Theorem 5.1] in the matrix case by proving that the
 300 problem (3.4) is partially calm in its optimal solution set. The partial calmness is defined in
 301 [28], which is also given in Appendix A.

302 **Theorem 3.1.** *Let $\phi \in \Phi$. The penalty problem (3.5) is a global exact penalty for (3.4).*

303 *Proof.* Let $(\mathcal{L}^*, \mathcal{M}^*, \mathcal{B}^*, \mathcal{S}^*)$ be an arbitrary global optimal solution of (3.4) and conse-
 304 quently $\mathcal{L}^* \neq 0$ and $\mathcal{M}^* \neq 0$. For all $i \in \{1, 2, \dots, n_3\}$, we write $r_i^* = \text{rank}(\widehat{\mathcal{L}}^{*(i)})$ and
 305 $s^* = \|\mathcal{M}^*\|_0$. Then $\sigma_{r_i^*}(\widehat{\mathcal{L}}^{*(i)}) > 0$ and $\pi_{s^*}(\mathcal{M}^*) > 0$. By the continuity of $\sigma_{r_i^*}(\cdot)$ and $\pi_{s^*}(\cdot)$,
 306 there exists $\varepsilon > 0$ such that for any $(\mathcal{L}, \mathcal{M}) \in \mathbb{B}((\mathcal{L}^*, \mathcal{M}^*), \varepsilon)$,

$$(3.6)$$

$$307 \sigma_{r_i^*}(\widehat{\mathcal{L}}^{*(i)}) \geq \alpha \quad \text{and} \quad \pi_{s^*}(\mathcal{M}) \geq \alpha \quad \text{with} \quad \alpha = \min(\sigma_{r_i^*}(\widehat{\mathcal{L}}^{*(i)}), \pi_{s^*}(\mathcal{M}^*)) / 2 \quad \forall i \in \{1, 2, \dots, n_3\}.$$

308 We consider the perturbed problem of (3.4) whose feasible set takes the following form:

$$309 \mathcal{F}_\epsilon := \left\{ (\mathcal{L}, \mathcal{M}, \mathcal{B}, \mathcal{S}) \mid \begin{aligned} & \frac{1}{n_3} \sum_{i=1}^{n_3} (\|\widehat{\mathcal{L}}^{(i)}\|_* - \langle \widehat{\mathcal{S}}^{(i)}, \widehat{\mathcal{L}}^{(i)} \rangle) + \lambda (\|\mathcal{M}\|_1 - \langle \mathcal{B}, |\mathcal{M}| \rangle) = \epsilon, \\ & 0 \leq \mathcal{B} \leq \mathcal{E}, \quad \|\widehat{\mathcal{S}}^{(i)}\| \leq 1, \quad \mathcal{P}_\Omega(\mathcal{L} + \mathcal{M}) = \mathcal{P}_\Omega(\mathcal{X}), \quad \|\mathcal{M}\|_\infty \leq b_m, \quad \|\mathcal{L}\| \leq b_l \end{aligned} \right\}.$$

310 Fix an arbitrary $\epsilon \in \mathbb{R}$. It suffices to consider the case $\epsilon \geq 0$. Let $(\mathcal{L}, \mathcal{M}, \mathcal{B}, \mathcal{S})$ be an arbitrary
 311 point from $\mathcal{F}_\epsilon \cap \mathbb{B}((\mathcal{L}^*, \mathcal{M}^*, \mathcal{B}^*, \mathcal{S}^*), \varepsilon)$. Then, with $\bar{\rho} = \phi'_-(1)/\alpha$,

$$(3.7)$$

$$\begin{aligned} & \frac{1}{n_3} \sum_{i=1}^{n_3} \sum_{j=1}^{\tilde{n}} \phi(\sigma_j(\widehat{\mathcal{S}}^{(i)})) + \lambda \sum_J^{(n_1, n_2, n_3)} \phi(\mathcal{B}_J) + \frac{\bar{\rho}}{n_3} \sum_{i=1}^{n_3} (\|\widehat{\mathcal{L}}^{(i)}\|_* - \langle \widehat{\mathcal{S}}^{(i)}, \widehat{\mathcal{L}}^{(i)} \rangle) \\ & + \bar{\rho} \lambda (\|\mathcal{M}\|_1 - \langle \mathcal{B}, |\mathcal{M}| \rangle) \\ & \geq \frac{1}{n_3} \sum_{i=1}^{n_3} \sum_{j=1}^{\tilde{n}} [\phi(\sigma_j(\widehat{\mathcal{S}}^{(i)})) + \bar{\rho} \sigma_j(\widehat{\mathcal{L}}^{(i)}) (1 - \sigma_j(\widehat{\mathcal{S}}^{(i)}))] + \lambda \sum_{j=1}^{n_1 n_2 n_3} [\phi(\pi_j(\mathcal{B})) + \bar{\rho} \pi_j(\mathcal{M}) (1 - \pi_j(\mathcal{B}))] \\ 312 & \geq \frac{1}{n_3} \sum_{i=1}^{n_3} \sum_{j=1}^{r_i^*} [\phi(\sigma_j(\widehat{\mathcal{S}}^{(i)})) + \bar{\rho} \sigma_{r_i^*}(\widehat{\mathcal{L}}^{(i)}) (1 - \sigma_j(\widehat{\mathcal{S}}^{(i)}))] + \lambda \sum_{j=1}^{s^*} [\phi(\pi_j(\mathcal{B})) + \bar{\rho} \pi_{s^*}(\mathcal{M}) (1 - \pi_j(\mathcal{B}))] \\ & \geq \frac{1}{n_3} \sum_{i=1}^{n_3} \sum_{j=1}^{r_i^*} [\phi(\sigma_j(\widehat{\mathcal{S}}^{(i)})) + \phi'_-(1) (1 - \sigma_j(\widehat{\mathcal{S}}^{(i)}))] + \lambda \sum_{j=1}^{s^*} [\phi(\pi_j(\mathcal{B})) + \phi'_-(1) (1 - \pi_j(\mathcal{B}))] \\ & \geq (\frac{1}{n_3} \sum_{i=1}^{n_3} r_i^* + \lambda s^*) \phi(1) = \frac{1}{n_3} \sum_{i=1}^{n_3} \text{rank}(\widehat{\mathcal{L}}^{*(i)}) + \lambda \|\mathcal{M}^*\|_0, \end{aligned}$$

313 where the first inequality is by the von Neumann's inequality and $\langle \mathcal{B}, |\mathcal{M}| \rangle \leq \langle \pi(\mathcal{B}), \pi(\mathcal{M}) \rangle$,
 314 the second one is by the nonnegativity of ϕ in $[0, 1]$, the third one is due to (3.6) and
 315 $\bar{\rho} = \phi'_-(1)/\alpha$, and the last one is using $\phi(t) \geq \phi(1) + \phi'_-(1)(t - 1)$ for $t \in [0, 1]$. Since
 316 $\frac{1}{n_3} \sum_{i=1}^{n_3} \text{rank}(\widehat{\mathcal{L}}^{*(i)}) + \lambda \|\mathcal{M}^*\|_0$ is exactly the optimal value of (3.4), by the arbitrariness of ϵ in
 317 \mathbb{R} and that of $(\mathcal{L}, \mathcal{M}, \mathcal{B}, \mathcal{S})$ in $\mathcal{F}_\epsilon \cap \mathbb{B}((\mathcal{L}^*, \mathcal{M}^*, \mathcal{B}^*, \mathcal{S}^*), \varepsilon)$, (3.7) shows that (3.4) is partially
 318 calm at $(\mathcal{L}^*, \mathcal{M}^*, \mathcal{B}^*, \mathcal{S}^*)$, where the definition of partial calmness and its properties are intro-
 319 duced in [28]. By the arbitrariness of $(\mathcal{L}^*, \mathcal{M}^*, \mathcal{B}^*, \mathcal{S}^*)$ in the global optimal solution set, it is
 320 partially calm in its optimal solution set. Since the feasible set of problem (3.5) is compact,
 321 the penalty problem (3.5) is a global exact penalty for (3.4) follows from [28, Proposition
 322 2.1(b)]. ■

323 Then, by letting $\psi(t) := \begin{cases} \phi(t), & t \in [0, 1], \\ +\infty, & \text{otherwise} \end{cases}$ and using the conjugate ψ^* of ψ , i.e., $\psi^*(s) :=$
 324 $\sup_{t \in \mathbb{R}} \{st - \psi(t)\}$, we can obtain the following conclusion.

325 **Corollary 3.2.** *Let $\phi \in \Phi$. There exists $\rho^* > 0$ such that the problem (3.1) has the same*
 326 *global optimal solution set as the following problem with $\rho > \rho^*$ does:*

$$327 \quad (3.8) \quad \min_{\mathcal{L}, \mathcal{M}} \frac{\rho}{n_3} \sum_{i=1}^{n_3} \|\widehat{\mathbf{L}}^{(i)}\|_* - \frac{1}{n_3} \sum_{i=1}^{n_3} \sum_{j=1}^{\tilde{n}} \psi^*(\rho \sigma_j(\widehat{\mathbf{L}}^{(i)})) + \lambda(\rho \|\mathcal{M}\|_1 - \sum_J \psi^*(\rho |\mathcal{M}_J|))$$

s.t. $\mathcal{P}_\Omega(\mathcal{L} + \mathcal{M}) = \mathcal{P}_\Omega(\mathcal{X}), \quad \|\mathcal{M}\|_\infty \leq b_m, \quad \|\mathcal{L}\| \leq b_l.$

328 Let $u > 0$. Denote

$$329 \quad (3.9) \quad \tilde{\theta}(s) := u\theta(\rho s)$$

330 with $\theta(s) := |s| - \psi^*(|s|)$. Then the problem (3.8) is equivalent to the following problem:

$$331 \quad (3.10) \quad \min_{\mathcal{L}, \mathcal{M}} \frac{1}{n_3} \sum_{i=1}^{n_3} \sum_{j=1}^{\tilde{n}} \tilde{\theta}(\sigma_j(\widehat{\mathbf{L}}^{(i)})) + \lambda \sum_J \tilde{\theta}(|\mathcal{M}_J|)$$

s.t. $\mathcal{P}_\Omega(\mathcal{L} + \mathcal{M}) = \mathcal{P}_\Omega(\mathcal{X}), \quad \|\mathcal{M}\|_\infty \leq b_m, \quad \|\mathcal{L}\| \leq b_l.$

332 It is worth noting that ϕ can be chosen as different functions satisfying $\phi \in \Phi$. In particular,
 333 if ϕ is chosen as the one in [Example 3.1](#), then $\tilde{\theta}$ becomes the MCP function (3.14); if ϕ is
 334 chosen as the one in [Example 3.2](#), then $\tilde{\theta}$ becomes the SCAD function (3.16).

335 **Example 3.1.** *Let $\phi(t) := \frac{\varphi(t)}{\varphi(1)}$ with $\varphi(t) := \frac{a^2}{4}t^2 - \frac{a^2}{2}t + at + \frac{(a-2)_+^2}{4}$, where $a > 0$ is*
 336 *a constant. Clearly, $\phi \in \Phi$ with $t_\phi^* = \frac{(a-2)_+}{a}$. Simple calculations show that ψ^* takes the*
 337 *following form:*

$$338 \quad \psi^*(s) = \begin{cases} -\frac{(a-2)_+^2}{4}, & \text{if } s \leq \frac{a-a^2/2}{\varphi(1)}, \\ \frac{1}{a^2\varphi(1)} \left(\frac{a^2-2a}{2} + s\varphi(1) \right)^2 - \frac{(a-2)_+^2}{4\varphi(1)}, & \text{if } \frac{a-a^2/2}{\varphi(1)} < s \leq \frac{a}{\varphi(1)}, \\ s-1, & \text{if } s > \frac{a}{\varphi(1)}. \end{cases}$$

339 When $a \geq 2$, we have $\varphi(1) = 1$ and $\theta(s) = |s| - \psi^*(|s|) = \begin{cases} \frac{2|s|}{a} - \frac{s^2}{a^2}, & |s| \leq a, \\ 1, & |s| > a. \end{cases}$ Set $s := \frac{as}{\gamma}$

340 for some constants $\gamma > 0$, we have $\frac{\gamma}{2}\theta(\frac{as}{\gamma}) = \frac{\gamma}{2} \left(\frac{a|s|}{\gamma} - \psi^*(\frac{a|s|}{\gamma}) \right) = \begin{cases} |s| - \frac{s^2}{2\gamma}, & |s| \leq \gamma, \\ \frac{\gamma}{2}, & |s| > \gamma. \end{cases}$ If

341 $\rho = \frac{a}{\gamma}$, $u = \frac{\gamma}{2}$ and $a \geq 2$, then the function $\tilde{\theta}(s)$ defined in (3.9) is the MCP function.

342 **Example 3.2.** *Let $\phi(t) := \frac{\varphi(t)}{\varphi(1)}$ with $\varphi(t) := \frac{a-1}{2}t^2 + t$, where $a > 1$ is a constant. Clearly,*
 343 *$\phi \in \Phi$. Then,*

$$344 \quad \psi^*(s) = \begin{cases} 0, & s \leq \frac{1}{\varphi(1)}, \\ s-1, & s > \frac{a}{\varphi(1)}, \\ \frac{1}{2(a-1)\varphi(1)} (s\varphi(1) - 1)^2, & \frac{1}{\varphi(1)} < s \leq \frac{a}{\varphi(1)}. \end{cases}$$

345 Then, $\theta(s) = |s| - \psi^*(|s|) = \begin{cases} |s|, & |s| \leq \frac{1}{\varphi(1)}, \\ 1, & |s| > \frac{a}{\varphi(1)}, \\ |s| - \frac{1}{2(a-1)\varphi(1)}(|s|\varphi(1) - 1)^2, & \frac{1}{\varphi(1)} < |s| \leq \frac{a}{\varphi(1)}. \end{cases}$ Set $s :=$
 346 $\frac{s}{\gamma\varphi(1)}$ for some constants $\gamma > 0$, we have

$$347 \quad \theta\left(\frac{s}{\gamma\varphi(1)}\right) = \frac{|s|}{\gamma\varphi(1)} - \psi^*\left(\frac{|s|}{\gamma\varphi(1)}\right) = \begin{cases} \frac{|s|}{\gamma\varphi(1)}, & |s| \leq \gamma, \\ 1, & |s| > a\gamma, \\ \frac{|s|}{\gamma\varphi(1)} - \frac{1}{2(a-1)\varphi(1)}(|s|/\gamma - 1)^2, & \gamma < |s| \leq a\gamma, \end{cases}$$

348 and $\gamma^2\varphi(1)\theta\left(\frac{s}{\gamma\varphi(1)}\right) = \gamma^2\varphi(1)\left(\frac{|s|}{\gamma\varphi(1)} - \psi^*\left(\frac{|s|}{\gamma\varphi(1)}\right)\right) = \begin{cases} \gamma|s|, & |s| \leq \gamma, \\ \frac{\gamma^2(a+1)}{2}, & |s| > a\gamma, \\ \frac{-s^2+2a|s|\gamma-\gamma^2}{2(a-1)}, & \gamma < |s| \leq a\gamma. \end{cases}$ If $\rho =$
 349 $\frac{1}{\gamma\varphi(1)}$, $u = \gamma^2\varphi(1)$ and $a > 1$, then the function $\tilde{\theta}(s)$ defined in (3.9) is the SCAD function.

350 **3.3. BCNRTC for RTC Problems.** From the above discussion, the equivalent surrogates
 351 problem (3.10) can be rewritten in a simplified bound constrained Nonconvex Robust Tensor
 352 Completion (BCNRTC for short) form as follows:

$$353 \quad (3.11) \quad \begin{aligned} \min_{\mathcal{L}, \mathcal{M}} \quad & \|\mathcal{L}\|_{\text{TNN}} - H_1(\mathcal{L}) + \lambda(\|\mathcal{M}\|_1 - H_2(\mathcal{M})) \\ \text{s.t.} \quad & \mathcal{P}_\Omega(\mathcal{L} + \mathcal{M}) = \mathcal{P}_\Omega(\mathcal{X}), \quad \|\mathcal{M}\|_\infty \leq b_m, \quad \|\mathcal{L}\| \leq b_l, \end{aligned}$$

354 where H_1 and H_2 are defined as

$$355 \quad (3.12) \quad H_1(\mathcal{L}) = \frac{1}{n_3} \sum_{i=1}^{n_3} g(\sigma(\hat{\mathbf{L}}^{(i)})), \quad H_2(\mathcal{M}) = \sum_{i=1}^{n_1} \sum_{j=1}^{n_2} \sum_{k=1}^{n_3} h(\mathcal{M}_{ijk}),$$

356 where $g(\mathbf{x}) = \sum_{j=1}^{\dim(\mathbf{x})} h(\mathbf{x}_j)$, h is a convex and continuous differentiable function which can be
 357 defined as

$$358 \quad (3.13) \quad h(x) := \begin{cases} \frac{x^2}{2\gamma}, & |x| \leq \gamma, \\ |x| - \frac{\gamma}{2}, & |x| > \gamma, \end{cases}$$

359 which is related to the MCP function ϖ_M with $h(x) = |x| - \varpi_M(x)$, where

$$360 \quad (3.14) \quad \varpi_M(x) = \begin{cases} |x| - \frac{x^2}{2\gamma}, & |x| \leq \gamma, \\ \frac{\gamma}{2}, & |x| > \gamma. \end{cases}$$

361 The convex function h can also be defined as

$$362 \quad (3.15) \quad h(x) := \begin{cases} 0, & |x| \leq \gamma_1, \\ \frac{x^2 - 2\gamma_1|x| + \gamma_1^2}{2(\gamma_2 - \gamma_1)}, & \gamma_1 < |x| \leq \gamma_2, \\ |x| - \frac{\gamma_1 + \gamma_2}{2}, & |x| > \gamma_2, \end{cases}$$

363 which is related to the SCAD function ϖ_S with $h(x) = |x| - \varpi_S(x)$, where

$$364 \quad (3.16) \quad \varpi_S(x) = \begin{cases} |x|, & |x| \leq \gamma_1, \\ \frac{2\gamma_2|x| - x^2 - \gamma_1^2}{2(\gamma_2 - \gamma_1)}, & \gamma_1 < |x| \leq \gamma_2, \\ \frac{\gamma_1 + \gamma_2}{2}, & |x| > \gamma_2. \end{cases}$$

365 *Remark 3.3.* When $H_1 \equiv 0$ and $H_2 \equiv 0$, the BCNRTC model (3.11) reduces to a convex
366 model (CRTC for short)

$$367 \quad (3.17) \quad \begin{aligned} & \min_{\mathcal{L}, \mathcal{M}} \|\mathcal{L}\|_{\text{TNN}} + \lambda \|\mathcal{M}\|_1 \\ & \text{s.t. } \mathcal{P}_\Omega(\mathcal{L} + \mathcal{M}) = \mathcal{P}_\Omega(\mathcal{X}), \quad \|\mathcal{M}\|_\infty \leq b_m, \quad \|\mathcal{L}\| \leq b_l, \end{aligned}$$

368 which is actually a reformulation of the Robust Tensor Completion (RTC ℓ_1) [18] with two
369 bound constraints. We use the symmetric Gauss-Seidel based alternating direction method of
370 multipliers (sGS-ADMM) to solve the CRTC which will be illustrated in Subsection 6.2 for a
371 warm start of BCNRTC.

372 Notice that the feasible set of the problem (3.11) is bounded and closed, and the objective
373 function is continuous and proper, by Weierstrass Theorem, the solution set of (3.11) is
374 nonempty and compact.

375 In the next section, we will propose an algorithm to solve the BCNRTC model (3.11).

376 **4. The Proximal Majorization-Minimization Algorithm.** In this section, we will develop
377 a proximal majorization-minimization (PMM) algorithm to solve the BCNRTC model (3.11).

378 By using the indicator function, we can rewrite the BCNRTC model (3.11) to an uncon-
379 strained optimization problem as follows:

$$380 \quad (4.1) \quad \min_{\mathcal{L}, \mathcal{M}} \|\mathcal{L}\|_{\text{TNN}} - H_1(\mathcal{L}) + \lambda(\|\mathcal{M}\|_1 - H_2(\mathcal{M})) + \delta_{\Gamma_1}(\mathcal{L}, \mathcal{M}) + \delta_{D_1}(\mathcal{M}) + \delta_{D_2}(\mathcal{L}),$$

381 where $D_1 := \{\mathcal{M} \mid \|\mathcal{M}\|_\infty \leq b_m\}$, $D_2 := \{\mathcal{L} \mid \|\mathcal{L}\| \leq b_l\}$, $\Gamma_1 := \{(\mathcal{L}, \mathcal{M}) \mid \mathcal{P}_\Omega(\mathcal{L} + \mathcal{M}) =$
382 $\mathcal{P}_\Omega(\mathcal{X})\}$, and $\delta_{D_1}(\mathcal{M})$ is the indicator function of the nonempty set D_1 .

383 The proposed PMM algorithm is to linearize the concave terms $-H_1(\cdot)$ and $-H_2(\cdot)$ in the
384 objective function of (4.1) at each iteration with respect to the current iterate, say $(\mathcal{L}^k, \mathcal{M}^k)$,
385 and generate the next iterate $(\mathcal{L}^{k+1}, \mathcal{M}^{k+1})$ by solving a convex subproblem inexactly:

$$386 \quad (4.2) \quad \begin{aligned} & \min_{\mathcal{L}, \mathcal{M}} \left\{ F(\mathcal{L}, \mathcal{M}; \mathcal{L}^k, \mathcal{M}^k) := \|\mathcal{L}\|_{\text{TNN}} - H_1(\mathcal{L}^k) - \langle \nabla H_1(\mathcal{L}^k), \mathcal{L} - \mathcal{L}^k \rangle + \lambda(\|\mathcal{M}\|_1 - H_2(\mathcal{M}^k)) \right. \\ & \quad \left. - \langle \nabla H_2(\mathcal{M}^k), \mathcal{M} - \mathcal{M}^k \rangle + \frac{\eta}{2} \|\mathcal{M} - \mathcal{M}^k\|_F^2 + \frac{\eta}{2} \|\mathcal{L} - \mathcal{L}^k\|_F^2 \right. \\ & \quad \left. + \delta_{\Gamma_1}(\mathcal{L}, \mathcal{M}) + \delta_{D_1}(\mathcal{M}) + \delta_{D_2}(\mathcal{L}) \right\}. \end{aligned}$$

387 Let $\mathcal{L}^k = \mathcal{U}^k * \Sigma^k * (\mathcal{V}^k)^H$ be the t-SVD, then it holds that $\nabla H_1(\mathcal{L}^k) = \mathcal{U}^k * \mathcal{R}^k * (\mathcal{V}^k)^H$, where
388 $\mathcal{R}^k = \text{ifft}(\widehat{\mathcal{R}}^k, [\], 3)$ and $\widehat{\mathcal{R}}^k = \text{Diag}(\nabla g(\text{diag}(\widehat{\Sigma}^k))) = \text{Diag}(\nabla g(\sigma(\widehat{\mathcal{L}}^k)))$. For brevity,
389 the proximal parameter $\eta > 0$ is assumed to be a constant, although it is frequently varying
390 in practice to accelerate convergence.

391 By casting some constants, the subproblem (4.2) can be rewritten as follows:

$$392 \quad (4.3) \quad \begin{aligned} & \min_{\mathcal{L}, \mathcal{M}} \|\mathcal{L}\|_{\text{TNN}} - \langle \nabla H_1(\mathcal{L}^k), \mathcal{L} \rangle + \lambda(\|\mathcal{M}\|_1 - \langle \nabla H_2(\mathcal{M}^k), \mathcal{M} \rangle) + \frac{\eta}{2} \|\mathcal{M} - \mathcal{M}^k\|_F^2 \\ & \quad + \frac{\eta}{2} \|\mathcal{L} - \mathcal{L}^k\|_F^2 + \delta_{\Gamma_1}(\mathcal{L}, \mathcal{M}) + \delta_{D_1}(\mathcal{M}) + \delta_{D_2}(\mathcal{L}). \end{aligned}$$

393 For convenience, we define $\mathcal{W} := (\mathcal{L}, \mathcal{M})$. Note that $F(\mathcal{W}; \mathcal{W}^k)$ is strongly convex, by [35,
394 Theorem 1.9, Theorem 2.6], we obtain that $F(\mathcal{W}; \mathcal{W}^k)$ has a unique minimizer.

395 Motivated by [3], we use an error criterion to describe the inexact solution in (4.3), i.e.,
396 we need to find \mathcal{W}^{k+1} and $\mathcal{C}^{k+1} := (\mathcal{C}_{\mathcal{L}}^{k+1}, \mathcal{C}_{\mathcal{M}}^{k+1})$ such that

$$397 \quad (4.4) \quad \mathcal{C}^{k+1} \in \partial F(\mathcal{L}^{k+1}, \mathcal{M}^{k+1}; \mathcal{L}^k, \mathcal{M}^k) \quad \text{and} \quad \|\mathcal{C}^{k+1}\|_F \leq \eta c \|\mathcal{W}^{k+1} - \mathcal{W}^k\|_F,$$

398 where $0 \leq c < \frac{1}{2}$ is a given constant.

399 Now, we summarize the PMM algorithm for solving the BCNRTC (3.11) in Algorithm 4.1.

Algorithm 4.1 The PMM algorithm for solving the BCNRTC (3.11).

- 1: **Input:** $\mathcal{L}^0, \mathcal{M}^0, \mathcal{P}_{\Omega}(\mathcal{X}), \lambda, \gamma$ and η . Set $k = 0$.
 - 2: Find $\mathcal{W}^{k+1}, \mathcal{C}^{k+1}$ such that $\mathcal{C}^{k+1} \in \partial F(\mathcal{L}^{k+1}, \mathcal{M}^{k+1}; \mathcal{L}^k, \mathcal{M}^k)$ and $\|\mathcal{C}^{k+1}\|_F \leq \eta c \|\mathcal{W}^{k+1} - \mathcal{W}^k\|_F$.
 - 3: If a termination criterion is met, set $\mathcal{L}^* := \mathcal{L}^{k+1}, \mathcal{M}^* := \mathcal{M}^{k+1}$; else, set $k := k + 1$, return to 2.
-

400 **4.1. Convergence Analysis.** In this section, we establish the global convergence of the
401 PMM algorithm when h is chosen as the one in (3.13) or (3.15). Recall that the notation
402 $\mathcal{W} := (\mathcal{L}, \mathcal{M})$. Let

$$403 \quad Q(\mathcal{W}) := \|\mathcal{L}\|_{\text{TNN}} - H_1(\mathcal{L}) + \lambda(\|\mathcal{M}\|_1 - H_2(\mathcal{M})) + \delta_{\Gamma_1}(\mathcal{L}, \mathcal{M}) + \delta_{D_1}(\mathcal{M}) + \delta_{D_2}(\mathcal{L}).$$

404 It is easy to see that $F(\mathcal{W}^k; \mathcal{W}^k) = Q(\mathcal{W}^k)$. Firstly, we show a descent lemma for $Q(\mathcal{W})$.

405 **Lemma 4.1.** *Let $\{\mathcal{W}^k\}_{k \in \mathbb{N}}$ be the sequence generated by Algorithm 4.1. Then, for any $\eta > 0$
406 and $0 \leq c < \frac{1}{2}$,*

$$407 \quad Q(\mathcal{W}^{k+1}) + \frac{\eta}{2}(1 - 2c)\|\mathcal{W}^{k+1} - \mathcal{W}^k\|_F^2 \leq Q(\mathcal{W}^k) \quad \forall k \geq 0,$$

408 *and furthermore, $\lim_{k \rightarrow \infty} \|\mathcal{W}^{k+1} - \mathcal{W}^k\|_F = 0$, where $\|\mathcal{W}^k\|_F = \sqrt{\|\mathcal{L}^k\|_F^2 + \|\mathcal{M}^k\|_F^2}$.*

409 Next, we show $Q(\mathcal{W})$ satisfies the relative error condition.

410 **Lemma 4.2.** *Let $\{\mathcal{W}^k\}_{k \in \mathbb{N}}$ be the sequence generated by Algorithm 4.1, \mathcal{W}^* be a cluster
411 point and $\mathcal{B}^{k+1} := (\mathcal{B}_{\mathcal{L}}^{k+1}, \mathcal{B}_{\mathcal{M}}^{k+1}) \in \partial Q(\mathcal{W}^{k+1})$. Then, there exist $\delta_0 > 0$ and $\tilde{m} > 0$ such that*

$$412 \quad \|\mathcal{B}^{k+1}\|_F \leq (\tilde{m} + \lambda/\gamma + \eta + \eta c)\|\mathcal{W}^{k+1} - \mathcal{W}^k\|_F \quad \forall \mathcal{W}^k, \mathcal{W}^{k+1} \in B(\mathcal{W}^*, \delta_0).$$

413 **Lemma 4.3.** *The function $Q(\mathcal{W})$ is a KL function when h is chosen as the one in (3.13)
414 or (3.15).*

415 The proofs of Lemma 4.1, Lemma 4.2 and Lemma 4.3 are given in Appendix C. Combining
416 Lemmas 4.1 - 4.3, we obtain the following convergence result of the PMM algorithm.

417 **Theorem 4.4.** *Let h be chosen as the one in (3.13) or (3.15), $\{\mathcal{W}^k\}_{k \in \mathbb{N}}$ be the sequence
418 generated by Algorithm 4.1 and \mathcal{W}^* be a cluster point. Then, for any $\eta > 0$ and $0 \leq c < \frac{1}{2}$,*

419 the sequence $\{\mathcal{W}^k\}_{k \in \mathbb{N}}$ converges to \mathcal{W}^* as k goes to infinity, and \mathcal{W}^* is a critical point of
 420 BCNRTC model (3.11), i.e., $0 \in \partial Q(\mathcal{W}^*)$. Moreover, the sequence $\{\mathcal{W}^k\}_{k \in \mathbb{N}}$ has a finite
 421 length, i.e., $\sum_{k=0}^{\infty} \|\mathcal{W}^{k+1} - \mathcal{W}^k\|_F < \infty$.

422 *Proof.* As mentioned in Lemma 4.2, the sequence $\{\mathcal{W}^k\}_{k \in \mathbb{N}}$ generated by Algorithm 4.1
 423 is bounded which admits a converging subsequence, i.e., there exists a subsequence \mathcal{W}^{k_j} such
 424 that $\mathcal{W}^{k_j} \rightarrow \mathcal{W}^*$, as $k_j \rightarrow \infty$. Moreover, \mathcal{W}^k belongs to Γ_1 , D_1 and D_2 , which leads to
 425 $\delta_{\Gamma_1}(\mathcal{L}^{k_j}, \mathcal{M}^{k_j}) = 0$, $\delta_{D_1}(\mathcal{M}^{k_j}) = 0$ and $\delta_{D_2}(\mathcal{L}^{k_j}) = 0$. So we have

$$\begin{aligned}
 Q(\mathcal{W}^{k_j}) &= \|\mathcal{L}^{k_j}\|_{\text{TNN}} - H_1(\mathcal{L}^{k_j}) + \lambda(\|\mathcal{M}^{k_j}\|_1 - H_2(\mathcal{M}^{k_j})) + \delta_{\Gamma_1}(\mathcal{L}^{k_j}, \mathcal{M}^{k_j}) \\
 &\quad + \delta_{D_1}(\mathcal{M}^{k_j}) + \delta_{D_2}(\mathcal{L}^{k_j}) \\
 426 \quad (4.5) \quad &= \|\mathcal{L}^{k_j}\|_{\text{TNN}} - H_1(\mathcal{L}^{k_j}) + \lambda(\|\mathcal{M}^{k_j}\|_1 - H_2(\mathcal{M}^{k_j})) \\
 &\rightarrow \|\mathcal{L}^*\|_{\text{TNN}} - H_1(\mathcal{L}^*) + \lambda(\|\mathcal{M}^*\|_1 - H_2(\mathcal{M}^*)), \text{ as } k_j \rightarrow \infty,
 \end{aligned}$$

427 where the last limit holds by the continuity of $\|\cdot\|_{\text{TNN}} - H_1(\cdot) + \lambda(\|\cdot\|_1 - H_2(\cdot))$. Since the
 428 sets Γ_1 , D_1 and D_2 are closed and \mathcal{W}^k belongs to Γ_1 , D_1 and D_2 , we have \mathcal{W}^* belongs to Γ_1 ,
 429 D_1 and D_2 , and so $Q(\mathcal{W}^*) = \|\mathcal{L}^*\|_{\text{TNN}} - H_1(\mathcal{L}^*) + \lambda(\|\mathcal{M}^*\|_1 - H_2(\mathcal{M}^*))$, which together with
 430 (4.5), implies that $Q(\mathcal{W}^{k_j}) \rightarrow Q(\mathcal{W}^*)$ as $k_j \rightarrow \infty$. Combining Lemma 4.1 - Lemma 4.3, the
 431 conclusion is obtained according to [3, Theorem 2.9]. This completes the proof. \blacksquare

432 **4.2. Solving the Subproblem.** In this section, the symmetric Gauss-Seidel based alter-
 433 nating direction method of multipliers (sGS-ADMM)[25] is applied to solve the subproblem
 434 in the PMM algorithm. Each PMM iteration solves a strongly convex subproblem of the
 435 following form inexactly:

$$\begin{aligned}
 436 \quad (4.6) \quad &\min_{\mathcal{L}, \mathcal{M}} \|\mathcal{L}\|_{\text{TNN}} - \langle \nabla H_1(\mathcal{L}^k), \mathcal{L} \rangle + \lambda(\|\mathcal{M}\|_1 - \langle \nabla H_2(\mathcal{M}^k), \mathcal{M} \rangle) + \frac{\eta}{2} \|\mathcal{M} - \mathcal{M}^k\|_F^2 + \frac{\eta}{2} \|\mathcal{L} - \mathcal{L}^k\|_F^2 \\
 &\text{s.t. } \mathcal{P}_{\Omega}(\mathcal{L} + \mathcal{M}) = \mathcal{P}_{\Omega}(\mathcal{X}), \|\mathcal{M}\|_{\infty} \leq b_m, \|\mathcal{L}\| \leq b_l.
 \end{aligned}$$

437 Let $\mathcal{L} + \mathcal{M} = \mathcal{Z}$ and add a proximal term. The problem (4.6) can be rewritten as

$$\begin{aligned}
 438 \quad (4.7) \quad &\min_{\mathcal{L}, \mathcal{M}, \mathcal{Z}} \|\mathcal{L}\|_{\text{TNN}} - \langle \nabla H_1(\mathcal{L}^k), \mathcal{L} \rangle + \lambda(\|\mathcal{M}\|_1 - \langle \nabla H_2(\mathcal{M}^k), \mathcal{M} \rangle) + \frac{\eta}{2} \|\mathcal{M} - \mathcal{M}^k\|_F^2 \\
 &\quad + \frac{\eta}{2} \|\mathcal{L} - \mathcal{L}^k\|_F^2 + \frac{\eta}{2} \|\mathcal{Z} - \mathcal{Z}^k\|_F^2 + \delta_{D_1}(\mathcal{M}) + \delta_{D_2}(\mathcal{L}) \\
 &\text{s.t. } \mathcal{L} + \mathcal{M} = \mathcal{Z}, \mathcal{P}_{\Omega}(\mathcal{X}) = \mathcal{P}_{\Omega}(\mathcal{Z}).
 \end{aligned}$$

439 Let $\Gamma_2 := \{\mathcal{Z} | \mathcal{P}_{\Omega}(\mathcal{X}) = \mathcal{P}_{\Omega}(\mathcal{Z})\}$. The augmented Lagrangian function associated with (4.7) is
 440 defined by

$$\begin{aligned}
 441 \quad \mathcal{L}(\mathcal{L}, \mathcal{M}, \mathcal{Z}; \mathcal{Y}) &:= \|\mathcal{L}\|_{\text{TNN}} - \langle \nabla H_1(\mathcal{L}^k), \mathcal{L} \rangle + \lambda(\|\mathcal{M}\|_1 - \langle \nabla H_2(\mathcal{M}^k), \mathcal{M} \rangle) + \langle \mathcal{Y}, \mathcal{Z} - \mathcal{L} - \mathcal{M} \rangle \\
 &\quad + \frac{\eta}{2} \|\mathcal{M} - \mathcal{M}^k\|_F^2 + \frac{\eta}{2} \|\mathcal{L} - \mathcal{L}^k\|_F^2 + \frac{\mu}{2} \|\mathcal{L} + \mathcal{M} - \mathcal{Z}\|_F^2 + \frac{\eta}{2} \|\mathcal{Z} - \mathcal{Z}^k\|_F^2 \\
 &\quad + \delta_{D_1}(\mathcal{M}) + \delta_{D_2}(\mathcal{L}),
 \end{aligned}$$

442 where $\mu > 0$ is the penalty parameter and \mathcal{Y} is a multiplier. The iterative scheme of sGS-
443 ADMM is given explicitly by

$$444 \quad (4.8) \quad \mathcal{Z}^{t+\frac{1}{2}} = \arg \min_{\mathcal{Z} \in \Gamma_2} \{\mathcal{L}(\mathcal{L}^t, \mathcal{M}^t, \mathcal{Z}; \mathcal{Y}^t)\},$$

$$445 \quad (4.9) \quad \mathcal{L}^{t+1} = \arg \min_{\mathcal{L}} \{\mathcal{L}(\mathcal{L}, \mathcal{M}^t, \mathcal{Z}^{t+\frac{1}{2}}; \mathcal{Y}^t)\},$$

$$446 \quad (4.10) \quad \mathcal{Z}^{t+1} = \arg \min_{\mathcal{Z} \in \Gamma_2} \{\mathcal{L}(\mathcal{L}^{t+1}, \mathcal{M}^t, \mathcal{Z}; \mathcal{Y}^t)\},$$

$$447 \quad (4.11) \quad \mathcal{M}^{t+1} = \arg \min_{\mathcal{M}} \{\mathcal{L}(\mathcal{L}^{t+1}, \mathcal{M}, \mathcal{Z}^{t+1}; \mathcal{Y}^t)\},$$

$$448 \quad (4.12) \quad \mathcal{Y}^{t+1} = \mathcal{Y}^t - \tau\mu(\mathcal{L}^{t+1} + \mathcal{M}^{t+1} - \mathcal{Z}^{t+1}),$$

450 where $\tau \in (0, (1 + \sqrt{5})/2)$ is the step-length. Next, we turn to compute the concrete forms of
451 solutions in each subproblem.

452 The optimal solution with respect to \mathcal{Z} is given explicitly by

$$453 \quad \mathcal{Z} = \mathcal{P}_{\Omega}(\mathcal{X}) + \frac{1}{\mu + \eta} \mathcal{P}_{\bar{\Omega}}(\mu(\mathcal{L} + \mathcal{M}) + \eta\mathcal{Z}^k - \mathcal{Y}).$$

454 Before giving the solution of the problem (4.9), we need to present the following lemma.

455 **Lemma 4.5.** *For any $\mathcal{Y} \in \mathbb{R}^{n_1 \times n_2 \times n_3}$, $\tau > 0$ and $\rho > 0$. Let $\mathcal{Y} = \mathcal{U} * \Sigma * \mathcal{V}^H$ be the t-SVD.
456 Then the optimal solution of the following problem*

$$457 \quad \min_{\mathcal{X} \in \mathbb{R}^{n_1 \times n_2 \times n_3}} \left\{ \tau \|\mathcal{X}\|_{\text{TNN}} + \frac{1}{2} \|\mathcal{X} - \mathcal{Y}\|_F^2 \mid \|\mathcal{X}\| \leq \rho \right\}$$

458 *is given by $\mathcal{X}^* = \mathcal{U} * \mathcal{D}_{\tau, \rho} * \mathcal{V}^H$, where $\mathcal{D}_{\tau, \rho} = \text{ifft}(\min\{\max\{\widehat{\Sigma} - \tau, 0\}, \rho\}, [\cdot], 3)$.*

459 **Lemma 4.5** can be proved easily. For brevity, we omit it here. It follows from **Lemma 4.5**
460 that the optimal solution with respect to \mathcal{L} in (4.9) can be given by

$$(4.13) \quad \begin{aligned} \mathcal{L}^{t+1} &= \arg \min_{\|\mathcal{L}\| \leq b_l} \left\{ \|\mathcal{L}\|_{\text{TNN}} - \langle \nabla H_1(\mathcal{L}^k) - \mathcal{Y}_1^t, \mathcal{L} \rangle + \frac{\mu}{2} \|\mathcal{L} + \mathcal{M}^t - \mathcal{Z}^{t+\frac{1}{2}}\|_F^2 + \frac{\eta}{2} \|\mathcal{L} - \mathcal{L}^k\|_F^2 \right\} \\ &= \arg \min_{\|\mathcal{L}\| \leq b_l} \left\{ \|\mathcal{L}\|_{\text{TNN}} + \frac{\eta + \mu}{2} \|\mathcal{L} - \mathcal{A}\|_F^2 \right\} = \mathcal{U}^t * \mathcal{D}_{\tau, \rho}^t * (\mathcal{V}^t)^H, \end{aligned}$$

463 where $\mathcal{A} = (-\mu\mathcal{M}^t + \mu\mathcal{Z}^{t+\frac{1}{2}} + \eta\mathcal{L}^k + \mathcal{Y}_1^t + \nabla H_1(\mathcal{L}^k))/(\eta + \mu) = \mathcal{U}^t * \Sigma^t * (\mathcal{V}^t)^H$ and $\mathcal{D}_{\tau, \rho}^t =$
464 $\text{ifft}(\min\{\max\{\widehat{\Sigma}^t - 1/(\eta + \mu), 0\}, b_l\}, [\cdot], 3)$.

465 On the other hand, the optimal solution with respect to (4.11) is given by

$$\begin{aligned} \mathcal{M}^{t+1} &= \arg \min_{\|\mathcal{M}\|_{\infty} \leq b_m} \left\{ \lambda(\|\mathcal{M}\|_1 - \langle \nabla H_2(\mathcal{M}^k), \mathcal{M} \rangle) - \langle \mathcal{Y}_1^t, \mathcal{M} \rangle + \frac{\eta}{2} \|\mathcal{M} - \mathcal{M}^k\|_F^2 \right. \\ &\quad \left. + \frac{\mu}{2} \|\mathcal{M} + \mathcal{L}^{t+1} - \mathcal{Z}^{t+1}\|_F^2 \right\} \\ &= \arg \min_{\|\mathcal{M}\|_{\infty} \leq b_m} \left\{ \|\mathcal{M}\|_1 + \frac{\eta + \mu}{2\lambda} \|\mathcal{M} - \mathcal{G}\|_F^2 \right\}, \end{aligned}$$

468 where $\mathcal{G} = (\lambda \nabla H_2(\mathcal{M}^k) + \mu \mathcal{Z}^{t+1} - \mu \mathcal{L}^{t+1} + \eta \mathcal{M}^k + \mathcal{Y}_1^t)/(\eta + \mu)$. Simple calculations show
 469 that the closed form solution with respect to \mathcal{M}^{t+1} can be given by

$$470 \quad (4.14) \quad \mathcal{M}_{ijk}^{t+1} = \begin{cases} \text{sign}(\mathcal{G}_{ijk}) \max\{|\mathcal{G}_{ijk}| - \lambda/(\mu + \eta), 0\}, & |\mathcal{G}_{ijk}| \leq b_m + \lambda/(\mu + \eta), \\ \text{sign}(\mathcal{G}_{ijk}) b_m, & |\mathcal{G}_{ijk}| > b_m + \lambda/(\mu + \eta). \end{cases}$$

471 Now we are ready to state the sGS-ADMM for solving (4.7) in Algorithm 4.2.

Algorithm 4.2 A symmetric Gauss-Seidel ADMM for solving (4.7).

- 1: **Input:** $\tau, \Omega, \lambda, \gamma, \mu, \eta, \mathcal{P}_\Omega(\mathcal{X}), \mathcal{L}^0, \mathcal{M}^0, \mathcal{Y}^0, \mathcal{M}^k, \mathcal{L}^k$ and \mathcal{Z}^k . Set $t = 0$.
 - 2: Compute $\mathcal{Z}^{t+\frac{1}{2}}$ by $\mathcal{Z}^{t+\frac{1}{2}} = \mathcal{P}_\Omega(\mathcal{X}) + \frac{1}{\mu+\eta} \mathcal{P}_\Omega(\mu(\mathcal{L}^t + \mathcal{M}^t) + \eta \mathcal{Z}^k - \mathcal{Y}^t)$.
 - 3: Compute \mathcal{L}^{t+1} via (4.13).
 - 4: Compute \mathcal{Z}^{t+1} by $\mathcal{Z}^{t+1} = \mathcal{P}_\Omega(\mathcal{X}) + \frac{1}{\mu+\eta} \mathcal{P}_\Omega(\mu(\mathcal{L}^{t+1} + \mathcal{M}^t) + \eta \mathcal{Z}^k - \mathcal{Y}^t)$.
 - 5: Compute \mathcal{M}^{t+1} via (4.14).
 - 6: Compute \mathcal{Y}^{t+1} by (4.12).
 - 7: If a termination criterion is not met, set $t := t + 1$ and return to 2.
-

472 Note that the objective function of (4.7) is nonsmooth with respect to \mathcal{L}, \mathcal{M} and quadratic
 473 with respect to \mathcal{Z} . By [25, Theorem 3], we can show the convergence of Algorithm 4.2, which
 474 is summarized in the following theorem.

475 **Theorem 4.6.** *Let $\{(\mathcal{L}^t, \mathcal{M}^t, \mathcal{Z}^t, \mathcal{Y}^t)\}_{t \in \mathbb{N}}$ be generated by Algorithm 4.2. Choose $\mu > 0$ and
 476 $\gamma \in (0, (\sqrt{5} + 1)/2)$, then the sequence $\{(\mathcal{L}^t, \mathcal{M}^t, \mathcal{Z}^t)\}_{t \in \mathbb{N}}$ converges to an optimal solution of
 477 the problem (4.7) and $\{\mathcal{Y}^t\}_{t \in \mathbb{N}}$ converges to an optimal solution of the dual problem of (4.7).*

478 *Proof.* Notice that the problem (4.7) has a unique minimizer and the following constraint
 479 qualification is satisfied:

$$480 \quad \text{There exists } (\mathcal{L}^*, \mathcal{M}^*, \mathcal{Z}^*) \in \text{ri}(D_2 \times D_1 \times \Gamma_2) \cap \mathfrak{C},$$

481 where $\mathfrak{C} := \{(\mathcal{L}, \mathcal{M}, \mathcal{Z}) | \mathcal{L} + \mathcal{M} = \mathcal{Z}\}$. By [25, Theorem 3], we can easily obtain the conclusion
 482 of this theorem. ■

483 **Remark 4.7.** Actually, Algorithm 4.2 shows the process of solving the CRTIC model if η ,
 484 $\mathcal{M}^k, \mathcal{L}^k$ and \mathcal{Z}^k are all equal to zero. For simplicity, we don't give the specific algorithm
 485 frame here.

486 Next we give the computational cost of algorithms. At each iteration of solving the sub-
 487 problem of PMM algorithm, we need to calculate (4.8)-(4.12). The main cost of (4.9) is tensor
 488 SVD. The number of the floating point operations of fft is $\mathcal{O}(n_3 \log_2(n_3))$, and we need to
 489 calculate $n_1 n_2$ times, so the total cost of tensor fft is $\mathcal{O}(n_3 \log_2(n_3) n_1 n_2)$. Meanwhile the cost
 490 of SVDs for n_3 n_1 -by- n_2 matrix is $\mathcal{O}(\tilde{n} \tilde{m}^2 n_3)$, where $\tilde{n} = \min\{n_1, n_2\}$ and $\tilde{m} = \max\{n_1, n_2\}$.
 491 Therefore, the total cost of tensor SVD is $\mathcal{O}(n_3 \log_2(n_3) n_1 n_2 + \tilde{n} \tilde{m}^2 n_3)$ operations. The
 492 complexities of computing $\mathcal{Z}^{t+1}, \mathcal{M}^{t+1}$ and \mathcal{Y}^{t+1} are all $\mathcal{O}(n_1 n_2 n_3)$ operations for the inde-
 493 pendency that operation on each entry of the tensor. Then the total cost of the subproblem
 494 of PMM algorithm at each iteration is $\mathcal{O}(n_3 \log_2(n_3) n_1 n_2 + \tilde{n} \tilde{m}^2 n_3)$. During the algorithm
 495 execution, the largest data we storage is the $n_1 \times n_2 \times n_3$ tensor, so the memory complexity
 496 is $\mathcal{O}(n_1 n_2 n_3)$.

497 **5. Error Bounds.** In this section, we establish the error bound between the optimal solu-
 498 tion $(\mathcal{L}^c, \mathcal{M}^c)$ of (4.3) and the ground-truth $(\mathcal{L}^*, \mathcal{M}^*)$ in Frobenius norm. Meanwhile, we give
 499 the analysis that the error bound of BCNRTC can be reduced compared with that of CRTC
 500 as long as the given initial estimator is not far from the ground truth.

501 We assume that $\|\mathcal{M}^*\|_0 = \tilde{s}$ and the tubal multi-rank of \mathcal{L}^* is $\mathbf{r} = (r_1, r_2, \dots, r_{n_3})$. Denote
 502 $\tilde{\Delta}_{\mathcal{L}} := \mathcal{L}^c - \mathcal{L}^*$ and $\tilde{\Delta}_{\mathcal{M}} := \mathcal{M}^c - \mathcal{M}^*$. Firstly, we provide the connection among $\|\tilde{\Delta}_{\mathcal{L}}\|_{\text{TNN}}$,
 503 $\|\tilde{\Delta}_{\mathcal{M}}\|_1$ and the Frobenius norms of $\tilde{\Delta}_{\mathcal{L}}$ and $\tilde{\Delta}_{\mathcal{M}}$. Similar results have been studied in [55],
 504 which established the relationship between the TNN and the Frobenius norm of the tensor
 505 by using the tubal rank. We show a structure constructed by the average rank, which may
 506 provide a more clear result of the error bound.

507 In order to display the structure, we study the subgradient of the TNN at first. Considering
 508 the $\bar{\mathbf{L}}^*$ with the structure $\bar{\mathbf{L}}^* = \text{Diag}(\widehat{\mathbf{L}}^{*(1)}, \widehat{\mathbf{L}}^{*(2)}, \dots, \widehat{\mathbf{L}}^{*(n_3)})$, where $\widehat{\mathbf{L}}^{*(i)} \in \mathbb{C}^{n_1 \times n_2}$ with the
 509 SVD $\widehat{\mathbf{L}}^{*(i)} = \mathbf{U}^{(i)} \mathbf{S}^{(i)} (\mathbf{V}^{(i)})^H$. Notice that $\text{rank}(\widehat{\mathbf{L}}^{*(i)}) = r_i$, by dividing the first r_i columns
 510 and the last $n_1 - r_i$ columns, we have the $\mathbf{U}^{(i)} = [\mathbf{U}_1^{(i)}, \mathbf{U}_2^{(i)}]$, where $\mathbf{U}_1^{(i)} \in \mathbb{C}^{n_1 \times r_i}$ and
 511 $\mathbf{U}_2^{(i)} \in \mathbb{C}^{n_1 \times (n_1 - r_i)}$. Similarly, $\mathbf{V}^{(i)} = [\mathbf{V}_1^{(i)}, \mathbf{V}_2^{(i)}]$, where $\mathbf{V}_1^{(i)} \in \mathbb{C}^{n_2 \times r_i}$ and $\mathbf{V}_2^{(i)} \in \mathbb{C}^{n_2 \times (n_2 - r_i)}$.
 512 From the subgradient of nuclear norm of the matrix, we have

$$513 \quad \left\{ \mathbf{U}_1^{(i)} (\mathbf{V}_1^{(i)})^H + \mathbf{U}_2^{(i)} \mathbf{W}^{(i)} (\mathbf{V}_2^{(i)})^H \mid \mathbf{W}^{(i)} \in \mathbb{C}^{(n_1 - r_i) \times (n_2 - r_i)}, \|\mathbf{W}^{(i)}\| \leq 1 \right\} = \partial \|\widehat{\mathbf{L}}^{*(i)}\|_*.$$

514 We denote that $\widehat{\mathbf{U}}_1^{(i)} = [\mathbf{U}_1^{(i)}, 0] \in \mathbb{C}^{n_1 \times r_{\max}}$, $\widehat{\mathbf{V}}_1^{(i)} = [\mathbf{V}_1^{(i)}, 0] \in \mathbb{C}^{n_2 \times r_{\max}}$, $\widehat{\mathbf{U}}_2^{(i)} = [0, \mathbf{U}_2^{(i)}] \in$
 515 $\mathbb{C}^{n_1 \times (n_1 - r_{\min})}$, $\widehat{\mathbf{V}}_2^{(i)} = [0, \mathbf{V}_2^{(i)}] \in \mathbb{C}^{n_2 \times (n_2 - r_{\min})}$ and

$$516 \quad \widehat{\mathbf{W}}^{(i)} = \begin{bmatrix} 0 & 0 \\ 0 & \mathbf{W}^{(i)} \end{bmatrix} \in \mathbb{C}^{(n_1 - r_{\min}) \times (n_2 - r_{\min})},$$

518 where $r_{\max} = \max\{r_1, r_2, \dots, r_{n_3}\}$, $r_{\min} = \min\{r_1, r_2, \dots, r_{n_3}\}$ and $\|\mathbf{W}^{(i)}\| \leq 1$. Then we
 519 have $\widehat{\mathbf{U}}_1^{(i)} (\widehat{\mathbf{V}}_1^{(i)})^H + \widehat{\mathbf{U}}_2^{(i)} \widehat{\mathbf{W}}^{(i)} (\widehat{\mathbf{V}}_2^{(i)})^H = \mathbf{U}_1^{(i)} (\mathbf{V}_1^{(i)})^H + \mathbf{U}_2^{(i)} \mathbf{W}^{(i)} (\mathbf{V}_2^{(i)})^H \in \partial \|\widehat{\mathbf{L}}^{*(i)}\|_*.$

520 Since $\widehat{\mathbf{U}}_1^{(i)} \in \mathbb{C}^{n_1 \times r_{\max}}$ have the same size for $i = 1, 2, \dots, n_3$, we can stack the matrices
 521 to form a tensor $\widehat{\mathcal{U}}_1 \in \mathbb{C}^{n_1 \times r_{\max} \times n_3}$. Let $\widehat{\mathcal{U}}_2$, $\widehat{\mathcal{V}}_1$, $\widehat{\mathcal{V}}_2$ and $\widehat{\mathcal{W}}$ are constructed likewise, we can
 522 see the following proposition holds.

523 **Proposition 5.1.** Let $\widehat{\mathcal{U}}_1$, $\widehat{\mathcal{U}}_2$, $\widehat{\mathcal{V}}_1$, $\widehat{\mathcal{V}}_2$ and $\widehat{\mathcal{W}}$ are defined as above, and $\mathcal{U}_1 = \text{ifft}(\widehat{\mathcal{U}}_1, [\cdot], 3)$,
 524 $\mathcal{U}_2 = \text{ifft}(\widehat{\mathcal{U}}_2, [\cdot], 3)$, $\mathcal{V}_1 = \text{ifft}(\widehat{\mathcal{V}}_1, [\cdot], 3)$, $\mathcal{V}_2 = \text{ifft}(\widehat{\mathcal{V}}_2, [\cdot], 3)$, $\mathcal{W} = \text{ifft}(\widehat{\mathcal{W}}, [\cdot], 3)$. Then we have
 (5.1)

$$525 \quad S(\mathcal{L}^*) := \left\{ \mathcal{U}_1 * \mathcal{V}_1^H + \mathcal{U}_2 * \mathcal{W} * \mathcal{V}_2^H \mid \mathcal{W} \in \mathbb{C}^{(n_1 - r_{\min}) \times (n_2 - r_{\min}) \times n_3}, \|\mathcal{W}\| \leq 1 \right\} = \partial \|\mathcal{L}^*\|_{\text{TNN}}.$$

526 The proof of the Proposition 5.1 is given in Appendix D.1. Obviously, $\mathcal{U}_1 \in \mathbb{R}^{n_1 \times r_{\max} \times n_3}$
 527 and $\mathcal{V}_1 \in \mathbb{R}^{n_2 \times r_{\max} \times n_3}$ have the same tubal multi-rank with \mathcal{L}^* .

Remark 5.2. A similar work is given in [29]:

$$G(\mathcal{L}^*) := \left\{ \mathcal{U}_s * \mathcal{V}_s^H + \mathcal{R} \mid \mathcal{U}_s^H * \mathcal{R} = \mathbf{0}, \mathcal{R} * \mathcal{V}_s = \mathbf{0}, \|\mathcal{R}\| \leq 1 \right\} = \partial \|\mathcal{L}^*\|_{\text{TNN}},$$

528 where $\mathcal{L}^* = \mathcal{U}_s * \mathcal{S}_s * \mathcal{V}_s^H$ is the skinny t-SVD of \mathcal{L}^* . However, its proof is not given, and it is
 529 not shown how to construct \mathcal{U}_s and \mathcal{V}_s . If \mathcal{U}_s and \mathcal{V}_s are constructed as same as those in [55]

530 similarly to the skinny SVD of matrix, then $S(\mathcal{L}^*) \supseteq G(\mathcal{L}^*)$, and the “equality” relationship
 531 holds when $r_i = r_{\max}$ for $i = 1, 2, \dots, n_3$. If \mathcal{U}_s and \mathcal{V}_s are constructed as same as ours, i.e.,
 532 $\mathcal{U}_s = \mathcal{U}_1$ and $\mathcal{V}_s = \mathcal{V}_1$, then $S(\mathcal{L}^*) = G(\mathcal{L}^*)$.

533 Denote the set \mathcal{T} by

$$534 \quad \mathcal{T} := \{\mathcal{U}_1 * \mathcal{Y}^H + \mathcal{W} * \mathcal{V}_1^H \mid \mathcal{Y} \in \mathbb{R}^{n_2 \times r_{\max} \times n_3}, \mathcal{W} \in \mathbb{R}^{n_1 \times r_{\max} \times n_3}\},$$

535 and its orthogonal complement by \mathcal{T}^\perp . The set \mathcal{T} is the tangent space with respect to the
 536 rank-constraint tensors $\{\mathcal{X} \in \mathbb{R}^{n_1 \times n_2 \times n_3} \mid \text{rank}_a(\mathcal{X}) \leq r_{\max}\}$ at \mathcal{L}^* .

537 **Proposition 5.3.** *For any tensor $\mathcal{X} \in \mathbb{R}^{n_1 \times n_2 \times n_3}$, the orthogonal projection of \mathcal{X} onto \mathcal{T}*
 538 *and \mathcal{T}^\perp are given by*

$$539 \quad \mathcal{P}_{\mathcal{T}}(\mathcal{X}) = \mathcal{U}_1 * \mathcal{U}_1^H * \mathcal{X} + \mathcal{X} * \mathcal{V}_1 * \mathcal{V}_1^H - \mathcal{U}_1 * \mathcal{U}_1^H * \mathcal{X} * \mathcal{V}_1 * \mathcal{V}_1^H,$$

540

$$541 \quad \mathcal{P}_{\mathcal{T}^\perp}(\mathcal{X}) = \mathcal{U}_2 * \mathcal{U}_2^H * \mathcal{X} * \mathcal{V}_2 * \mathcal{V}_2^H.$$

542 The proof of the **Proposition 5.3** is given in **Appendix D.2**. For simplicity of subsequently
 543 analysis, we denote

$$544 \quad (5.2) \quad d_{\mathcal{L}} := \frac{1}{\sqrt{r}} \|\mathcal{U}_1 * \mathcal{V}_1^H - \nabla H_1(\mathcal{L}^k)\|_F, \quad d_{\mathcal{M}} := \frac{1}{\sqrt{s}} \|\text{sign}(\mathcal{M}^*) - \nabla H_2(\mathcal{M}^k)\|_F,$$

$$545 \quad r := \frac{\sum_{i=1}^{n_3} r_i}{n_3}, \quad |\Omega| := m, \quad \tilde{\Delta} := \tilde{\Delta}_{\mathcal{L}} + \tilde{\Delta}_{\mathcal{M}}.$$

546 Denote Θ_{ijk} as a unit tensor with the (i, j, k) -th nonzero entry equaling 1. Let the set of
 547 the standard orthogonal basis of $\mathbb{R}^{n_1 \times n_2 \times n_3}$ be denoted by $\Theta := \{\Theta_{ijk} \mid 1 \leq i \leq n_1, 1 \leq j \leq$
 548 $n_2, 1 \leq k \leq n_3\}$. For each unit tensor Θ_{ijk} , there exists a unique index $\omega_l = j + (i-1)n_2 +$
 549 $(k-1)n_1n_2$ such that $\Theta_{\omega_l} = \Theta_{ijk}$, $\omega_l \in \{1, 2, \dots, n_1n_2n_3\}$, which is a bijective mapping from
 550 $\{1, 2, \dots, n_1\} \times \{1, 2, \dots, n_2\} \times \{1, 2, \dots, n_3\}$ to $\{1, 2, \dots, n_1n_2n_3\}$. Then Ω be the multiset of
 551 all sampled i.i.d. indices $\omega_1, \dots, \omega_m$ mapping to the subset of $\{1, 2, \dots, n_1\} \times \{1, 2, \dots, n_2\} \times$
 552 $\{1, 2, \dots, n_3\}$.

553 **Lemma 5.4.** *For any $\eta > 0$ and $\lambda > 0$, we have*

$$554 \quad (5.3) \quad \|\tilde{\Delta}_{\mathcal{L}}\|_{TNN} \leq p_1 \|\tilde{\Delta}_{\mathcal{L}}\|_F + p_2 \|\tilde{\Delta}_{\mathcal{M}}\|_F, \quad \|\tilde{\Delta}_{\mathcal{M}}\|_1 \leq q_1 \|\tilde{\Delta}_{\mathcal{L}}\|_F + q_2 \|\tilde{\Delta}_{\mathcal{M}}\|_F,$$

555 where $p_1 := \sqrt{2r} + d_{\mathcal{L}}\sqrt{r} + \eta \|\mathcal{L}^* - \mathcal{L}^k\|_F$, $p_2 := \lambda d_{\mathcal{M}}\sqrt{s} + \eta \|\mathcal{M}^* - \mathcal{M}^k\|_F$, $q_1 := (d_{\mathcal{L}}\sqrt{r} +$
 556 $\eta \|\mathcal{L}^* - \mathcal{L}^k\|_F)/\lambda$ and $q_2 := \sqrt{s} + d_{\mathcal{M}}\sqrt{s} + \eta \|\mathcal{M}^* - \mathcal{M}^k\|_F/\lambda$.

557 The proof of the **Lemma 5.4** is given in **Appendix D.3**. Let p_{ijk} denote the probability
 558 to observe the (i, j, k) -th entry of \mathcal{X} , we suppose that each element is sampled with positive
 559 probability.

560 **Assumption 5.1.** *There exists a positive constant $\mu_1 \geq 1$ such that $p_{ijk} \geq (\mu_1 n_1 n_2 n_3)^{-1}$.*

561 Note that **Assumption 5.1** implies that

$$562 \quad (5.4) \quad \mathbb{E}[\langle \Theta, \mathcal{X} \rangle^2] = \sum_{i=1}^{n_1} \sum_{j=1}^{n_2} \sum_{k=1}^{n_3} p_{ijk} \mathcal{X}_{ijk}^2 \geq (\mu_1 n_1 n_2 n_3)^{-1} \|\mathcal{X}\|_F^2.$$

563 Define the operator $\mathfrak{D}_\Omega : \mathbb{R}^{n_1 \times n_2 \times n_3} \rightarrow \mathbb{R}^m$ by $\mathfrak{D}_\Omega(\mathcal{X}) := (\langle \Theta_{\omega_1}, \mathcal{X} \rangle, \dots, \langle \Theta_{\omega_m}, \mathcal{X} \rangle)^T$. The
 564 adjoint $\mathfrak{D}_\Omega^* : \mathbb{R}^m \rightarrow \mathbb{R}^{n_1 \times n_2 \times n_3}$ by $\mathfrak{D}_\Omega^*(\mathfrak{D}_\Omega(\mathcal{X})) = \sum_{l=1}^m \langle \Theta_{\omega_l}, \mathcal{X} \rangle \Theta_{\omega_l}$. Let $\epsilon = (\epsilon_1, \dots, \epsilon_m)^T$ be
 565 independent and identically distributed (i.i.d.) Rademacher sequence, i.e., i.i.d. sequence of
 566 Bernoulli random variables taking the values 1 and -1 with probability $\frac{1}{2}$. Define

$$567 \quad (5.5) \quad \beta_{\mathcal{L}} := \mathbb{E} \left\| \frac{1}{m} \mathfrak{D}_\Omega^*(\epsilon) \right\|, \quad \beta_{\mathcal{M}} := \mathbb{E} \left\| \frac{1}{m} \mathfrak{D}_\Omega^*(\epsilon) \right\|_\infty.$$

568 The following Lemma shows that the sampling operator \mathcal{P}_Ω satisfies some property spec-
 569 ified in a certain set with high probability. Similar results can also be found in [21].

570 **Lemma 5.5.** *Suppose that Assumption 5.1 holds. Given any positive numbers $p_1, p_2, q_1,$
 571 q_2 and t , define*

$$572 \quad (5.6) \quad K(p, q, t) := \{ \Delta = \Delta_{\mathcal{L}} + \Delta_{\mathcal{M}} \mid \|\Delta_{\mathcal{L}}\|_{TNN} \leq p_1 \|\Delta_{\mathcal{L}}\|_F + p_2 \|\Delta_{\mathcal{M}}\|_F, \\ \|\Delta_{\mathcal{M}}\|_1 \leq q_1 \|\Delta_{\mathcal{L}}\|_F + q_2 \|\Delta_{\mathcal{M}}\|_F, \|\Delta\|_\infty = 1, \|\Delta_{\mathcal{L}}\|_F^2 + \|\Delta_{\mathcal{M}}\|_F^2 \geq t \mu_1 n_1 n_2 n_3 \},$$

573 where $p := (p_1, p_2)$ and $q := (q_1, q_2)$. Denote $\beta_S := (\beta_{\mathcal{L}}^2 p_1^2 + \beta_{\mathcal{L}}^2 p_2^2 + \beta_{\mathcal{M}}^2 q_1^2 + \beta_{\mathcal{M}}^2 q_2^2)^{\frac{1}{2}}$. Then, it
 574 holds that for all $\Delta \in K(p, q, t)$,

$$575 \quad (5.7) \quad \frac{1}{m} \|\mathcal{P}_\Omega(\Delta)\|_F^2 \geq \mathbb{E}[\langle \Theta, \Delta \rangle^2] - \frac{\|\Delta_{\mathcal{L}}\|_F^2 + \|\Delta_{\mathcal{M}}\|_F^2}{2\mu_1 n_1 n_2 n_3} - 256\mu_1 n_1 n_2 n_3 \beta_S^2$$

576 with probability at least $1 - \frac{\exp[-mt^2 \log(2)/64]}{1 - \exp[-mt^2 \log(2)/64]}$. In particular, the inequality (5.7) holds with
 577 probability at least $1 - \frac{1}{n_1 + n_2 + n_3}$ if $t = 8\sqrt{\frac{\log(n_1 + n_2 + n_3 + 1)}{m \log(2)}}$.

578 The proof of the Lemma 5.5 is given in Appendix D.4.

579 **Proposition 5.6.** *Suppose that Assumption 5.1 holds. Then, there exists $C_2 > 0$, such that,
 580 it holds that either*

$$581 \quad \frac{\|\tilde{\Delta}_{\mathcal{L}}\|_F^2 + \|\tilde{\Delta}_{\mathcal{M}}\|_F^2}{n_1 n_2 n_3} \leq 32(b_m + b_l)^2 \mu_1 \sqrt{\frac{\log(n_1 + n_2 + n_3 + 1)}{m \log(2)}}$$

582 or

$$\begin{aligned} \frac{\|\tilde{\Delta}_{\mathcal{L}}\|_F^2 + \|\tilde{\Delta}_{\mathcal{M}}\|_F^2}{n_1 n_2 n_3} &\leq \frac{64b_l^2}{n_1 n_2 n_3} \left[\frac{(d_{\mathcal{L}}\sqrt{r} + \eta\|\mathcal{L}^* - \mathcal{L}^k\|_F)^2}{\lambda^2} + \left(\sqrt{\tilde{s}} + d_{\mathcal{M}}\sqrt{\tilde{s}} + \frac{\eta\|\mathcal{M}^* - \mathcal{M}^k\|_F}{\lambda} \right)^2 \right] \\ &+ C_2 \left[\beta_{\mathcal{L}}^2 (\sqrt{2r} + d_{\mathcal{L}}\sqrt{r} + \eta\|\mathcal{L}^* - \mathcal{L}^k\|_F)^2 \right. \\ 583 &+ \beta_{\mathcal{L}}^2 (\lambda d_{\mathcal{M}}\sqrt{\tilde{s}} + \eta\|\mathcal{M}^* - \mathcal{M}^k\|_F)^2 + \frac{\beta_{\mathcal{M}}^2 (d_{\mathcal{L}}\sqrt{r} + \eta\|\mathcal{L}^* - \mathcal{L}^k\|_F)^2}{\lambda^2} \\ &\left. + \beta_{\mathcal{M}}^2 \left(\sqrt{\tilde{s}} + d_{\mathcal{M}}\sqrt{\tilde{s}} + \frac{\eta\|\mathcal{M}^* - \mathcal{M}^k\|_F}{\lambda} \right)^2 \right] \end{aligned}$$

584 with probability at least $1 - \frac{1}{n_1 + n_2 + n_3}$.

585 *Proof.* Let $\tilde{b} := \|\tilde{\Delta}\|_\infty$. Since $(\mathcal{L}^c, \mathcal{M}^c)$ is the optimal and $(\mathcal{L}^*, \mathcal{M}^*)$ is feasible to the
 586 problem (4.3), we have $\|\tilde{\Delta}_{\mathcal{M}}\|_\infty \leq 2b_m$ and $\|\tilde{\Delta}_{\mathcal{L}}\|_\infty \leq \|\mathcal{L}^c\| + \|\mathcal{L}^*\| \leq 2b_l$. Hence, $\tilde{b} \leq$
 587 $\|\tilde{\Delta}_{\mathcal{L}}\|_\infty + \|\tilde{\Delta}_{\mathcal{M}}\|_\infty \leq 2(b_m + b_l)$. We consider the following two cases:

588 Case 1: Suppose that $\|\tilde{\Delta}_{\mathcal{L}}\|_F^2 + \|\tilde{\Delta}_{\mathcal{M}}\|_F^2 \leq 8\tilde{b}^2\mu_1n_1n_2n_3\sqrt{\frac{\log(n_1+n_2+n_3+1)}{m\log(2)}}$. Then we im-
 589 mediately obtain that

$$590 \frac{\|\tilde{\Delta}_{\mathcal{L}}\|_F^2 + \|\tilde{\Delta}_{\mathcal{M}}\|_F^2}{n_1n_2n_3} \leq 32(b_m + b_l)^2\mu_1\sqrt{\frac{\log(n_1 + n_2 + n_3 + 1)}{m\log(2)}}.$$

591 Case 2: Suppose that $\|\tilde{\Delta}_{\mathcal{L}}\|_F^2 + \|\tilde{\Delta}_{\mathcal{M}}\|_F^2 \geq 8\tilde{b}^2\mu_1n_1n_2n_3\sqrt{\frac{\log(n_1+n_2+n_3+1)}{m\log(2)}}$. It follows from
 592 the definition of \tilde{b} that $\tilde{\Delta}/\tilde{b} \in K(p, q, t)$, where $t = 8\sqrt{\frac{\log(n_1+n_2+n_3+1)}{m\log(2)}}$, and $p = (p_1, p_2)$ and
 593 $q = (q_1, q_2)$ are given in Lemma 5.4. Due to (5.4) and Lemma 5.5, we obtain that with
 594 probability at least $1 - \frac{1}{n_1+n_2+n_3}$,

$$595 (5.8) \quad \frac{\|\tilde{\Delta}\|_F^2}{n_1n_2n_3} \leq \frac{\mu_1}{m}\|\mathcal{P}_\Omega(\tilde{\Delta})\|_F^2 + \frac{\|\tilde{\Delta}_{\mathcal{L}}\|_F^2 + \|\tilde{\Delta}_{\mathcal{M}}\|_F^2}{2n_1n_2n_3} + 256\mu_1^2n_1n_2n_3\beta_S^2\tilde{b}^2.$$

596 Since $(\mathcal{L}^c, \mathcal{M}^c)$ is the optimal solution of (4.3) and $(\mathcal{L}^*, \mathcal{M}^*)$ is the true tensor, we obtain
 597 $\mathcal{P}_\Omega(\tilde{\Delta}) = 0$. In addition, due to $\|\tilde{\Delta}_{\mathcal{L}}\|_\infty \leq 2b_l$, we then derive from (5.3) that

$$598 (5.9) \quad \begin{aligned} \|\tilde{\Delta}\|_F^2 &\geq \|\tilde{\Delta}_{\mathcal{L}}\|_F^2 + \|\tilde{\Delta}_{\mathcal{M}}\|_F^2 - 2\|\tilde{\Delta}_{\mathcal{L}}\|_\infty\|\tilde{\Delta}_{\mathcal{M}}\|_1 \\ &\geq \|\tilde{\Delta}_{\mathcal{L}}\|_F^2 + \|\tilde{\Delta}_{\mathcal{M}}\|_F^2 - 4b_l(q_1\|\tilde{\Delta}_{\mathcal{L}}\|_F + q_2\|\tilde{\Delta}_{\mathcal{M}}\|_F) \\ &\geq \|\tilde{\Delta}_{\mathcal{L}}\|_F^2 + \|\tilde{\Delta}_{\mathcal{M}}\|_F^2 - 16b_l^2(q_1^2 + q_2^2) - \frac{\|\tilde{\Delta}_{\mathcal{L}}\|_F^2 + \|\tilde{\Delta}_{\mathcal{M}}\|_F^2}{4} \\ &= \frac{3}{4}(\|\tilde{\Delta}_{\mathcal{L}}\|_F^2 + \|\tilde{\Delta}_{\mathcal{M}}\|_F^2) - 16b_l^2(q_1^2 + q_2^2). \end{aligned}$$

599 By combining (5.8) with (5.9), we obtain that

$$600 (5.10) \quad \frac{\|\tilde{\Delta}_{\mathcal{L}}\|_F^2 + \|\tilde{\Delta}_{\mathcal{M}}\|_F^2}{n_1n_2n_3} \leq \frac{64b_l^2(q_1^2 + q_2^2)}{n_1n_2n_3} + 1024\mu_1^2n_1n_2n_3\beta_S^2\tilde{b}^2.$$

601 Recall that $\beta_S := (\beta_{\mathcal{L}}^2p_1^2 + \beta_{\mathcal{L}}^2p_2^2 + \beta_{\mathcal{M}}^2q_1^2 + \beta_{\mathcal{M}}^2q_2^2)^{\frac{1}{2}}$. By plugging this together with Lemma 5.4
 602 into (5.10) and taking $C_2 := 4096\mu_1^2n_1n_2n_3(b_m + b_l)^2$, we complete the proof. \blacksquare

603 For the third-order tensor, we need to avoid the case that each fiber is sampled with very high
 604 probability. Let $R_{:jk} := \sum_{i=1}^{n_1}p_{ijk}$, $C_{i:k} := \sum_{j=1}^{n_2}p_{ijk}$, $T_{ij:} := \sum_{k=1}^{n_3}p_{ijk}$, the following assumption
 605 is used to avoid this situation.

606 **Assumption 5.2.** *There exists a positive constant $\mu_2 \geq 1$ such that $\max_{\{i,j,k\}}\{R_{:jk}, C_{i:k},$
 607 $T_{ij:}\} \leq \frac{\mu_2}{\min\{n_1, n_2, n_3\}}$.*

608 We now estimate an upper bound of $\mathbb{E}\|\frac{1}{m}\mathfrak{D}_\Omega^*(\epsilon)\|$. First, we give a brief introduction about
 609 Orlicz ψ_s -norm. Given any $s \geq 1$, the Orlicz ψ_s -norm of a random variable z is defined by
 610 $\|z\|_{\psi_s} := \inf\{t > 0 | \mathbb{E}\exp(|z|^s/t^s) \leq 2\}$. The proofs of the followings two lemmas are given in
 611 Appendix D.5 and Appendix D.6, respectively.

Lemma 5.7. Under *Assumption 5.2*, for $m \geq \tilde{n} \log((n_1 + n_2)n_3)(\log(\tilde{n}))^2/\mu_2$, there exists a positive constant C_1 such that

$$\beta_{\mathcal{L}} = \mathbb{E} \left\| \frac{1}{m} \mathfrak{D}_{\Omega}^*(\epsilon) \right\| \leq C_1 \sqrt{\frac{3e\mu_2 \log((n_1 + n_2)n_3)}{\tilde{n}m}},$$

612 where $\tilde{n} := \min\{n_1, n_2\}$.

Lemma 5.8. There exist $C > 0$ and $M > 0$ that depend on the Orlicz ψ_1 -norm of ϵ_l such that

$$\beta_{\mathcal{M}} = \mathbb{E} \left\| \frac{1}{m} \mathfrak{D}_{\Omega}^*(\epsilon) \right\|_{\infty} \leq \frac{M(\log(2m) + 1)}{Cm}.$$

613 We first define two fundamental terms

$$614 \begin{cases} \Upsilon_1 := \left(\frac{d_{\mathcal{L}}\sqrt{r} + \eta \|\mathcal{L}^* - \mathcal{L}^k\|_F}{\lambda} \right)^2 + (\sqrt{\tilde{s}} + d_{\mathcal{M}}\sqrt{\tilde{s}} + \frac{\eta \|\mathcal{M}^* - \mathcal{M}^k\|_F}{\lambda})^2, \\ \Upsilon_2 := (\sqrt{2r} + d_{\mathcal{L}}\sqrt{r} + \eta \|\mathcal{L}^* - \mathcal{L}^k\|_F)^2 + (d_{\mathcal{M}}\sqrt{\tilde{s}}\lambda + \eta \|\mathcal{M}^* - \mathcal{M}^k\|_F)^2. \end{cases}$$

615 By combining *Proposition 5.6* with *Lemma 5.7* and *Lemma 5.8*, we can easily establish the
616 following error bound results.

617 **Theorem 5.9.** Suppose that *Assumption 5.1* and *Assumption 5.2* hold. Then, for $m \geq$
618 $\tilde{n} \log((n_1 + n_2)n_3)(\log(\tilde{n}))^2/\mu_2$, there exist constants $C > 0$, $C_1 > 0$ and $C_2 > 0$ such that

$$619 \quad (5.11) \quad \frac{\|\tilde{\Delta}_{\mathcal{L}}\|_F^2 + \|\tilde{\Delta}_{\mathcal{M}}\|_F^2}{n_1 n_2 n_3} \leq \frac{64b_l^2}{n_1 n_2 n_3} \Upsilon_1 + C_2 \left[\frac{C_1^2 3e\mu_2 \log((n_1 + n_2)n_3)}{\tilde{n}m} \Upsilon_2 + \left(\frac{M(\log(2m) + 1)}{Cm} \right)^2 \Upsilon_1 \right]$$

620 with probability at least $1 - \frac{1}{n_1 + n_2 + n_3}$.

621 When $H_1 \equiv 0$, $H_2 \equiv 0$ and $\eta \equiv 0$, the error bound in *Theorem 5.9* is just the error bound
622 of the CRTC problem (3.17). From *Theorem 5.9*, we can see that the second term in the
623 maximum of (5.11) dominates the first term. Thus, the error bound is dominated by the
624 second term. Now, we denote the second term as \mathfrak{L}_m . In fact, when $H_1 \equiv 0$ and $H_2 \equiv 0$, we
625 obtain that $d_{\mathcal{L}} = 1$ and $d_{\mathcal{M}} = 1$ according to (5.2). In this case, we denote the second term
626 as \mathfrak{L}'_m . Note that $\mathfrak{L}_m < \mathfrak{L}'_m$ when $d_{\mathcal{L}} < 1$ and $d_{\mathcal{M}} < 1$.

627 Let $\widehat{\mathbf{U}}_1^{k(i)}$ and $\widehat{\mathbf{V}}_1^{k(i)}$ denote the first r_i columns of $\widehat{\mathbf{U}}^k(i)$ and $\widehat{\mathbf{V}}^k(i)$. Next, we show that
628 the error bound of (4.3) is lower than that of (3.17), i.e., $d_{\mathcal{L}} < 1$ and $d_{\mathcal{M}} < 1$.

629 **Theorem 5.10.** Let $\varepsilon_{\nabla H_1}(\widehat{\mathbf{L}}^{k(i)}) := \frac{1}{\sqrt{r_i}} \left\| \widehat{\nabla H_1}(\widehat{\mathcal{L}}^k(i)) - \widehat{\mathbf{U}}_1^{k(i)} (\widehat{\mathbf{V}}_1^{k(i)})^H \right\|_F$ for $i = 1, \dots, n_3$,

630 and assume that

$$631 \quad (5.12) \quad \frac{\|\widehat{\mathbf{L}}^{k(i)} - \widehat{\mathbf{L}}^{*k(i)}\|_F}{\sigma_{r_i}(\widehat{\mathbf{L}}^{*k(i)})} < \min \left\{ \frac{1}{\sqrt{2}} \left(1 - \exp \left(-\sqrt{2r_i} \left(1 - \varepsilon_{\nabla H_1}(\widehat{\mathbf{L}}^{k(i)}) \right) \right) \right), \frac{1}{2} \right\},$$

632 then $d_{\mathcal{L}} < 1$.

633 *Proof.* Let $\widehat{\mathbf{L}}^{\star(i)} = \mathbf{U}^{(i)} \mathbf{S}^{(i)} (\mathbf{V}^{(i)})^H$ with $\mathbf{U}^{(i)} = [\mathbf{U}_1^{(i)}, \mathbf{U}_2^{(i)}]$ and $\mathbf{V}_i = [\mathbf{V}_1^{(i)}, \mathbf{V}_2^{(i)}]$, $\mathbf{U}_1^{(i)} \in$
 634 $\mathbb{C}^{n_1 \times r_i}$, $\mathbf{V}_1^{(i)} \in \mathbb{C}^{n_2 \times r_i}$, for $i = 1, \dots, n_3$. Note that

$$635 \quad \|\widehat{\mathbf{U}}_1^{k(i)} (\widehat{\mathbf{V}}_1^{k(i)})^H - \mathbf{U}_1^{(i)} (\mathbf{V}_1^{(i)})^H\|_F \leq -\frac{1}{\sqrt{2}} \log \left(1 - \sqrt{2} \frac{\|\widehat{\mathbf{L}}^k(i) - \widehat{\mathbf{L}}^{\star(i)}\|_F}{\sigma_{r_i}(\widehat{\mathbf{L}}^{\star(i)})} \right) < \sqrt{r_i} (1 - \varepsilon_{\nabla H_1}(\widehat{\mathbf{L}}^k(i))),$$

636 where the first inequality follows from the proof of [31, Theorem 3] and the second inequality
 637 is due to the inequality (5.12). So we obtain

$$638 \quad \|\nabla \widehat{H}_1(\mathcal{L}^k)^{(i)} - \mathbf{U}_1^{(i)} (\mathbf{V}_1^{(i)})^H\|_F \leq \|\nabla \widehat{H}_1(\mathcal{L}^k)^{(i)} - \widehat{\mathbf{U}}_1^{k(i)} (\widehat{\mathbf{V}}_1^{k(i)})^H\|_F + \|\widehat{\mathbf{U}}_1^{k(i)} (\widehat{\mathbf{V}}_1^{k(i)})^H - \mathbf{U}_1^{(i)} (\mathbf{V}_1^{(i)})^H\|_F \\ < \sqrt{r_i} \varepsilon_{\nabla H_1}(\widehat{\mathbf{L}}^k(i)) + \sqrt{r_i} (1 - \varepsilon_{\nabla H_1}(\widehat{\mathbf{L}}^k(i))) = \sqrt{r_i}.$$

639 On the other hand, it follows from $\widehat{\mathbf{U}}_1^{(i)} = [\mathbf{U}_1^{(i)}, 0] \in \mathbb{C}^{n_1 \times r_{\max}}$ and $\widehat{\mathbf{V}}_1^{(i)} = [\mathbf{V}_1^{(i)}, 0] \in$
 640 $\mathbb{C}^{n_2 \times r_{\max}}$ that

$$641 \quad d_{\mathcal{L}}^2 = \frac{1}{r} \|\mathcal{U}_1 * \mathcal{V}_1^H - \nabla H_1(\mathcal{L}^k)\|_F^2 = \frac{1}{rn_3} \sum_{i=1}^{n_3} \|\nabla \widehat{H}_1(\mathcal{L}^k)^{(i)} - \widehat{\mathbf{U}}_1^{(i)} (\widehat{\mathbf{V}}_1^{(i)})^H\|_F^2 < \frac{1}{rn_3} \sum_{i=1}^{n_3} r_i = 1.$$

642 This completes the proof. ■

643 **Theorem 5.10** guarantees that $d_{\mathcal{L}} < 1$ if the estimator \mathcal{L}^k does not deviate too much from
 644 \mathcal{L}^{\star} .

645 **Remark 5.11.** **Theorem 5.10** removes the rank constraint condition $r_1 < \frac{6}{4n_3-7}(r_2 + \dots +$
 646 $r_{n_3})$ in [54, Lemma 4.2].

647 **Theorem 5.12.** Let $\mathbf{M}^{\star} := \text{Diag}(\text{vec}(\mathcal{M}^{\star}))$, $\mathbf{M}^k := \text{Diag}(\text{vec}(\mathcal{M}^k))$, and $\varepsilon_{\nabla H_2}(\mathcal{M}^k) :=$
 648 $\frac{1}{\sqrt{s}} \|\nabla H_2(\mathcal{M}^k) - \text{sign}(\mathcal{M}^k)\|_F$. Assume that

$$649 \quad \frac{\|\mathbf{M}^k - \mathbf{M}^{\star}\|_F}{\sigma_{\tilde{s}}(\mathbf{M}^{\star})} < \min \left\{ \frac{1}{\sqrt{2}} (1 - \exp(-\sqrt{2\tilde{s}}(1 - \varepsilon_{\nabla H_2}(\mathcal{M}^k)))) , \frac{1}{2} \right\},$$

650 where $\sigma_{\tilde{s}}(\mathbf{M}^{\star}) := \min\{|\mathcal{M}_{ijk}^{\star}| | \mathcal{M}_{ijk}^{\star} \neq 0\}$. Then, we have $d_{\mathcal{M}} < 1$.

651 *Proof.* We can obtain the following decomposition

$$652 \quad \mathbf{M}^{\star} = \text{Diag}(\text{vec}(\text{sign}(\mathcal{M}^{\star}))) \text{Diag}(\text{vec}(|\mathcal{M}^{\star}|)) \text{Diag}(\text{vec}(\text{sign}^2(\mathcal{M}^{\star}))) \\ = \text{Diag}(\text{vec}(\text{sign}(\mathcal{M}^{\star}))) \mathbf{P}_1 \mathbf{P}_2 \dots \mathbf{P}_{\tilde{s}} \text{Diag}(\pi(\text{vec}(|\mathcal{M}^{\star}|))) \\ \mathbf{P}_{\tilde{s}}^H \mathbf{P}_{\tilde{s}-1}^H \dots \mathbf{P}_1^H \text{Diag}(\text{vec}(\text{sign}^2(\mathcal{M}^{\star}))),$$

653 where $\mathbf{P}_1, \mathbf{P}_2, \dots, \mathbf{P}_{\tilde{s}}$ are elementary transformation matrices. Let $\mathbf{M}^{\star} = \mathbf{U}^{\star} \mathbf{\Sigma}^{\star} (\mathbf{V}^{\star})^H$ be
 654 the SVD, where $\mathbf{U}^{\star} = [\mathbf{U}_1^{\star} \ \mathbf{U}_2^{\star}]$, $\mathbf{V}^{\star} = [\mathbf{V}_1^{\star} \ \mathbf{V}_2^{\star}]$, $\mathbf{U}_1^{\star} \in \mathbb{R}^{n_1 n_2 n_3 \times \tilde{s}}$ and $\mathbf{V}_1^{\star} \in \mathbb{R}^{n_1 n_2 n_3 \times \tilde{s}}$. This
 655 implies that

$$656 \quad (5.13) \quad \mathbf{U}_1^{\star} (\mathbf{V}_1^{\star})^H = [\mathbf{U}_1^{\star} \ 0] \begin{bmatrix} (\mathbf{V}_1^{\star})^H \\ 0 \end{bmatrix} = \mathbf{U}^{\star} (\mathbf{V}^{\star})^H \\ = \text{Diag}(\text{vec}(\text{sign}(\mathcal{M}^{\star}))) \mathbf{P}_1 \mathbf{P}_2 \dots \mathbf{P}_{\tilde{s}} \mathbf{P}_{\tilde{s}}^H \mathbf{P}_{\tilde{s}-1}^H \dots \mathbf{P}_1^H \text{Diag}(\text{vec}(\text{sign}^2(\mathcal{M}^{\star}))) \\ = \text{Diag}(\text{vec}(\text{sign}(\mathcal{M}^{\star}))).$$

657 Notice that $\sigma_{\tilde{s}}(\mathbf{M}^*) = \min\{|\mathcal{M}_{ijk}^*| \mid \mathcal{M}_{ijk}^* \neq 0\}$, we have

$$\begin{aligned}
d_{\mathcal{M}} &= \frac{1}{\sqrt{\tilde{s}}} \|\nabla H_2(\mathcal{M}^k) - \text{sign}(\mathcal{M}^*)\|_F = \frac{1}{\sqrt{\tilde{s}}} \|\text{Diag}(\text{vec}(\nabla H_2(\mathcal{M}^k))) - \text{Diag}(\text{vec}(\text{sign}(\mathcal{M}^*)))\|_F \\
658 &= \frac{1}{\sqrt{\tilde{s}}} \|\text{Diag}(\text{vec}(\nabla H_2(\mathcal{M}^k))) - \mathbf{U}_1^* (\mathbf{V}_1^*)^H\|_F \\
&\leq -\frac{1}{\sqrt{2\tilde{s}}} \log \left(1 - \sqrt{2} \frac{\|\mathbf{M}^k - \mathbf{M}^*\|_F}{\sigma_{\tilde{s}}(\mathbf{M}^*)} \right) + \varepsilon_{\nabla H_2}(\mathcal{M}^k) < 1,
\end{aligned}$$

659 where the third equation follows from (5.13), and the first inequality follows from [31, Theorem
660 3]. ■

661 The above theorem demonstrates that $d_{\mathcal{M}} < 1$ if \mathcal{M}^k does not deviate too much from
662 \mathcal{M}^* .

663 Now, we analyze the constructions of ∇H_1 and ∇H_2 . In order to get a small error bound,
664 according to Theorem 5.9, we desire $d_{\mathcal{L}}$ and $d_{\mathcal{M}}$ as small as possible, i.e., $\nabla H_1(\mathcal{L}^k)$ is close to
665 $\mathcal{U}_1 * \mathcal{V}_1^H$ and $\nabla H_2(\mathcal{M}^k)$ is close to $\text{sign}(\mathcal{M}^*)$. Firstly, let $\nabla H_1(\mathcal{L}^k) = \mathcal{U}^k * \mathcal{R}^k * (\mathcal{V}^k)^H$, where
666 $\mathcal{U}^k = [\mathcal{U}_1^k \ \mathcal{U}_2^k]$ and $\mathcal{V}^k = [\mathcal{V}_1^k \ \mathcal{V}_2^k]$ with $\mathcal{U}_1^k \in \mathbb{R}^{n_1 \times r_{\max} \times n_3}$ and $\mathcal{V}_1^k \in \mathbb{R}^{n_2 \times r_{\max} \times n_3}$. If \mathcal{L}^k is close
667 to \mathcal{L}^* , we desire $\nabla H_1(\mathcal{L}^k)$ is close to $\mathcal{U}_1^k * (\mathcal{V}_1^k)^H$. Notice from (3.13) that

$$668 \quad (5.14) \quad h'(x) := \begin{cases} \frac{x}{\gamma}, & |x| \leq \gamma, \\ \text{sign}(x), & |x| > \gamma. \end{cases}$$

669 It is observed from (5.14) that the function h' is S-shaped with two inflection points at $\pm\gamma$
670 and the parameter γ mainly controls the shape of h' , the steepness of h' increase when γ
671 decrease. So, there exist some $\gamma \in (0, b_l]$ such that the following property holds:

$$672 \quad (5.15) \quad (\nabla g(\sigma(\widehat{\mathbf{L}}^k(i))))_j = h'(\sigma_j(\widehat{\mathbf{L}}^k(i))) \approx \begin{cases} 1, & 1 \leq j \leq r_i, \\ 0, & \text{otherwise,} \end{cases} \quad \forall i = 1, \dots, n_3.$$

673 Similarly, the SVD of \mathbf{M}^k is given by $\tilde{\mathbf{U}} \tilde{\Sigma} (\tilde{\mathbf{V}})^H$. Let $\tilde{\mathbf{U}}_1$ and $\tilde{\mathbf{V}}_1$ denote the first \tilde{s} columns
674 of $\tilde{\mathbf{U}}$ and $\tilde{\mathbf{V}}$. If \mathcal{M}^k is close to \mathcal{M}^* , we desire $\text{Diag}(\text{vec}(\nabla H_2(\mathcal{M}^k)))$ is close to $\tilde{\mathbf{U}}_1 \tilde{\mathbf{V}}_1^H$. So,
675 there also exist some $\gamma \in (0, b_m]$ such that the following property holds:

$$676 \quad (5.16) \quad h'(\mathbf{M}_{jj}^k) \approx \begin{cases} 1, & \mathbf{M}_{jj}^k > 0, \\ -1, & \mathbf{M}_{jj}^k < 0, \\ 0, & \text{otherwise.} \end{cases}$$

677 *Remark 5.13.* Notice that if ∇H_1 and ∇H_2 are obtained from the derivative of (3.15),
678 i.e.,

$$679 \quad (5.17) \quad h'(x) := \begin{cases} 0, & |x| \leq \gamma_1, \\ \frac{x - \gamma_1 \text{sign}(x)}{\gamma_2 - \gamma_1}, & \gamma_1 < |x| \leq \gamma_2, \\ \text{sign}(x), & |x| > \gamma_2, \end{cases}$$

680 then, the properties (5.15) and (5.16) hold. And the results can also be established if ∇H_1
681 and ∇H_2 are chosen as the correction function in [31].

682 *Remark 5.14.* By numerical experiments, we verify that $d_{\mathcal{L}} < 1$ and $d_{\mathcal{M}} < 1$ when h is
683 chosen as the one in (3.13). The relevant results can be found in Table 1.

684 **6. Numerical Experiments.** In this section, we present numerical experiments to show
 685 the effectiveness of our BCNRTC method in recovering color images and multispectral images,
 686 and compare it with the Robust Tensor Ring Completion (RTRC) [17], the Robust Tensor
 687 Completion ($\text{RTC}\ell_1$) [18] and the Nonconvex Robust Tensor Completion (NCRTC) [58]. The
 688 $\text{RTC}\ell_1$ model is a convex model and the NCRTC model is nonconvex, which gives the non-
 689 convex approximation of the sparse term compared to the $\text{RTC}\ell_1$. The superior performance
 690 of NCRTC compared to the $\text{RTC}\ell_1$ in terms of recovery quality has been demonstrated in
 691 [58] via extensive numerical results. To show the effectiveness of the BCNRTC more clearly,
 692 we also present results of $\text{RTC}\ell_1$. For fair comparisons, the parameters in each method are
 693 tuned to give optimal performance. All experiments are performed on an Intel i7-2600 CPU
 694 desktop computer with 8 GB of RAM and MATLAB R2020a.

695 We define the sample ratio (SR) as $\text{SR} := \frac{|\Omega|}{n_1 n_2 n_3}$ for an $n_1 \times n_2 \times n_3$ tensor, where Ω is
 696 generated uniformly at random and $|\Omega|$ represents the cardinality of Ω . Meanwhile, we use α
 697 to represent the impulse noise level. For each tensor, we randomly add the salt-and-pepper
 698 impulse noise with ratio α , and the observed tensor $\mathcal{P}_\Omega(\mathcal{X})$ is generated by the given SR.

699 To evaluate the performance of different methods, the peak signal-to-noise ratio (PSNR)
 700 is used to measure the quality of the recovered tensors, which is defined as follows:

$$701 \quad \text{PSNR}(\mathcal{L}) := 10 \log_{10} \frac{n_1 n_2 n_3 (\max_{i,j,k} \mathcal{L}^* - \min_{i,j,k} \mathcal{L}^*)^2}{\|\mathcal{L}^* - \mathcal{L}\|_F^2},$$

702 where \mathcal{L} and \mathcal{L}^* are the recovered tensor and the ground-truth tensor, respectively. The
 703 relative error (RE) between the recovered and the true tensor is defined by $\text{RE} := \frac{\|\mathcal{L} - \mathcal{L}^*\|_F}{\|\mathcal{L}^*\|_F}$.

704 6.1. Stopping Criteria.

705 **6.1.1. The stopping criterion for the PMM algorithm.** For the nonconvex BCNRTC
 706 model (3.11), we adopt the relative KKT residual

$$707 \quad (6.1) \quad \eta_{\text{kkt}} := \max\{\eta_{\mathcal{L}}, \eta_{\mathcal{M}}, \eta_P\} \leq 3 \times 10^{-3}$$

708 to measure the accuracy of an approximate optimal solution obtained by the PMM algorithm,
 709 where

$$710 \quad (6.2) \quad \eta_P := \frac{\|\mathcal{L} + \mathcal{M} - \mathcal{Z}\|_F}{1 + \|\mathcal{Z}\|_F + \|\mathcal{L}\|_F + \|\mathcal{M}\|_F}, \quad \eta_{\mathcal{L}} := \frac{\|\mathcal{L} - \text{Prox}_{\|\cdot\|_{\text{TNN}} + \delta_{D_2}(\cdot)}(\mathcal{Y} + \mathcal{L} + \nabla H_1(\mathcal{L}))\|_F}{1 + \|\mathcal{Y}\|_F + \|\mathcal{L}\|_F + \|\nabla H_1(\mathcal{L})\|_F},$$

$$\eta_{\mathcal{M}} := \frac{\|\mathcal{M} - \text{Prox}_{\lambda\|\cdot\|_1 + \delta_{D_1}(\cdot)}(\mathcal{Y} + \mathcal{M} + \lambda \nabla H_2(\mathcal{M}))\|_F}{1 + \|\mathcal{Y}\|_F + \|\mathcal{M}\|_F + \|\lambda \nabla H_2(\mathcal{M})\|_F}$$

711 with

$$712 \quad \text{Prox}_{\lambda f}(\mathbf{x}) := \arg \min_{\mathbf{w} \in \mathbb{R}^p} f(\mathbf{w}) + \frac{1}{2\lambda} \|\mathbf{w} - \mathbf{x}\|_F^2$$

713 denoting the proximal mapping of f with parameter λ [35].

714 **6.1.2. The stopping criterion for the sGS-ADMM algorithm.** In order to evaluate the
 715 performance of sGS-ADMM for solving convex subproblem (4.7), we use the primal infeasibility
 716 η_P and relative duality gap defined by

$$717 \quad \eta_{\text{gap}} := \frac{|\text{pobj} - \text{dobj}|}{1 + |\text{pobj}| + |\text{dobj}|},$$

718 where

$$719 \quad \begin{aligned} \text{pobj} := & \|\mathcal{L}\|_{\text{TNN}} - \langle \nabla H_1(\mathcal{L}^k), \mathcal{L} \rangle + \lambda(\|\mathcal{M}\|_1 - \langle \nabla H_2(\mathcal{M}^k), \mathcal{M} \rangle) + \frac{\eta}{2} \|\mathcal{M} - \mathcal{M}^k\|_F^2 \\ & + \frac{\eta}{2} \|\mathcal{L} - \mathcal{L}^k\|_F^2 + \frac{\eta}{2} \|\mathcal{Z} - \mathcal{Z}^k\|_F^2, \end{aligned}$$

720 and

$$721 \quad \begin{aligned} \text{dobj} := & \lambda \min_{\|\mathcal{M}\|_\infty \leq b_m} \left[\|\mathcal{M}\|_1 + \frac{\eta}{2\lambda} \left\| \mathcal{M} - \left(\mathcal{M}^k + \frac{\lambda \nabla H_2(\mathcal{M}^k) + \mathcal{Y}}{\eta} \right) \right\|_F^2 \right] - \frac{\eta}{2} \left\| \mathcal{L}^k + \frac{\mathcal{Y} + \nabla H_1(\mathcal{L}^k)}{\eta} \right\|_F^2 \\ & + \min_{\|\mathcal{L}\| \leq b_l} \left[\|\mathcal{L}\|_{\text{TNN}} + \frac{\eta}{2} \left\| \mathcal{L} - \left(\mathcal{L}^k + \frac{\mathcal{Y} + \nabla H_1(\mathcal{L}^k)}{\eta} \right) \right\|_F^2 \right] - \frac{\eta}{2} \left\| \mathcal{M}^k + \frac{\lambda \nabla H_2(\mathcal{M}^k) + \mathcal{Y}}{\eta} \right\|_F^2 \\ & + \min_{\mathcal{P}_\Omega(\mathcal{X}) = \mathcal{P}_\Omega(\mathcal{Z})} \left[\frac{\eta}{2} \left\| \mathcal{Z} - \left(\mathcal{Z}^k - \frac{\mathcal{Y}}{\eta} \right) \right\|_F^2 \right] + \langle \mathcal{Y}, \mathcal{Z}^k \rangle + \frac{\eta}{2} \|\mathcal{L}^k\|_F^2 + \frac{\eta}{2} \|\mathcal{M}^k\|_F^2 - \frac{1}{2\eta} \|\mathcal{Y}\|_F^2 \end{aligned}$$

722 are the primal and dual objective function values, respectively. For given tolerance Tol_S ,
 723 we will terminate the sGS-ADMM when $\max\{\eta_{\text{gap}}, \eta_P\} \leq \text{Tol}_S$ or the number of iterations
 724 reaches the maximum of 200. We initialize Tol_S^0 to be 3×10^{-2} and decrease it by a ratio, i.e.,
 725 $\text{Tol}_S^{k+1} = \text{Tol}_S^k / 1.1$.

726 **6.2. The Setting of Parameters.** In order to improve the convergence speed of **Algo-**
 727 **rithm 4.2**, based on the KKT optimality conditions of problem (4.7), we adopt the following
 728 relative residuals of \mathcal{L} and \mathcal{M} to update the penalty parameter μ in the augmented Lagrangian
 729 function:

$$730 \quad \begin{aligned} \eta_{D_1} &= \frac{\left\| \mathcal{L} - \text{Prox}_{\frac{1}{\eta}}(\|\cdot\|_{\text{TNN}} + \delta_{D_2}(\cdot)) \left(\mathcal{L}^k + \frac{\mathcal{Y} + \nabla H_1(\mathcal{L}^k)}{\eta} \right) \right\|_F}{1 + \frac{1}{\eta} \|\mathcal{Y}\|_F + \|\mathcal{L}^k\|_F + \frac{1}{\eta} \|\nabla H_1(\mathcal{L}^k)\|_F}, \\ \eta_{D_2} &= \frac{\left\| \mathcal{M} - \text{Prox}_{\frac{1}{\eta}}(\lambda \|\cdot\|_1 + \delta_{D_1}(\cdot)) \left(\mathcal{M}^k + \frac{\mathcal{Y} + \lambda \nabla H_2(\mathcal{M}^k)}{\eta} \right) \right\|_F}{1 + \frac{1}{\eta} \|\mathcal{Y}\|_F + \|\mathcal{M}^k\|_F + \frac{\lambda}{\eta} \|\nabla H_2(\mathcal{M}^k)\|_F}, \end{aligned}$$

731 which is a similar strategy as [23]. Let $\eta_D := \max\{\eta_{D_1}, \eta_{D_2}\}$. Specifically, set $\mu^0 = 0.1$. At
 732 the t -th iteration, compute $\chi^{t+1} = \frac{\eta_D^{t+1}}{\eta_D^t}$ and then set

$$733 \quad \mu^{t+1} = \begin{cases} \xi \mu^t, & \chi^{t+1} > 7, \\ \xi^{-1} \mu^t, & \frac{1}{\chi^{t+1}} > 7, \\ \mu^t, & \text{otherwise} \end{cases} \quad \text{with} \quad \xi = \begin{cases} 1.1, & \max \left\{ \chi^{t+1}, \frac{1}{\chi^{t+1}} \right\} \leq 50, \\ 2, & \max \left\{ \chi^{t+1}, \frac{1}{\chi^{t+1}} \right\} > 500, \\ 1.5, & \text{otherwise.} \end{cases}$$

734 For the proximal term in the PMM algorithm, the parameter η^0 is initialized as 10^{-4} and
 735 gradually decreased by some factors $\varsigma \in (0, 1)$, i.e., $\eta^{k+1} = \varsigma\eta^k$, where η^k denotes the penalty
 736 parameter value at the k -th PMM iteration.

737 In our following experiments, the function h in (3.13) which is related to the MCP func-
 738 tion is used in both H_1 and H_2 for simplicity. Meanwhile, we use γ_1 and γ_2 to denote the
 739 parameters in H_1 and H_2 , respectively. The parameters λ , γ_1 and γ_2 are sensitive to the
 740 recovery performance. For different sample ratios and different noise levels, we use the grid
 741 search method to get the best values of λ , γ_1 and γ_2 in terms of PSNR values of recovered
 742 images. These best values show that the value of λ depends on the sample ratio, noise level,
 743 γ_2 and the size of tensors. By using the data fitting method, we obtain the fitting function
 744 of λ , i.e., $\lambda = \frac{\tilde{c}}{\sqrt{SR\gamma_2\alpha n_3\tilde{m}}}$, where \tilde{c} is chosen from $\{0.4, 0.5, 0.6, 0.7\}$ to get the best recovery
 745 performance. The parameter γ_1 is chosen as $10(1.2 - SR)$ and γ_2 is chosen from $\{0.3, 0.4\}$,
 746 respectively. For practical problems, we adjust the above parameters slightly to obtain the
 747 best possible results. The step length τ in (4.12) can vary in the range $(0, (\sqrt{5} + 1)/2)$ [25]. In
 748 our numerical test, we find that the larger the step length, the faster the convergence speed.
 749 Hence, we set $\tau = 1.618$ in all the experiments. In experiments, all testing images are normal-
 750 ized to $[0, 1]$. Therefore, we set $b_m = 1$ and $\|\mathcal{L}\|_\infty \leq 1$. According to the equivalence between
 751 norms, we have $\|\mathcal{L}\| \leq \sqrt{n_1 n_2 n_3} \|\mathcal{L}\|_\infty$. So we set $b_l = \sqrt{n_1 n_2 n_3}$ in our numerical experiments.

752 As mentioned in Theorem 5.10 and Theorem 5.12, a lower recovery error bound can be
 753 obtained if the estimator $(\mathcal{L}^k, \mathcal{M}^k)$ in the PMM algorithm does not deviate from the ground-
 754 truth $(\mathcal{L}^*, \mathcal{M}^*)$ too much. Therefore, we use the solution obtained from solving the CRTC
 755 problem (3.17) as the initial estimator to warm-start our PMM algorithm. The sGS-ADMM
 756 is implemented to solve the CRTC method and will be terminated if (6.1) is satisfied or the
 757 number of iterations reaches the maximum of 200, where $\nabla H_1(\cdot)$ and $\nabla H_2(\cdot)$ in (6.2) vanish.
 758 We use the grid search method to get the best choice of λ , i.e., a value that gives nearly the
 759 highest possible PSNR value. And we use a similar strategy as [23] to update the penalty
 760 parameter μ .

761 **6.3. Error Bounds and the Performance of the PMM Algorithm.** In this subsection, we
 762 test error bounds and the performance of the PMM algorithm in different outer iterations. The
 763 test image is Pepper, and the test results are given in Table 1 which reports $d_{\mathcal{L}}$, $d_{\mathcal{M}}$, relative
 764 error and PSNR values of the CRTC and the first three outer iterations. In all experiments in
 765 Table 1, the stopping criterion of the PMM algorithm is achieved in the third outer iteration.

766 We can see from Table 1 that $d_{\mathcal{L}} = 1$ and $d_{\mathcal{M}} = 1$ in CRTC, and $d_{\mathcal{L}} < 1$ and $d_{\mathcal{M}} < 1$
 767 in each outer iteration of PMM algorithm, which verifies the results of Theorem 5.10 and
 768 Theorem 5.12. The PMM algorithm substantially reduces $d_{\mathcal{L}}$ and $d_{\mathcal{M}}$ in the first iteration.
 769 The first outer iteration improves the recovery quality at least 33% in terms of the relative
 770 error with respect to the CRTC model.

771 Table 1 also shows that $d_{\mathcal{L}}$ and $d_{\mathcal{M}}$ continue to decrease as the number of outer iterations
 772 increases, which implies that the upper error bounds in (5.11) in Theorem 5.9 continue to
 773 decrease. The PMM algorithm significantly improves the recovery quality in terms of both
 774 the relative error and the PSNR values.

Table 1

The values of $d_{\mathcal{L}}$, $d_{\mathcal{M}}$ and the performance of the PMM algorithm for Pepper image in different outer iterations with different sample ratios and noise levels.

SR	α		CRTC	1	2	3
0.8	0.2	$d_{\mathcal{L}}$	1	0.9432	0.923	0.9131
		$d_{\mathcal{M}}$	1	0.5317	0.5153	0.5104
		RE	0.0681	0.0393	0.0294	0.0257
		PSNR	29.27	34.04	36.56	37.72
	0.3	$d_{\mathcal{L}}$	1	0.963	0.9379	0.9262
		$d_{\mathcal{M}}$	1	0.5339	0.5195	0.5146
		RE	0.094	0.0584	0.0447	0.039
		PSNR	26.47	30.6	32.93	34.12
	0.4	$d_{\mathcal{L}}$	1	0.9817	0.9559	0.9451
		$d_{\mathcal{M}}$	1	0.5364	0.5241	0.5195
		RE	0.1279	0.0866	0.0692	0.0611
		PSNR	23.8	27.18	29.13	30.21
0.7	0.2	$d_{\mathcal{L}}$	1	0.952	0.935	0.926
		$d_{\mathcal{M}}$	1	0.6143	0.6011	0.5968
		RE	0.0773	0.0478	0.0377	0.0334
		PSNR	28.17	32.34	34.4	35.46
	0.3	$d_{\mathcal{L}}$	1	0.9672	0.9474	0.9386
		$d_{\mathcal{M}}$	1	0.6262	0.6201	0.619
		RE	0.1054	0.0668	0.0535	0.0491
		PSNR	25.47	29.43	31.37	32.11
	0.4	$d_{\mathcal{L}}$	1	0.9802	0.963	0.9552
		$d_{\mathcal{M}}$	1	0.6253	0.6213	0.6209
		RE	0.1415	0.0961	0.079	0.0727
		PSNR	22.91	26.28	27.98	28.7

775 **6.4. Random data.** In this section, we present the results to analyze the success ratio on
776 random data. We present the colormap of 3-order random tensors \mathcal{L} with size $100 \times 100 \times 30$
777 and all entries $\mathcal{L}_{ijk} \in [0, 1]$. The tensor average ranks are 2, 5 and 8, respectively. The sample
778 ratio SR increases from 0.3 to 0.8 with increment 0.1 and the noise level α increases from
779 0.1 to 0.6 with increment 0.1. For each pair (SR, α) , we simulate 100 test instances. We
780 consider two kinds of success ratios. One is defined by the percentage of successful entries
781 ($|\mathcal{L}_{ijk} - \mathcal{L}_{ijk}^*| < 10^{-2}$) from total entries. The another is defined by the relative error. If the
782 relative error is smaller than 10^{-2} , then the tensor recovery is regarded as successful and the
783 success ratio is denoted by 1(= 100%). Figure 1 reports the fraction of successful recovery
784 for each pair. The first row reports the success ratio defined by the percentage of successful
785 entries from total entries, and the second row reports the success ratio defined by relative
786 error. The success ratio in the second row is defined by 1 if the recovered tensor \mathcal{L} satisfies
787 $\|\mathcal{L} - \mathcal{L}^*\|_F / \|\mathcal{L}^*\|_F < 10^{-2}$, and defined by 0 for others. Figure 1 shows: (1) the recovery
788 success ratio is higher when the average rank is smaller; (2) the tensor data is more difficult to
789 recover when the sample rate is lower and the noise level is higher; (3) in some cases, the entire
790 tensor is judged to be failed to recover, but there are still some entries that can be successfully
791 recovered. Numerical results in Figure 1 also show that the rank and noise level of tensors
792 greatly affect the recovery of tensors. For example, under the setting that the average rank is
793 8 and the noise level is 0.6, it's hard to recover the data with sample rates from 0.3 to 0.7.

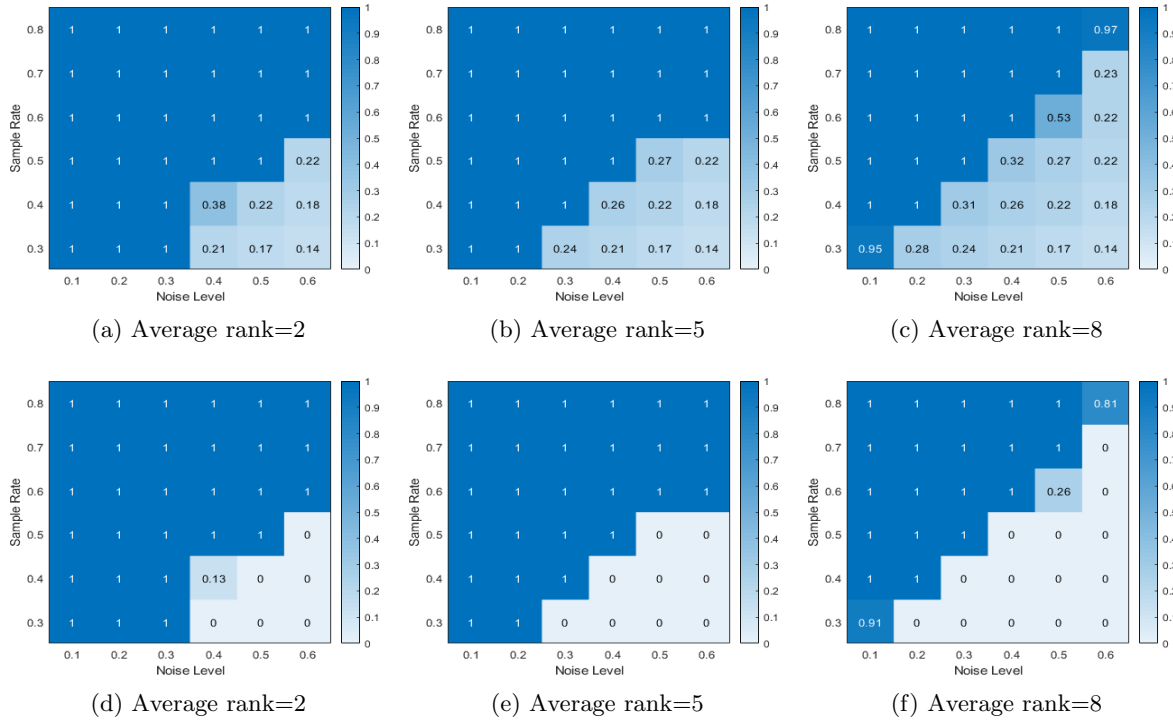


Figure 1. The success ratio for varying sample ratio and noise level under different average ranks, where the success ratio in the first row is defined by the percentage of successful entries from total entries, and the success ratio in the second row is defined by relative error.

794 **6.5. Experiments on Color Images.** In this subsection, we test color images including
 795 Pepper ($512 \times 512 \times 3$), Lena ($512 \times 512 \times 3$)¹ and Flower ($321 \times 481 \times 3$)². Although the
 796 color images are not low-rank exactly, most information on each frontal slice of the color
 797 images is dominated by a few top singular values. In our experiments, these testing images
 798 are normalized on $[0, 1]$ and are all corrupted by removing arbitrary voxels and adding salt-
 799 and-pepper noise.

800 **Figure 2** and **Figure 3** show the recovered results and corresponding zoomed regions of
 801 RTRC, $RTCl_1$, NCRTC and BCNRTC. It can be observed that the BCNRTC performs better
 802 than others in terms of PSNR values and visual quality, where the BCNRTC preserves more
 803 details for Pepper image and many more sharp edges for Flower image than others.

804 In **Table 2**, we report the PSNR values of RTRC, $RTCl_1$, NCRTC and BCNRTC for
 805 three color images. We set $SR = 0.6, 0.7$ and 0.8 to illustrate the performance of methods
 806 and noise levels are considered as $\alpha \in \{0.2, 0.3, 0.4, 0.5\}$ simultaneously. It can be observed
 807 that the PSNR values obtained by our proposed BCNRTC model are much higher than those
 808 obtained by RTRC, $RTCl_1$ and NCRTC, especially for low noise levels. The PSNR values of
 809 the restored image by the BCNRTC increase at least 3dB relative to those of the $RTCl_1$ model.

¹<http://sipi.usc.edu/database/>

²<https://www2.eecs.berkeley.edu/Research/Projects/CS/vision/bsds/>

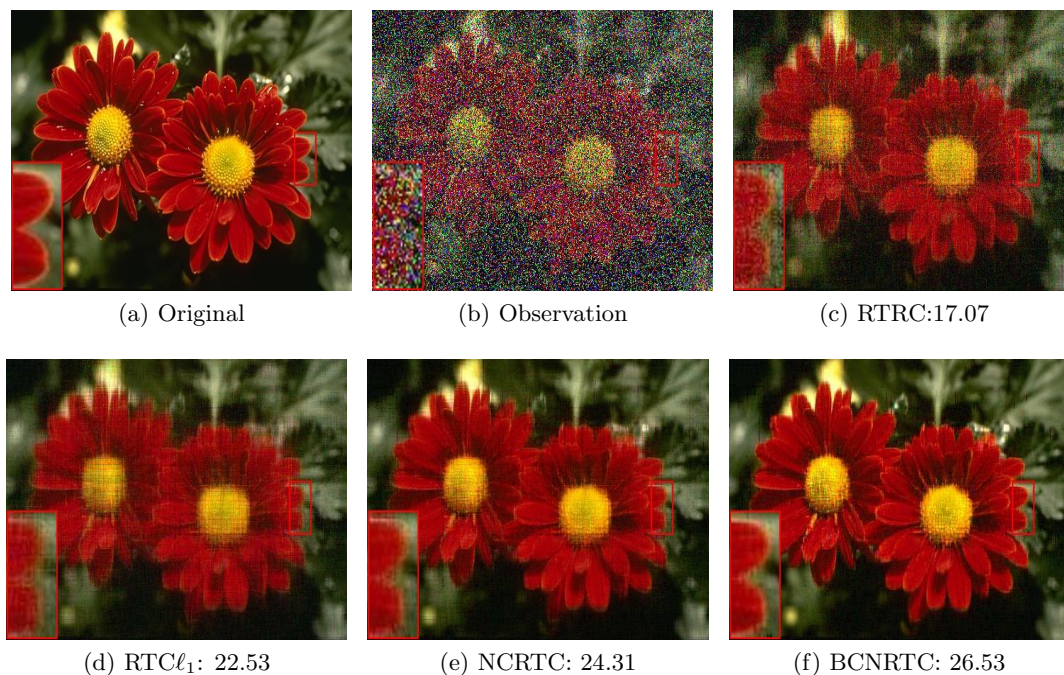


Figure 2. Recovered images (with PSNR(dB)) and zoomed regions of four different methods for the Flower image, where $SR=0.8$ and $\alpha=0.4$.

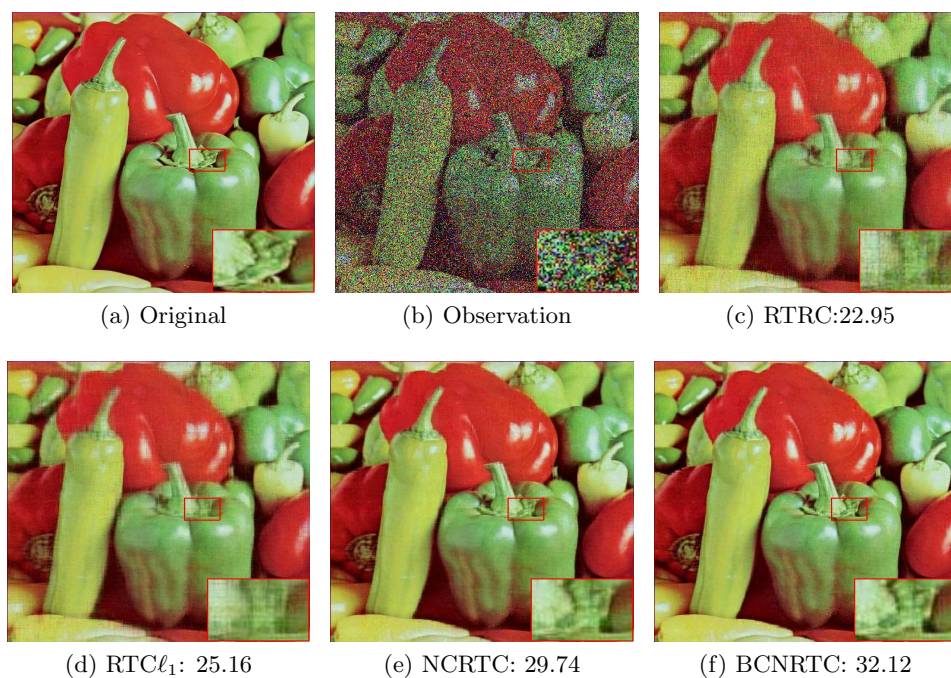


Figure 3. Recovered images (with PSNR(dB)) and zoomed regions of four different methods for the Pepper image, where $SR=0.7$ and $\alpha=0.3$.

Table 2

PSNR(dB) values for restoring results of different methods for color images corrupted by sample losing and salt-and-pepper noise. The boldface numbers are the best performance.

sample ratios	noise level	Pepper				Lena				Flower			
		RTRC	RTCl ₁	NCRTC	BCNRTC	RTRC	RTCl ₁	NCRTC	BCNRTC	RTRC	RTCl ₁	NCRTC	BCNRTC
0.8	0.2	27.98	29.08	34.99	37.72	28.12	29.5	34.36	36.31	25.92	26.97	29.85	32.54
	0.3	24.15	26.09	31.24	34.12	24.78	26.98	31.48	33.84	23.68	24.64	26.85	29.48
	0.4	17.07	23.56	27.39	30.21	17.41	24.96	28.44	30.6	19.62	22.5	24.25	26.37
	0.5	11.66	21.25	23.87	26.86	11.79	23.07	25.26	27.33	14.9	20.36	21.72	23.31
0.7	0.2	27.01	27.85	32.82	35.46	27.25	28.43	32.58	35.02	25.17	26.02	28.55	30.77
	0.3	22.95	25.12	29.74	32.11	23.73	26.17	30.16	31.98	22.84	23.84	25.84	28.03
	0.4	16.11	22.71	25.98	28.7	16.44	24.3	27.29	29.29	18.88	21.75	23.37	25.33
	0.5	11.48	20.51	22.94	25.1	11.67	22.51	24.62	26.48	14.55	19.61	20.76	22.11
0.6	0.2	25.86	26.56	30.69	33.31	26.3	27.34	30.98	32.92	24.3	25.01	27.15	29.07
	0.3	21.6	24.09	27.98	30.27	22.52	25.32	28.72	30.31	21.86	22.94	24.8	26.67
	0.4	15.17	21.82	24.77	27.05	15.52	23.57	26.18	27.96	18.1	20.9	22.43	24.17
	0.5	11.32	19.75	21.94	23.57	11.54	21.81	23.86	25.38	14.19	18.82	19.69	21.06

810 The performance of the nonconvex BCNRTC model can be improved greatly compared with
811 that of the convex RTCl₁ model. The PSNR values of the restored image by the BCNRTC
812 is at least 2dB higher than that of the nonconvex NCRTC model, which shows that both
813 low-rank and sparse terms are nonconvex better than only sparse term is nonconvex.

814 **6.6. Experiments on Multispectral Images.** In this subsection, we test the multispectral
815 images datasets including Cloth ($521 \times 521 \times 31$)³ and the Indian Pines dataset ($145 \times 145 \times$
816 224)⁴, which is a synthetic data. Since the Cloth dataset is too large, we resize the Cloth
817 dataset to 128×128 in each image, and the size of the resulting tensor is $128 \times 128 \times 31$.
818 This testing image is normalized on $[0, 1]$. For Multispectral Images, we compute the PSNR
819 values between each ground-truth band and the recovered band, and then averaged them.
820 This metric is denoted as mean PSNR (MPSNR).

821 In Figure 4, we show the 20-th band of the recovered images and corresponding zoomed
822 regions of different methods for the Indian dataset, where SR= 0.5 and $\alpha = 0.2$. It is obvious
823 that the details of the zoomed region obtained by BCNRTC are more clear than those obtained
824 by RTRC and RTCl₁. The performance of NCRTC and BCNRTC is almost the same for the
825 testing images in terms of visual quality. But PSNR values also show the BCNRTC is quite
826 effective than NCRTC.

827 Table 3 presents detailed comparison results of four different methods for the two multi-
828 spectral images with different sample ratios and noise levels, where the MPSNR values, the
829 relative error (RE), the number of iterations (Iter) and the CPU time (in seconds) are given.
830 Note that for the columns “Iter” and “Time” in the BCNRTC, we list the total inner sGS-
831 ADMM iterations and CPU times outside brackets. Meanwhile, the values in brackets in this
832 table mean the number of iterations and CPU times of CRTTC for a warm start. In addition,
833 the outer PMM iterations in Indian are four when SR= 0.8, 0.7, and the rest of cases are
834 three. Table 3 shows the advantage of BCNRTC over other three methods no matter in terms
835 of MPSNR values (largest) or relative errors (smallest). Meanwhile, the BCNRTC takes less

³<https://www.cs.columbia.edu/CAVE/databases/multispectral/stuff/>

⁴<https://engineering.purdue.edu/biehl/MultiSpec/hyperspectral.html>

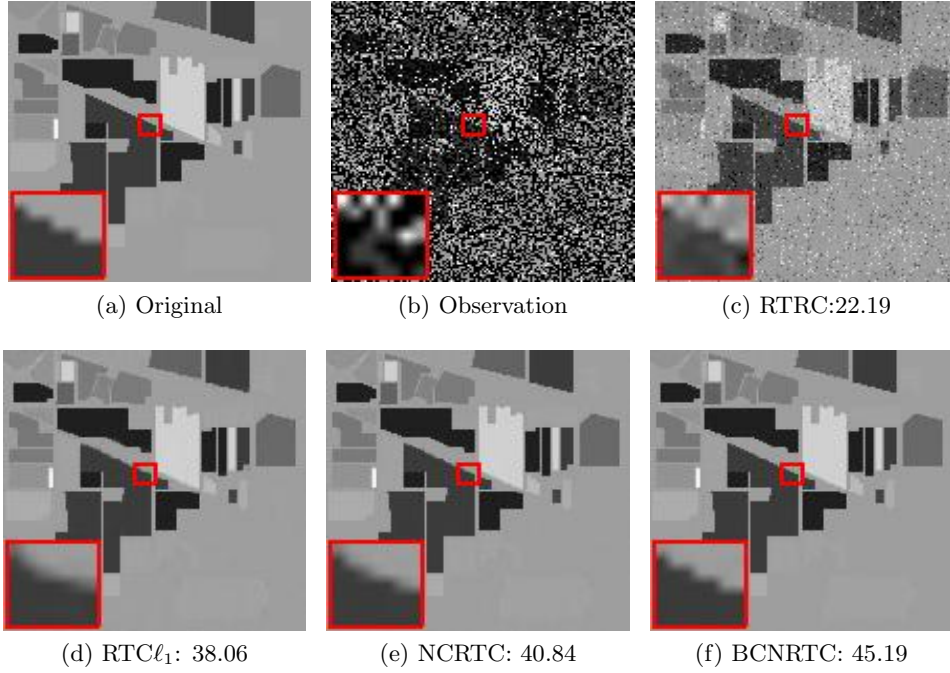


Figure 4. The 20-th band of recovered images (with PSNR(dB)) and zoomed regions of four different methods for the Indian dataset, where $SR=0.5$ and $\alpha = 0.2$.

Table 3

Numerical results of different methods for the multispectral images dataset with different SRs and α .

Images	α	SR	RTRC				RTC ℓ_1				NCRTC				BCNRTC			
			MPSNR	RE	Iter	Time	MPSNR	RE	Iter	Time	MPSNR	RE	Iter	Time	MPSNR	RE	Iter	Time
Indian	0.2	0.8	23.19	1.17e-1	100	308	38.06	3.24e-2	68	349	42.7	2.54e-2	55	211	50.47	1.3e-2	26(26)	87(78)
		0.7	22.74	1.23e-1	100	291	37.87	3.26e-2	69	345	41.11	2.72e-2	57	219	48.66	1.46e-2	27(34)	89(100)
		0.6	22.25	1.3e-1	100	292	36.33	3.67e-2	69	339	39.61	2.97e-2	59	225	45.98	1.79e-2	24(35)	78(101)
		0.5	21.67	1.39e-1	100	295	35.39	3.92e-2	69	332	37.59	3.38e-2	59	225	43.74	2.03e-2	28(42)	89(119)
Cloth	0.4	0.8	18.34	5.53e-1	100	28	32.53	1.29e-1	58	20	37.18	7.39e-2	41	17	39.68	5.81e-2	233(15)	12(8)
		0.7	17.69	5.98e-1	100	27	31.25	1.42e-1	57	19	35.84	8.51e-2	42	17	38.14	6.67e-2	236(17)	13(6)
		0.6	17.45	6.14e-1	100	27	30.24	1.64e-1	58	19	34.1	1.02e-1	45	18	36.59	7.67e-2	240(17)	15(5)
		0.5	17.24	6.28e-1	100	27	28.96	1.88e-1	58	19	31.89	1.31e-1	50	20	34.85	1.25e-1	146(17)	17(5)

836 CPU time and iteration numbers than the others when a suitable initial point is given. Specif-
 837 ically, BCNRTC is able to outperform others by a factor of about 2-4 in terms of computation
 838 times for the Indian dataset.

839 **7. Conclusions.** In this paper, we propose a BCNRTC model for the RTC problem which
 840 aims to recover a third-order low-rank tensor from partial observations corrupted by impulse
 841 noise. Then, we prove the equivalence of global solutions between RTC problems and our
 842 proposed nonconvex model, which gives the theoretical guarantee that the nonconvex penalties
 843 are superior to convex penalties. Due to the nonconvexity, the resulting model is difficult to
 844 solve. To tackle this problem, we devise the PMM algorithm to solve the nonconvex model and

845 show that the sequence generated by the PMM algorithm globally converges to a critical point
 846 of the problem. Next, we establish a recovery error bound and give the theoretical guarantee
 847 that the proposed model can get lower error bounds when the initial estimator is close to
 848 the ground truth. Extensive numerical experiments including color images and multispectral
 849 images demonstrate that the proposed BCNRTC method outperforms several state-of-the-art
 850 methods.

851 In the future, it would be of great interest to extend the BCNRTC to higher-order tensors
 852 since some real datasets are higher-order tensors, such as color videos or traffic data.

Appendix A. Partial Calmness. The partial calmness is defined in detail in [28], which is used in the proof of [Theorem 3.1](#). Let $\theta : \mathbb{R}^n \rightarrow (-\infty, +\infty]$ be a proper lsc function, $h : \mathbb{R}^n \rightarrow \mathbb{R}$ be a continuous function, and Δ be a nonempty closed set of \mathbb{R}^n . Consider the following problem:

$$(MP) \quad \min_z \{\theta(z) : h(z) = 0, z \in \Delta\}.$$

Let \mathcal{F} and \mathcal{F}^* denote the feasible set and the global optimal solution set of (MP), respectively, and $v^*(MP)$ is the optimal value of (MP). Assume that $\mathcal{F}^* \neq \emptyset$. Consider the perturbed problem of (MP):

$$(MP_\epsilon) \quad \min_z \{\theta(z) : h(z) = \epsilon, z \in \Delta\},$$

853 where $\epsilon \in \mathbb{R}$, \mathcal{F}_ϵ denotes the feasible set of (MP_ϵ) associated to ϵ .

854 **Definition A.1.** *The problem (MP) is said to be partially calm at a solution point z^* if*
 855 *there exist $\epsilon > 0$ and $\mu > 0$ such that for all $\epsilon \in [-\epsilon, \epsilon]$ and all $z \in (z^* + \epsilon\mathbb{B}) \cap \mathcal{F}_\epsilon$, one has*
 856 *$\theta(z) - \theta(z^*) + \mu|h(z)| \geq 0$.*

857 The partial calmness plays a critical role in the proof of [Theorem 3.1](#). [28, Proposition
 858 2.1] shows that under the compactness of feasible set of problem (3.5), the partial calmness
 859 of (3.4) over its global optimal solution set implies the global exact penalization of (3.5).

860 **Appendix B. The Kurdyka-Łojasiewicz property.** The Kurdyka-Łojasiewicz property is
 861 defined in detailed in [3], which is used in the proof of [Lemma 4.3](#).

862 **Definition B.1.** *Let $f : \mathbb{R}^n \rightarrow (-\infty, +\infty]$ be a proper and lower semicontinuous function.*

(i) The function f is said to have the KL property at $\mathbf{x} \in \text{dom}(\partial f)$ if there exist $\eta \in (0, +\infty]$, a neighborhood \mathfrak{U} of \mathbf{x} and a continuous concave function $\varphi : [0, \eta) \rightarrow [0, +\infty)$ such that: (a) $\varphi(0) = 0$; (b) φ is continuously differentiable on $(0, \eta)$, and continuous at 0; (c) $\varphi'(s) > 0$ for all $s \in (0, \eta)$; (d) for all $\mathbf{y} \in \mathfrak{U} \cap \{\mathbf{y} \in \mathbb{R}^n : f(\mathbf{x}) < f(\mathbf{y}) < f(\mathbf{x}) + \eta\}$, the following KL inequality holds:

$$\varphi'(f(\mathbf{y}) - f(\mathbf{x})) \text{dist}(0, \partial f(\mathbf{y})) \geq 1.$$

863 *(ii) If f satisfies the KL property at each point of $\text{dom}(\partial f)$, then f is called a KL function.*

864 **Appendix C. Proofs of the results in Section 4.** This part includes the proofs of part
 865 of results in [Section 4](#).

866 **C.1. Proof of Lemma 4.1.** From the definition of Q , we have

$$(C.1) \quad \begin{aligned} 867 \quad Q(\mathcal{W}) - F(\mathcal{W}; \mathcal{W}^k) &= H_1(\mathcal{L}^k) - H_1(\mathcal{L}) + \langle \nabla H_1(\mathcal{L}^k), \mathcal{L} - \mathcal{L}^k \rangle \\ &\quad + \lambda(H_2(\mathcal{M}^k) - H_2(\mathcal{M}) + \langle \nabla H_2(\mathcal{M}^k), \mathcal{M} - \mathcal{M}^k \rangle) - \frac{\eta}{2} \|\mathcal{W} - \mathcal{W}^k\|_F^2. \end{aligned}$$

868 On the other hand, the convexity of H_1 and H_2 implies that

$$(C.2) \quad H_1(\mathcal{L}) \geq H_1(\mathcal{L}^k) + \langle \nabla H_1(\mathcal{L}^k), \mathcal{L} - \mathcal{L}^k \rangle, \quad H_2(\mathcal{M}) \geq H_2(\mathcal{M}^k) + \langle \nabla H_2(\mathcal{M}^k), \mathcal{M} - \mathcal{M}^k \rangle.$$

870 Combining (C.1) with (C.2), we obtain that $Q(\mathcal{W}) - F(\mathcal{W}; \mathcal{W}^k) \leq -\frac{\eta}{2} \|\mathcal{W} - \mathcal{W}^k\|_F^2$. Thus, we
871 obtain

$$(C.3) \quad Q(\mathcal{W}^{k+1}) + \frac{\eta}{2} \|\mathcal{W}^{k+1} - \mathcal{W}^k\|_F^2 \leq F(\mathcal{W}^{k+1}; \mathcal{W}^k).$$

873 Since $\mathcal{C}^{k+1} \in \partial F(\mathcal{W}^{k+1}; \mathcal{W}^k)$, we have

$$(C.4) \quad \begin{aligned} Q(\mathcal{W}^k) = F(\mathcal{W}^k; \mathcal{W}^k) &\geq F(\mathcal{W}^{k+1}; \mathcal{W}^k) + \langle \mathcal{C}^{k+1}, \mathcal{W}^k - \mathcal{W}^{k+1} \rangle \\ &\geq F(\mathcal{W}^{k+1}; \mathcal{W}^k) - \|\mathcal{C}^{k+1}\|_F \|\mathcal{W}^{k+1} - \mathcal{W}^k\|_F \\ &\geq F(\mathcal{W}^{k+1}; \mathcal{W}^k) - \eta c \|\mathcal{W}^{k+1} - \mathcal{W}^k\|_F^2, \end{aligned}$$

875 where the last inequality follows from (4.4). Combining (C.3) with (C.4), we have

$$(C.5) \quad Q(\mathcal{W}^{k+1}) + \frac{\eta}{2} (1 - 2c) \|\mathcal{W}^{k+1} - \mathcal{W}^k\|_F^2 \leq Q(\mathcal{W}^k),$$

877 which completes the first part of the proof. Let N be a positive integer. Summing (C.5) from
878 $k = 0$ to $N - 1$, we get

$$879 \quad \sum_{k=0}^{N-1} (\|\mathcal{L}^{k+1} - \mathcal{L}^k\|_F^2 + \|\mathcal{M}^{k+1} - \mathcal{M}^k\|_F^2) = \sum_{k=0}^{N-1} \|\mathcal{W}^{k+1} - \mathcal{W}^k\|_F^2 \leq \frac{2}{\eta(1-2c)} (Q(\mathcal{W}^0) - Q(\mathcal{W}^N)),$$

880 where the inequality is valid since the condition $\eta(1-2c) > 0$ holds. By the inequality
881 (C.5), we can get the sequence $\{Q(\mathcal{W}^k)\}_{k \in \mathbb{N}}$ is non-increasing. Since $Q(\mathcal{W})$ is bounded be-
882 low, the sequence $\{Q(\mathcal{W}^k)\}_{k \in \mathbb{N}}$ converges. Taking the limit as $N \rightarrow \infty$, we obtain that
883 $\sum_{k=0}^{\infty} \|\mathcal{W}^{k+1} - \mathcal{W}^k\|_F^2 < \infty$ and the sequence $\{\|\mathcal{W}^{k+1} - \mathcal{W}^k\|_F\}_{k \in \mathbb{N}}$ converges to zero. There-
884 fore, the conclusion is obtained.

885 **C.2. Proof of Lemma 4.2.** By [2, Proposition 2.1], [35, Exercise 8.8(c)] and $\mathcal{C}^{k+1} \in$
886 $\partial F(\mathcal{W}^{k+1}; \mathcal{W}^k)$, we have

$$(C.6) \quad \mathcal{C}_{\mathcal{L}}^{k+1} = \tilde{Y}^{k+1} - \nabla H_1(\mathcal{L}^k) + \eta(\mathcal{L}^{k+1} - \mathcal{L}^k), \quad \mathcal{C}_{\mathcal{M}}^{k+1} = \tilde{Z}^{k+1} - \nabla H_2(\mathcal{M}^k) + \eta(\mathcal{M}^{k+1} - \mathcal{M}^k)$$

888 for some $\tilde{Y}^{k+1} \in \partial_{\mathcal{L}}[\|\mathcal{L}\|_{\text{TNN}} + \delta_{\Gamma_1}(\mathcal{L}, \mathcal{M}) + \delta_{D_2}(\mathcal{L})]_{\mathcal{W}=\mathcal{W}^{k+1}}$, $\tilde{Z}^{k+1} \in \partial_{\mathcal{M}}[\lambda\|\mathcal{M}\|_1 + \delta_{\Gamma_1}(\mathcal{L}, \mathcal{M}) +$
889 $\delta_{D_1}(\mathcal{M})]_{\mathcal{W}=\mathcal{W}^{k+1}}$. From the definition of Q , we get

$$890 \quad \partial_{\mathcal{L}} Q(\mathcal{W}) = \partial_{\mathcal{L}}[\|\mathcal{L}\|_{\text{TNN}} + \delta_{\Gamma_1}(\mathcal{L}, \mathcal{M}) + \delta_{D_2}(\mathcal{L})] - \nabla H_1(\mathcal{L}),$$

891
892

$$\partial_{\mathcal{M}}Q(\mathcal{W}) = \partial_{\mathcal{M}}[\lambda\|\mathcal{M}\|_1 + \delta_{\Gamma_1}(\mathcal{L}, \mathcal{M}) + \delta_{D_1}(\mathcal{M})] - \nabla H_2(\mathcal{M}).$$

893 By the definitions of \tilde{Y}^{k+1} and \tilde{Z}^{k+1} , we obtain that

$$894 \quad \mathcal{B}_{\mathcal{L}}^{k+1} := \tilde{Y}^{k+1} - \nabla H_1(\mathcal{L}^{k+1}) \in \partial_{\mathcal{L}}Q(\mathcal{W}^{k+1}), \quad \mathcal{B}_{\mathcal{M}}^{k+1} := \tilde{Z}^{k+1} - \nabla H_2(\mathcal{M}^{k+1}) \in \partial_{\mathcal{M}}Q(\mathcal{W}^{k+1}).$$

895 Then, we have $\mathcal{B}^{k+1} \in \partial Q(\mathcal{W}^{k+1})$. Define

$$896 \quad (\text{C.7}) \quad \mathcal{H}_{\mathcal{L}}^{k+1} := \tilde{Y}^{k+1} - \nabla H_1(\mathcal{L}^k), \quad \mathcal{H}_{\mathcal{M}}^{k+1} := \tilde{Z}^{k+1} - \lambda \nabla H_2(\mathcal{M}^k).$$

897 We now have to estimate the norm of \mathcal{B}^{k+1} . By the definitions of \mathcal{B}^{k+1} and \mathcal{H}^{k+1} , we have

$$898 \quad (\text{C.8}) \quad \|\mathcal{B}^{k+1} - \mathcal{H}^{k+1}\|_F = \|(\nabla H_1(\mathcal{L}^k) - \nabla H_1(\mathcal{L}^{k+1}), \lambda(\nabla H_2(\mathcal{M}^k) - \nabla H_2(\mathcal{M}^{k+1}))\|_F.$$

899 Since \mathcal{W}^k is an approximate solution of $F(\mathcal{W}; \mathcal{W}^{k-1})$, by the definition of the indicator func-
900 tion, we get that \mathcal{W}^k belongs to Γ_1 , D_1 and D_2 . Thus, $\{\mathcal{W}^k\}_{k \in \mathbb{N}}$ is bounded and \mathcal{W}^* is a
901 cluster point. Then, it follows from [11, Theorem 3.10] that there exist constants $\delta_0 > 0$ and
902 $\tilde{m} > 0$ such that for any $\mathcal{W}^k, \mathcal{W}^{k+1} \in B(\mathcal{W}^*, \delta_0)$,

$$903 \quad (\text{C.9}) \quad \|\nabla H_1(\mathcal{L}^k) - \nabla H_1(\mathcal{L}^{k+1})\|_F \leq \tilde{m} \|\mathcal{L}^{k+1} - \mathcal{L}^k\|_F.$$

904 It follows from ∇H_2 is Lipschitz continuous with constant $\frac{1}{\gamma}$ that

$$905 \quad (\text{C.10}) \quad \lambda \|\nabla H_2(\mathcal{M}^k) - \nabla H_2(\mathcal{M}^{k+1})\|_F \leq \frac{\lambda}{\gamma} \|\mathcal{M}^{k+1} - \mathcal{M}^k\|_F.$$

906 By combining (C.6) with (C.7), we have that $\mathcal{H}^{k+1} = \mathcal{C}^{k+1} - \eta(\mathcal{W}^{k+1} - \mathcal{W}^k)$. Moreover, by
907 $\|\mathcal{B}^{k+1} - \mathcal{H}^{k+1}\|_F \geq \|\mathcal{B}^{k+1}\|_F - \|\mathcal{H}^{k+1}\|_F$, we obtain that

$$\begin{aligned} & \|\mathcal{B}^{k+1}\|_F \leq \|\mathcal{B}^{k+1} - \mathcal{H}^{k+1}\|_F + \|\mathcal{H}^{k+1}\|_F \\ 908 \quad & \leq \tilde{m} \|\mathcal{L}^{k+1} - \mathcal{L}^k\|_F + \frac{\lambda}{\gamma} \|\mathcal{M}^{k+1} - \mathcal{M}^k\|_F + \|\mathcal{C}^{k+1}\|_F + \eta \|\mathcal{W}^{k+1} - \mathcal{W}^k\|_F \\ & \leq (\tilde{m} + \lambda/\gamma + \eta + \eta c) \|\mathcal{W}^{k+1} - \mathcal{W}^k\|_F, \end{aligned}$$

909 where the second inequality holds by (C.8) and the last inequality holds by (4.4), (C.9) and
910 (C.10). The desired result is proven.

911 **C.3. Proof of Lemma 4.3.** It is easy to see that δ_{Γ_1} , δ_{D_1} and δ_{D_2} are semialgebraic [6].
912 On the other hand, the MCP function and the SCAD function are shown to be semialgebraic
913 in [50], and $\|\mathcal{L}\|_{\text{TNN}}$ is also shown to be semi-algebraic in [58]. Hence, the function $Q(\mathcal{W})$ is
914 semi-algebraic since it is the finite sum of semialgebraic functions. Since $Q(\mathcal{W})$ is also proper
915 lower semicontinuous, and it follows from [6, Theorem 3] that the function Q is a KL function,
916 which completes the proof.

917 **Appendix D. Proofs of the results in Section 5.** This part includes the proofs of part of
918 results in Section 5.

919 **D.1. Proof of Proposition 5.1.** Recall that

$$920 \quad S(\mathcal{L}^*) := \left\{ \mathcal{U}_1 * \mathcal{V}_1^H + \mathcal{U}_2 * \mathcal{W} * \mathcal{V}_2^H \mid \mathcal{W} \in \mathbb{C}^{(n_1-r_{\min}) \times (n_2-r_{\min}) \times n_3}, \|\mathcal{W}\| \leq 1 \right\}.$$

921 First we are going to show that $S(\mathcal{L}^*) \subseteq \partial\|\mathcal{L}^*\|_{\text{TNN}}$. For any $\mathcal{Z} \in S(\mathcal{L}^*)$, we have

$$\begin{aligned} 922 \quad \langle \mathcal{Z}, \mathcal{L}^* \rangle &= \langle \mathcal{U}_1 * \mathcal{V}_1^H + \mathcal{U}_2 * \mathcal{W} * \mathcal{V}_2^H, \mathcal{U} * \mathcal{S} * \mathcal{V}^H \rangle \\ 923 \quad &= \frac{1}{n_3} \sum_{i=1}^{n_3} \left\langle \widehat{\mathbf{U}}_1^{(i)} (\widehat{\mathbf{V}}_1^{(i)})^H + \widehat{\mathbf{U}}_2^{(i)} \widehat{\mathbf{W}}^{(i)} (\widehat{\mathbf{V}}_2^{(i)})^H, \widehat{\mathbf{U}}^{(i)} \widehat{\mathbf{S}}^{(i)} (\widehat{\mathbf{V}}^{(i)})^H \right\rangle \\ 924 \quad &= \frac{1}{n_3} \sum_{i=1}^{n_3} \left\langle \mathbf{U}_1^{(i)} (\mathbf{V}_1^{(i)})^H + \mathbf{U}_2^{(i)} \mathbf{W}^{(i)} (\mathbf{V}_2^{(i)})^H, \mathbf{U}^{(i)} \mathbf{S}^{(i)} (\mathbf{V}^{(i)})^H \right\rangle \\ 925 \quad &= \frac{1}{n_3} \sum_{i=1}^{n_3} \left\langle \mathbf{U}^{(i)} \begin{pmatrix} \mathbf{I}_{r_i} & 0 \\ 0 & \mathbf{W}^{(i)} \end{pmatrix} (\mathbf{V}^{(i)})^H, \mathbf{U}^{(i)} \begin{pmatrix} \text{Diag}(\sigma(\widehat{\mathbf{L}}^{*(i)})) & 0 \\ 0 & 0 \end{pmatrix} (\mathbf{V}^{(i)})^H \right\rangle \\ 926 \quad &= \frac{1}{n_3} \sum_{i=1}^{n_3} \|\widehat{\mathbf{L}}^{*(i)}\|_* \\ 927 \quad &= \|\mathcal{L}^*\|_{\text{TNN}}. \end{aligned}$$

929 It is easy to verify that $\|\mathcal{Z}\| \leq 1$. Then, by [47], we have $\mathcal{Z} \in \partial\|\mathcal{L}^*\|_{\text{TNN}}$. So we have
930 $S(\mathcal{L}^*) \subseteq \partial\|\mathcal{L}^*\|_{\text{TNN}}$.

931 Next, we are going to prove that $\partial\|\mathcal{L}^*\|_{\text{TNN}} \subseteq S(\mathcal{L}^*)$. We argue it by contradiction.
932 Assume that exist $\mathcal{G}' \in \partial\|\mathcal{L}^*\|_{\text{TNN}}$ but $\mathcal{G}' \notin S(\mathcal{L}^*)$. It can be verified that $S(\mathcal{L}^*)$ is convex
933 and closed. Then, by Strict Separation Theorem [5], there exists $\mathcal{R} \in \mathbb{R}^{n_1 \times n_2 \times n_3}$ satisfying
934 $\langle \mathcal{G}', \mathcal{R} \rangle > \langle \mathcal{H}, \mathcal{R} \rangle$ for any $\mathcal{H} \in S(\mathcal{L}^*)$. So that

$$935 \quad \max_{\mathcal{G} \in \partial\|\mathcal{L}^*\|_{\text{TNN}}} \langle \mathcal{G}, \mathcal{R} \rangle > \max_{\mathcal{H} \in S(\mathcal{L}^*)} \langle \mathcal{H}, \mathcal{R} \rangle.$$

936 Let $f(\mathcal{L}^*) := \|\mathcal{L}^*\|_{\text{TNN}}$. We use $f'(\mathcal{L}^*; \mathcal{R})$ to denote the directional derivative of f at \mathcal{L}^* with
937 the direction \mathcal{R} . It follows from [34, Theorem 23.4] that $f'(\mathcal{L}^*; \mathcal{R}) = \max_{\mathcal{G} \in \partial\|\mathcal{L}^*\|_{\text{TNN}}} \langle \mathcal{G}, \mathcal{R} \rangle$.

938 Moreover,

$$\begin{aligned}
939 \quad f'(\mathcal{L}^*; \mathcal{R}) &= \lim_{\gamma \rightarrow 0^+} \frac{\|\mathcal{L}^* + \gamma \mathcal{R}\|_{\text{TNN}} - \|\mathcal{L}^*\|_{\text{TNN}}}{\gamma} \\
940 \quad &= \lim_{\gamma \rightarrow 0^+} \frac{1}{n_3} \sum_{i=1}^{n_3} \frac{\|\widehat{\mathbf{L}^*} + \gamma \widehat{\mathbf{R}}^{(i)}\|_* - \|\widehat{\mathbf{L}^*}\|_*}{\gamma} \\
941 \quad &= \frac{1}{n_3} \sum_{i=1}^{n_3} \lim_{\gamma \rightarrow 0^+} \frac{\|\widehat{\mathbf{L}^*} + \gamma \widehat{\mathbf{R}}^{(i)}\|_* - \|\widehat{\mathbf{L}^*}\|_*}{\gamma} \\
942 \quad &= \frac{1}{n_3} \sum_{i=1}^{n_3} \max_{\mathbf{d}^{(i)} \in \partial \|\boldsymbol{\sigma}^{(i)}\|_1} \sum_{j=1}^{n_1} \mathbf{d}_j^{(i)} (\mathbf{u}_j^{(i)})^H \widehat{\mathbf{R}}^{(i)} \mathbf{v}_j^{(i)} \\
943 \quad &= \frac{1}{n_3} \sum_{i=1}^{n_3} \max_{\mathbf{d}^{(i)} \in \partial \|\boldsymbol{\sigma}^{(i)}\|_1} \left\langle \sum_{j=1}^{n_1} \mathbf{d}_j^{(i)} \mathbf{u}_j^{(i)} (\mathbf{v}_j^{(i)})^H, \widehat{\mathbf{R}}^{(i)} \right\rangle \\
944 \quad &= \frac{1}{n_3} \sum_{i=1}^{n_3} \max_{\mathbf{d}^{(i)} \in \partial \|\boldsymbol{\sigma}^{(i)}\|_1} \langle \mathbf{U}^{(i)} \text{Diag}(\mathbf{d}^{(i)}) \mathbf{V}^{(i)H}, \widehat{\mathbf{R}}^{(i)} \rangle \\
945 \quad &= \frac{1}{n_3} \sum_{i=1}^{n_3} \max_{\mathbf{d}^{(i)} \in \partial \|\boldsymbol{\sigma}^{(i)}\|_1} \left\langle \begin{bmatrix} \mathbf{U}_1^{(i)} & \mathbf{U}_2^{(i)} \\ 0 & 0 \end{bmatrix} \begin{bmatrix} \text{Diag}(\mathbf{d}_{\leq r_i}^{(i)}) & 0 \\ 0 & \text{Diag}(\mathbf{d}_{> r_i}^{(i)}) \end{bmatrix} \begin{bmatrix} (\mathbf{V}_1^{(i)})^H \\ (\mathbf{V}_2^{(i)})^H \end{bmatrix}, \widehat{\mathbf{R}}^{(i)} \right\rangle \\
946 \quad &= \frac{1}{n_3} \sum_{i=1}^{n_3} \max_{\mathbf{d}^{(i)} \in \partial \|\boldsymbol{\sigma}^{(i)}\|_1} \left\langle \mathbf{U}_1^{(i)} (\mathbf{V}_1^{(i)})^H + \mathbf{U}_2^{(i)} \text{Diag}(\mathbf{d}_{> r_i}^{(i)}) (\mathbf{V}_2^{(i)})^H, \widehat{\mathbf{R}}^{(i)} \right\rangle \\
947 \quad &= \frac{1}{n_3} \sum_{i=1}^{n_3} \max_{\mathbf{d}^{(i)} \in \partial \|\boldsymbol{\sigma}^{(i)}\|_1} \left\langle \widehat{\mathbf{U}}_1^{(i)} (\widehat{\mathbf{V}}_1^{(i)})^H + \widehat{\mathbf{U}}_2^{(i)} \begin{bmatrix} 0 & 0 \\ 0 & \text{Diag}(\mathbf{d}_{> r_i}^{(i)}) \end{bmatrix} (\widehat{\mathbf{V}}_2^{(i)})^H, \widehat{\mathbf{R}}^{(i)} \right\rangle, \\
948 \quad &
\end{aligned}$$

949 where $\mathbf{u}_j^{(i)}$ is the j -th column of the $\mathbf{U}^{(i)}$ (also the j -th column of $\widehat{\mathbf{U}}^{(i)}$ when $j \leq r_i$) and the
950 fourth equality is due to [47, Theorem 1]. Notice that $|\mathbf{d}_j^{(i)}| \leq 1$ when $j > r_i$. Denote

$$\begin{aligned}
951 \quad \widehat{\mathbf{D}}^{(i)} &:= \begin{bmatrix} 0 & 0 \\ 0 & \text{Diag}(\mathbf{d}_{> r_i}^{(i)}) \end{bmatrix} \in \mathbb{C}^{(n_1 - r_{\min}) \times (n_2 - r_{\min})}. \\
952 \quad &
\end{aligned}$$

953 Then we have $\widehat{\mathbf{D}}^{(i)} \in \{\widehat{\mathbf{W}}^{(i)} \|\widehat{\mathbf{W}}^{(i)}\| \leq 1\}$, which means that

$$\begin{aligned}
954 \quad \{\widehat{\mathbf{D}}^{(i)} \mid \text{diag}(\widehat{\mathbf{D}}^{(i)}) = (0, \mathbf{d}_{> r_i}^{(i)})^H, \mathbf{d}^{(i)} \in \partial \|\boldsymbol{\sigma}^{(i)}\|_1\} &\subseteq \{\widehat{\mathbf{W}}^{(i)} \|\widehat{\mathbf{W}}^{(i)}\| \leq 1\}.
\end{aligned}$$

955 Let $\Lambda^{(i)} := \{\widehat{\mathbf{D}}^{(i)} \mid \text{diag}(\widehat{\mathbf{D}}^{(i)}) = (0, \mathbf{d}_{>r_i}^{(i)})^H, \mathbf{d}^{(i)} \in \partial \|\boldsymbol{\sigma}^{(i)}\|_1\}$. Then we have

$$\begin{aligned}
956 & \max_{\mathcal{H} \in S(\mathcal{L}^*)} \langle \mathcal{H}, \mathcal{R} \rangle \\
957 & = \max_{\|\mathcal{W}\| \leq 1} \langle \mathcal{U}_1 * \mathcal{V}_1^H + \mathcal{U}_2 * \mathcal{W} * \mathcal{V}_2^H, \mathcal{R} \rangle \\
958 & = \frac{1}{n_3} \sum_{i=1}^{n_3} \max_{\|\widehat{\mathbf{W}}^{(i)}\| \leq 1} \left\langle \widehat{\mathbf{U}}_1^{(i)} \widehat{\mathbf{V}}_1^{(i)H} + \widehat{\mathbf{U}}_2^{(i)} \widehat{\mathbf{W}}^{(i)} (\widehat{\mathbf{V}}_2^{(i)})^H, \widehat{\mathbf{R}}^{(i)} \right\rangle \\
959 & \geq \frac{1}{n_3} \sum_{i=1}^{n_3} \max_{\widehat{\mathbf{W}}^{(i)} \in \Lambda^{(i)}} \left\langle \widehat{\mathbf{U}}_1^{(i)} \widehat{\mathbf{V}}_1^{(i)H} + \widehat{\mathbf{U}}_2^{(i)} \widehat{\mathbf{W}}^{(i)} (\widehat{\mathbf{V}}_2^{(i)})^H, \widehat{\mathbf{R}}^{(i)} \right\rangle \\
960 & = f'(\mathcal{L}^*; \mathcal{R}),
\end{aligned}$$

962 which implies $\max_{\mathcal{H} \in S(\mathcal{L}^*)} \langle \mathcal{H}, \mathcal{R} \rangle \geq \max_{\mathcal{G} \in \partial \|\mathcal{L}^*\|_{\text{TNN}}} \langle \mathcal{G}, \mathcal{R} \rangle$. This contradicts the assumption.
963 Therefore, we have $\partial \|\mathcal{L}^*\|_{\text{TNN}} \subseteq S(\mathcal{L}^*)$. This completes the proof.

964 **D.2. Proof of Proposition 5.3.** Considering $\overline{\mathbf{X}} = \text{Diag}(\widehat{\mathbf{X}}^{(1)}, \widehat{\mathbf{X}}^{(2)}, \dots, \widehat{\mathbf{X}}^{(n_3)})$, $\forall i =$
965 $1, 2, \dots, n_3$, we have

$$\begin{aligned}
966 & \widehat{\mathbf{X}}^{(i)} = [\mathbf{U}_1^{(i)}, \mathbf{U}_2^{(i)}][\mathbf{U}_1^{(i)}, \mathbf{U}_2^{(i)}]^H \widehat{\mathbf{X}}^{(i)} [\mathbf{V}_1^{(i)}, \mathbf{V}_2^{(i)}][\mathbf{V}_1^{(i)}, \mathbf{V}_2^{(i)}]^H \\
967 & = [\mathbf{U}_1^{(i)}, \mathbf{U}_2^{(i)}] \begin{bmatrix} (\mathbf{U}_1^{(i)})^H \widehat{\mathbf{X}}^{(i)} \mathbf{V}_1^{(i)} & (\mathbf{U}_1^{(i)})^H \widehat{\mathbf{X}}^{(i)} \mathbf{V}_2^{(i)} \\ (\mathbf{U}_2^{(i)})^H \widehat{\mathbf{X}}^{(i)} \mathbf{V}_1^{(i)} & 0 \end{bmatrix} [\mathbf{V}_1^{(i)}, \mathbf{V}_2^{(i)}]^H + \\
968 & \quad [\mathbf{U}_1^{(i)}, \mathbf{U}_2^{(i)}] \begin{bmatrix} 0 & 0 \\ 0 & (\mathbf{U}_2^{(i)})^H \widehat{\mathbf{X}}^{(i)} \mathbf{V}_2^{(i)} \end{bmatrix} [\mathbf{V}_1^{(i)}, \mathbf{V}_2^{(i)}]^H \\
969 & = \mathbf{U}_1^{(i)} (\mathbf{U}_1^{(i)})^H \widehat{\mathbf{X}}^{(i)} + \widehat{\mathbf{X}}^{(i)} \mathbf{V}_1^{(i)} (\mathbf{V}_1^{(i)})^H - \mathbf{U}_1^{(i)} (\mathbf{U}_1^{(i)})^H \widehat{\mathbf{X}}^{(i)} \mathbf{V}_1^{(i)} (\mathbf{V}_1^{(i)})^H \\
970 & \quad + \mathbf{U}_2^{(i)} (\mathbf{U}_2^{(i)})^H \widehat{\mathbf{X}}^{(i)} \mathbf{V}_2^{(i)} (\mathbf{V}_2^{(i)})^H \\
971 & = \widehat{\mathbf{U}}_1^{(i)} (\widehat{\mathbf{U}}_1^{(i)})^H \widehat{\mathbf{X}}^{(i)} + \widehat{\mathbf{X}}^{(i)} \widehat{\mathbf{V}}_1^{(i)} (\widehat{\mathbf{V}}_1^{(i)})^H - \widehat{\mathbf{U}}_1^{(i)} (\widehat{\mathbf{U}}_1^{(i)})^H \widehat{\mathbf{X}}^{(i)} \widehat{\mathbf{V}}_1^{(i)} (\widehat{\mathbf{V}}_1^{(i)})^H \\
972 & \quad + \widehat{\mathbf{U}}_2^{(i)} (\widehat{\mathbf{U}}_2^{(i)})^H \widehat{\mathbf{X}}^{(i)} \widehat{\mathbf{V}}_2^{(i)} (\widehat{\mathbf{V}}_2^{(i)})^H,
\end{aligned}$$

974 which means that

$$975 \quad \overline{\mathbf{X}} = \overline{\mathbf{U}}_1 \overline{\mathbf{U}}_1^H \overline{\mathbf{X}} + \overline{\mathbf{X}} \overline{\mathbf{V}}_1 \overline{\mathbf{V}}_1^H - \overline{\mathbf{U}}_1 \overline{\mathbf{U}}_1^H \overline{\mathbf{X}} \overline{\mathbf{V}}_1 \overline{\mathbf{V}}_1^H + \overline{\mathbf{U}}_2 \overline{\mathbf{U}}_2^H \overline{\mathbf{X}} \overline{\mathbf{V}}_2 \overline{\mathbf{V}}_2^H.$$

976 So we have

$$977 \quad \mathcal{X} = \mathcal{U}_1 * \mathcal{U}_1^H * \mathcal{X} + \mathcal{X} * \mathcal{V}_1 * \mathcal{V}_1^H - \mathcal{U}_1 * \mathcal{U}_1^H * \mathcal{X} * \mathcal{V}_1 * \mathcal{V}_1^H + \mathcal{U}_2 * \mathcal{U}_2^H * \mathcal{X} * \mathcal{V}_2 * \mathcal{V}_2^H.$$

978 By the definition of \mathcal{T} , we can see that

$$979 \quad \mathcal{P}_{\mathcal{T}}(\mathcal{X}) = \mathcal{U}_1 * \mathcal{U}_1^H * \mathcal{X} + \mathcal{X} * \mathcal{V}_1 * \mathcal{V}_1^H - \mathcal{U}_1 * \mathcal{U}_1^H * \mathcal{X} * \mathcal{V}_1 * \mathcal{V}_1^H.$$

980 Therefore, it follows from $\mathcal{X} = \mathcal{P}_{\mathcal{T}}(\mathcal{X}) + \mathcal{P}_{\mathcal{T}^\perp}(\mathcal{X})$ that

$$981 \quad \mathcal{P}_{\mathcal{T}^\perp}(\mathcal{X}) = \mathcal{U}_2 * \mathcal{U}_2^H * \mathcal{X} * \mathcal{V}_2 * \mathcal{V}_2^H.$$

982 This completes the proof.

983 **D.3. Proof of Lemma 5.4.** Since $(\mathcal{L}^c, \mathcal{M}^c)$ is optimal and $(\mathcal{L}^*, \mathcal{M}^*)$ is feasible to the
984 problem (4.3), we have

(D.1)

$$985 \quad 0 \geq (\|\mathcal{L}^c\|_{\text{TNN}} - \|\mathcal{L}^*\|_{\text{TNN}} - \langle \nabla H_1(\mathcal{L}^k), \tilde{\Delta}_{\mathcal{L}} \rangle) + \lambda(\|\mathcal{M}^c\|_1 - \langle \nabla H_2(\mathcal{M}^k), \tilde{\Delta}_{\mathcal{M}} \rangle - \|\mathcal{M}^*\|_1) \\ + \frac{\eta}{2}(\|\mathcal{L}^c - \mathcal{L}^k\|_F^2 - \|\mathcal{L}^* - \mathcal{L}^k\|_F^2) + \frac{\eta}{2}(\|\mathcal{M}^c - \mathcal{M}^k\|_F^2 - \|\mathcal{M}^* - \mathcal{M}^k\|_F^2).$$

986 By (5.1), we know that $\{\mathcal{U}_1 * \mathcal{V}_1^H + \mathcal{U}_2 * \mathcal{W} * \mathcal{V}_2^H \mid \|\mathcal{W}\| \leq 1\} = \partial\|\mathcal{L}^*\|_{\text{TNN}}$. Thus, by the
987 convexity of $\|\cdot\|_{\text{TNN}}$, we have

$$988 \quad \begin{aligned} & \|\mathcal{L}^c\|_{\text{TNN}} - \|\mathcal{L}^*\|_{\text{TNN}} - \langle \nabla H_1(\mathcal{L}^k), \tilde{\Delta}_{\mathcal{L}} \rangle \\ & \geq \langle \mathcal{U}_1 * \mathcal{V}_1^H + \mathcal{U}_2 * \mathcal{W} * \mathcal{V}_2^H, \tilde{\Delta}_{\mathcal{L}} \rangle - \langle \nabla H_1(\mathcal{L}^k), \tilde{\Delta}_{\mathcal{L}} \rangle \\ & = \frac{1}{n_3} \langle \overline{\mathcal{U}_1} \overline{\mathcal{V}_1}^H - \overline{\nabla H_1(\mathcal{L}^k)}, \tilde{\Delta}_{\mathcal{L}} \rangle + \frac{1}{n_3} \langle \overline{\mathcal{U}_2} \overline{\mathcal{W}} \overline{\mathcal{V}_2}^H, \tilde{\Delta}_{\mathcal{L}} \rangle \\ & \geq \frac{1}{n_3} \sup_{\|\overline{\mathcal{W}}\| \leq 1} \langle \overline{\mathcal{W}}, \overline{\mathcal{U}_2}^H \tilde{\Delta}_{\mathcal{L}} \overline{\mathcal{V}_2} \rangle - \frac{1}{n_3} \|\overline{\mathcal{U}_1} \overline{\mathcal{V}_1}^H - \overline{\nabla H_1(\mathcal{L}^k)}\|_F \|\tilde{\Delta}_{\mathcal{L}}\|_F \\ & = \frac{1}{n_3} \|\overline{\mathcal{U}_2}^H \tilde{\Delta}_{\mathcal{L}} \overline{\mathcal{V}_2}\|_* - \frac{1}{n_3} \|\overline{\mathcal{U}_1} \overline{\mathcal{V}_1}^H - \overline{\nabla H_1(\mathcal{L}^k)}\|_F \|\tilde{\Delta}_{\mathcal{L}}\|_F \\ & = \|\mathcal{U}_2 * \tilde{\Delta}_{\mathcal{L}} * \mathcal{V}_2^H\|_{\text{TNN}} - \|\mathcal{U}_1 * \mathcal{V}_1^H - \nabla H_1(\mathcal{L}^k)\|_F \|\tilde{\Delta}_{\mathcal{L}}\|_F \\ & = \|\mathcal{P}_{\mathcal{T}^\perp}(\tilde{\Delta}_{\mathcal{L}})\|_{\text{TNN}} - d_{\mathcal{L}} \sqrt{r} \|\tilde{\Delta}_{\mathcal{L}}\|_F, \end{aligned}$$

989 where the second equality directly from the definition of dual norm.

990 Similarly, we know that $\{\text{sign}(\mathcal{M}^*) + \mathcal{F} | \mathcal{P}_{\text{supp}_{\mathcal{M}^*}}(\mathcal{F}) = 0, \|\mathcal{F}\|_\infty \leq 1\} \subseteq \partial\|\mathcal{M}^*\|_1$, where
991 $\text{supp}_{\mathcal{X}} := \{(i, j, k) \mid \langle \Theta_{ijk}, \mathcal{X} \rangle \neq 0\}$. Thus, by the convexity of $\|\cdot\|_1$, we have

$$992 \quad \begin{aligned} & \|\mathcal{M}^c\|_1 - \|\mathcal{M}^*\|_1 - \langle \nabla H_2(\mathcal{M}^k), \tilde{\Delta}_{\mathcal{M}} \rangle \\ & \geq \langle \text{sign}(\mathcal{M}^*) + \mathcal{P}_{\text{supp}_{\mathcal{M}^*}}^c(\mathcal{F}), \tilde{\Delta}_{\mathcal{M}} \rangle - \langle \nabla H_2(\mathcal{M}^k), \tilde{\Delta}_{\mathcal{M}} \rangle \\ & \geq \sup_{\|\mathcal{F}\|_\infty \leq 1} \langle \mathcal{F}, \mathcal{P}_{\text{supp}_{\mathcal{M}^*}}^c(\tilde{\Delta}_{\mathcal{M}}) \rangle - \|\text{sign}(\mathcal{M}^*) - \nabla H_2(\mathcal{M}^k)\|_F \|\tilde{\Delta}_{\mathcal{M}}\|_F \\ & = \|\mathcal{P}_{\text{supp}_{\mathcal{M}^*}}^c(\tilde{\Delta}_{\mathcal{M}})\|_1 - d_{\mathcal{M}} \sqrt{s} \|\tilde{\Delta}_{\mathcal{M}}\|_F. \end{aligned}$$

993 By the convexity of $\|\cdot\|_F^2$, we also have

$$994 \quad \begin{aligned} & \frac{\eta}{2}(\|\mathcal{L}^c - \mathcal{L}^k\|_F^2 - \|\mathcal{L}^* - \mathcal{L}^k\|_F^2) + \frac{\eta}{2}(\|\mathcal{M}^c - \mathcal{M}^k\|_F^2 - \|\mathcal{M}^* - \mathcal{M}^k\|_F^2) \\ & \geq \eta(\langle \mathcal{L}^* - \mathcal{L}^k, \mathcal{L}^c - \mathcal{L}^* \rangle + \langle \mathcal{M}^* - \mathcal{M}^k, \mathcal{M}^c - \mathcal{M}^* \rangle) \\ & \geq -\eta \|\mathcal{L}^* - \mathcal{L}^k\|_F \|\tilde{\Delta}_{\mathcal{L}}\|_F - \eta \|\mathcal{M}^* - \mathcal{M}^k\|_F \|\tilde{\Delta}_{\mathcal{M}}\|_F. \end{aligned}$$

995 By substituting (D.2), (D.3) and (D.4) into (D.1), we get that

$$996 \quad \begin{aligned} & \|\mathcal{P}_{\mathcal{T}^\perp}(\tilde{\Delta}_{\mathcal{L}})\|_{\text{TNN}} + \lambda \|\mathcal{P}_{\text{supp}_{\mathcal{M}^*}}^c(\tilde{\Delta}_{\mathcal{M}})\|_1 \\ & \leq (d_{\mathcal{L}} \sqrt{r} + \eta \|\mathcal{L}^* - \mathcal{L}^k\|_F) \|\tilde{\Delta}_{\mathcal{L}}\|_F + (\lambda d_{\mathcal{M}} \sqrt{s} + \eta \|\mathcal{M}^* - \mathcal{M}^k\|_F) \|\tilde{\Delta}_{\mathcal{M}}\|_F. \end{aligned}$$

997 Thus,

$$998 \quad (D.5) \quad \begin{aligned} & \max\{\|\mathcal{P}_{\mathcal{T}^\perp}(\tilde{\Delta}_{\mathcal{L}})\|_{\text{TNN}}, \lambda\|\mathcal{P}_{\text{supp}_{\mathcal{M}^*}^c}(\tilde{\Delta}_{\mathcal{M}})\|_1\} \\ & \leq (d_{\mathcal{L}}\sqrt{r} + \eta\|\mathcal{L}^* - \mathcal{L}^k\|_F)\|\tilde{\Delta}_{\mathcal{L}}\|_F + (\lambda d_{\mathcal{M}}\sqrt{\tilde{s}} + \eta\|\mathcal{M}^* - \mathcal{M}^k\|_F)\|\tilde{\Delta}_{\mathcal{M}}\|_F. \end{aligned}$$

999 It follows from [Proposition 5.3](#) that $\text{rank}_a(\mathcal{P}_{\mathcal{T}}(\tilde{\Delta}_{\mathcal{L}})) \leq 2r$, which together with $\|\mathcal{P}_{\text{supp}_{\mathcal{M}^*}}(\tilde{\Delta}_{\mathcal{M}})\|_0 \leq \tilde{s}$, we have

$$1001 \quad (D.6) \quad \begin{aligned} \|\mathcal{P}_{\mathcal{T}}(\tilde{\Delta}_{\mathcal{L}})\|_{\text{TNN}} &= \frac{1}{n_3} \|\overline{\mathcal{P}_{\mathcal{T}}(\tilde{\Delta}_{\mathcal{L}})}\|_* \leq \frac{\sqrt{2rn_3}}{n_3} \|\overline{\mathcal{P}_{\mathcal{T}}(\tilde{\Delta}_{\mathcal{L}})}\|_F = \sqrt{2r}\|\mathcal{P}_{\mathcal{T}}(\tilde{\Delta}_{\mathcal{L}})\|_F \leq \sqrt{2r}\|\tilde{\Delta}_{\mathcal{L}}\|_F, \\ \|\mathcal{P}_{\text{supp}_{\mathcal{M}^*}}(\tilde{\Delta}_{\mathcal{M}})\|_1 &\leq \sqrt{\tilde{s}}\|\mathcal{P}_{\text{supp}_{\mathcal{M}^*}}(\tilde{\Delta}_{\mathcal{M}})\|_F \leq \sqrt{\tilde{s}}\|\tilde{\Delta}_{\mathcal{M}}\|_F. \end{aligned}$$

1002 Note that $\|\tilde{\Delta}_{\mathcal{L}}\|_{\text{TNN}} \leq \|\mathcal{P}_{\mathcal{T}}(\tilde{\Delta}_{\mathcal{L}})\|_{\text{TNN}} + \|\mathcal{P}_{\mathcal{T}^\perp}(\tilde{\Delta}_{\mathcal{L}})\|_{\text{TNN}}$ and $\|\tilde{\Delta}_{\mathcal{M}}\|_1 \leq \|\mathcal{P}_{\text{supp}_{\mathcal{M}^*}}(\tilde{\Delta}_{\mathcal{M}})\|_1 +$
1003 $\|\mathcal{P}_{\text{supp}_{\mathcal{M}^*}^c}(\tilde{\Delta}_{\mathcal{M}})\|_1$. By combining [\(D.5\)](#) and [\(D.6\)](#) together with the above inequalities, we
1004 complete the proof.

1005 **D.4. Proof of Lemma 5.5.** First, we will show that the following event holds with small
1006 probability:

$$1007 \quad E := \left\{ \exists \Delta \in K(p, q, t) \text{ such that } \left| \frac{1}{m} \|\mathcal{P}_{\Omega}(\Delta)\|_F^2 - \mathbb{E}[\langle \Theta, \Delta \rangle^2] \right| \geq \frac{\|\Delta_{\mathcal{L}}\|_F^2 + \|\Delta_{\mathcal{M}}\|_F^2}{2\mu_1 n_1 n_2 n_3} + 256\mu_1 n_1 n_2 n_3 \beta_S^2 \right\}.$$

1008 It is clear that the complement of the interested event is included in E . Now we estimate the
1009 probability of the event E . We decompose the set $K(p, q, t)$ into

$$1010 \quad K(p, q, t) = \bigcup_{j=1}^{\infty} \left\{ \Delta \in K(p, q, t) \mid 2^{j-1}t \leq \frac{\|\Delta_{\mathcal{L}}\|_F^2 + \|\Delta_{\mathcal{M}}\|_F^2}{\mu_1 n_1 n_2 n_3} \leq 2^j t \right\}.$$

1011 For any $s \geq t$, we define the set

$$1012 \quad K(p, q, t, s) := \left\{ \Delta \in K(p, q, t) \mid \frac{\|\Delta_{\mathcal{L}}\|_F^2 + \|\Delta_{\mathcal{M}}\|_F^2}{\mu_1 n_1 n_2 n_3} \leq s \right\}.$$

1013 Let

$$1014 \quad E_j := \left\{ \exists \Delta \in K(p, q, t, 2^j t) \text{ s.t. } \left| \frac{1}{m} \|\mathcal{P}_{\Omega}(\Delta)\|_F^2 - \mathbb{E}[\langle \Theta, \Delta \rangle^2] \right| \geq 2^{j-2}t + 256\mu_1 n_1 n_2 n_3 \beta_S^2 \right\}.$$

1015 Note that $E \subseteq \bigcup_{j=1}^{\infty} E_j$. In the following, we estimate the probability of the event E_j . Let

$$1016 \quad Z_s := \sup_{\Delta \in K(p, q, t, s)} \left| \frac{1}{m} \|\mathcal{P}_{\Omega}(\Delta)\|_F^2 - \mathbb{E}[\langle \Theta, \Delta \rangle^2] \right|,$$

1017 we have

$$1018 \quad (\text{D.7}) \quad \frac{1}{m} \|\mathcal{P}_\Omega(\Delta)\|_F^2 - \mathbb{E}[\langle \Theta, \Delta \rangle^2] = \frac{1}{m} \sum_{l=1}^m (\langle \Theta_{\omega_l}, \Delta \rangle^2 - \mathbb{E}[\langle \Theta, \Delta \rangle^2]).$$

1019 Since $\|\Delta\|_\infty = 1$ for all $\Delta \in K(p, q, t)$, it follows that

$$1020 \quad |\langle \Theta_{\omega_l}, \Delta \rangle^2 - \mathbb{E}[\langle \Theta, \Delta \rangle^2]| \leq \max\{\langle \Theta_{\omega_l}, \Delta \rangle^2, \mathbb{E}[\langle \Theta, \Delta \rangle^2]\} \leq 1.$$

1021 Thus, it follows from Massart's Hoeffding type concentration inequality [30, Theorem 1.4] that

$$1022 \quad (\text{D.8}) \quad \mathbb{P}(Z_s \geq \mathbb{E}[Z_s] + \varepsilon) \leq \exp\left(-\frac{m\varepsilon^2}{2}\right), \quad \forall \varepsilon > 0.$$

1023 In order to be able to apply the inequality (D.8), we need to estimate an upper bound of
1024 $\mathbb{E}[Z_s]$. By (D.7), we have

$$\begin{aligned} \mathbb{E}[Z_s] &= \mathbb{E} \left[\sup_{\Delta \in K(p, q, t, s)} \left| \frac{1}{m} \|\mathcal{P}_\Omega(\Delta)\|_F^2 - \mathbb{E}[\langle \Theta, \Delta \rangle^2] \right| \right] \leq 2\mathbb{E} \left[\sup_{\Delta \in K(p, q, t, s)} \left| \frac{1}{m} \sum_{l=1}^m \epsilon_l \langle \Theta_{\omega_l}, \Delta \rangle^2 \right| \right] \\ &\leq 8\mathbb{E} \left[\sup_{\Delta \in K(p, q, t, s)} \left| \frac{1}{m} \sum_{l=1}^m \langle \epsilon_l \Theta_{\omega_l}, \Delta \rangle \right| \right] = 8\mathbb{E} \left[\sup_{\Delta \in K(p, q, t, s)} \left| \frac{1}{m} \langle \mathfrak{D}_\Omega^*(\epsilon), \Delta \rangle \right| \right] \\ 1025 \quad &\leq 8\mathbb{E} \left[\sup_{\Delta \in K(p, q, t, s)} \left\| \frac{1}{m} \overline{\mathfrak{D}_\Omega^*(\epsilon)} \right\| \left\| \frac{1}{n_3} \overline{\Delta_{\mathcal{L}}} \right\|_* + \sup_{\Delta \in K(p, q, t, s)} \left\| \frac{1}{m} \mathfrak{D}_\Omega^*(\epsilon) \right\|_\infty \|\Delta_{\mathcal{M}}\|_1 \right] \\ &= 8\mathbb{E} \left[\sup_{\Delta \in K(p, q, t, s)} \left\| \frac{1}{m} \mathfrak{D}_\Omega^*(\epsilon) \right\| \|\Delta_{\mathcal{L}}\|_{\text{TNN}} + \sup_{\Delta \in K(p, q, t, s)} \left\| \frac{1}{m} \mathfrak{D}_\Omega^*(\epsilon) \right\|_\infty \|\Delta_{\mathcal{M}}\|_1 \right] \\ &\leq 8\mathbb{E} \left\| \frac{1}{m} \mathfrak{D}_\Omega^*(\epsilon) \right\| \left(\sup_{\Delta \in K(p, q, t, s)} \|\Delta_{\mathcal{L}}\|_{\text{TNN}} \right) + 8\mathbb{E} \left\| \frac{1}{m} \mathfrak{D}_\Omega^*(\epsilon) \right\|_\infty \left(\sup_{\Delta \in K(p, q, t, s)} \|\Delta_{\mathcal{M}}\|_1 \right), \end{aligned}$$

1026 where the first inequality is due to the symmetrization theorem [7, Theorem 14.3] and the
1027 second inequality follows from the contraction theorem [7, Theorem 14.4]. Notice that for any
1028 $u \geq 0, v \geq 0$ and $\Delta \in K(p, q, t, s)$,

$$1029 \quad u\|\Delta_{\mathcal{L}}\|_F + v\|\Delta_{\mathcal{M}}\|_F \leq 32\mu_1 n_1 n_2 n_3 (u^2 + v^2) + \frac{\|\Delta_{\mathcal{L}}\|_F^2 + \|\Delta_{\mathcal{M}}\|_F^2}{128\mu_1 n_1 n_2 n_3} \leq 32\mu_1 n_1 n_2 n_3 (u^2 + v^2) + \frac{s}{128},$$

1030 where the first inequality follows from the fact $2ab \leq a^2 + b^2$. Then, follows from (5.5), (5.6),
1031 the definition of $K(p, q, t)$ and the above inequality, we derive that

$$1032 \quad (\text{D.9}) \quad \mathbb{E}[Z_s] \leq 8 \left[\sup_{\Delta \in K(p, q, t, s)} \beta_{\mathcal{L}}(p_1 \|\Delta_{\mathcal{L}}\|_F + p_2 \|\Delta_{\mathcal{M}}\|_F) + \sup_{\Delta \in K(p, q, t, s)} \beta_{\mathcal{M}}(q_1 \|\Delta_{\mathcal{L}}\|_F + q_2 \|\Delta_{\mathcal{M}}\|_F) \right] \\ \leq 256\mu_1 n_1 n_2 n_3 \beta_S^2 + \frac{s}{8}.$$

1033 Then it follows from (D.8) and (D.9) that

$$1034 \quad \mathbb{P} \left(Z_s \geq 256\mu_1 n_1 n_2 n_3 \beta_S^2 + \frac{s}{4} \right) \leq \mathbb{P} \left(Z_s \geq \mathbb{E}[Z_s] + \frac{s}{8} \right) \leq \exp \left(-\frac{ms^2}{128} \right).$$

1035 This, together with the choice of $s = 2^j t$, implies that $\mathbb{P}(E_j) \leq \exp\left(-\frac{4^j m t^2}{128}\right)$. Therefore, it
 1036 follows from the simple fact $4^j > \log(4^j) = 2j \log(2)$ that

$$1037 \quad \mathbb{P}(E) \leq \sum_{j=1}^{\infty} \mathbb{P}(E_j) \leq \sum_{j=1}^{\infty} \exp\left(-\frac{4^j m t^2}{128}\right) \leq \sum_{j=1}^{\infty} \exp\left(-\frac{j m t^2 \log(2)}{64}\right) \leq \frac{\exp[-m t^2 \log(2)/64]}{1 - \exp[-m t^2 \log(2)/64]}.$$

1038 Then, taking $t = 8\sqrt{\frac{\log(n_1+n_2+n_3+1)}{m \log(2)}}$, we obtain that $\mathbb{P}(E) \leq \frac{1}{n_1+n_2+n_3}$. The proof is completed.

1039 **D.5. Proof of Lemma 5.7.** For $l = 1, \dots, m$, define the random tensor $\mathcal{Z}_{\omega_l} := \epsilon_l \Theta_{\omega_l}$.
 1040 Then $\frac{1}{m} \mathfrak{D}_{\Omega}^*(\epsilon) = \frac{1}{m} \sum_{l=1}^m \mathcal{Z}_{\omega_l}$. Since ϵ_l is an i.i.d. Rademacher sequence, we have that $|\epsilon_l| \leq 1$,
 1041 $\mathbb{E}[\epsilon_l] = 0$ and $\mathbb{E}[\epsilon_l^2] = 1$. Notice that ϵ_l and Θ_{ω_l} are independent, we get $\mathbb{E}[\mathcal{Z}_{\omega_l}] = \mathbb{E}[\epsilon_l] \mathbb{E}[\Theta_{\omega_l}] = 0$.
 1042 Since $\|\Theta_{\omega_l}\|_F = 1$, we have

$$1043 \quad \|\mathcal{Z}_{\omega_l}\| \leq \|\mathcal{Z}_{\omega_l}\|_F = |\epsilon_l| \|\Theta_{\omega_l}\|_F = |\epsilon_l|.$$

1044 It is easy to obtain that there exists a constant $M > 0$ such that $\|\|\mathcal{Z}_{\omega_l}\|\|_{\psi_1} \leq \|\epsilon_l\|_{\psi_1} \leq M$
 1045 and $\mathbb{E}^{\frac{1}{2}}[\|\mathcal{Z}_{\omega_l}\|^2] \leq \mathbb{E}^{\frac{1}{2}}[\epsilon_l^2] = 1$. Define

$$1046 \quad \sigma_{\mathcal{Z}} := \max \left\{ \left\| \frac{1}{m} \sum_{l=1}^m \mathbb{E}[\mathcal{Z}_{\omega_l} * \mathcal{Z}_{\omega_l}^H] \right\|^{\frac{1}{2}}, \left\| \frac{1}{m} \sum_{l=1}^m \mathbb{E}[\mathcal{Z}_{\omega_l}^H * \mathcal{Z}_{\omega_l}] \right\|^{\frac{1}{2}} \right\}.$$

1047 By direct calculations we can see that $\mathbb{E}[\mathcal{Z}_{\omega_l} * \mathcal{Z}_{\omega_l}^H] = \mathbb{E}[\epsilon_l^2 \Theta_{\omega_l} * \Theta_{\omega_l}^H] = \mathbb{E}[\Theta_{\omega_l} * \Theta_{\omega_l}^H]$. The
 1048 calculation for $\mathbb{E}[\mathcal{Z}_{\omega_l}^H * \mathcal{Z}_{\omega_l}]$ is similar. We obtain from [Assumption 5.2](#) that $\sigma_{\mathcal{Z}}^2 \leq \frac{\mu_2}{\tilde{n}}$. By
 1049 applying [[48](#), Lemma 2.6], we obtain

$$1050 \quad \left\| \frac{1}{m} \mathfrak{D}_{\Omega}^*(\epsilon) \right\| \leq C_1 \left\{ \sqrt{\frac{\mu_2(t + \log((n_1 + n_2)n_3))}{\tilde{n}m}}, \frac{(t + \log((n_1 + n_2)n_3)) \log(\tilde{n})}{m} \right\}$$

1051 with probability at least $1 - \exp(-t)$. Set $\tau^* = \frac{\mu_2 C_1}{\tilde{n} \log(\tilde{n})}$. Then we can derive

$$1052 \quad (\text{D.10}) \quad \mathbb{P} \left[\left\| \frac{1}{m} \mathfrak{D}_{\Omega}^*(\epsilon) \right\| > \tau \right] \leq \begin{cases} ((n_1 + n_2)n_3) \exp\left(-\frac{\tau^2 \tilde{n} m}{C_1^2 \mu_2}\right), & \tau \leq \tau^*, \\ ((n_1 + n_2)n_3) \exp\left(-\frac{\tau m}{C_1 \log(\tilde{n})}\right), & \tau > \tau^*. \end{cases}$$

1053 We set $v_1 = \frac{\tilde{n}m}{C_1^2 \mu_2}$ and $v_2 = \frac{m}{C_1 \log(\tilde{n})}$. By Hölder's inequality, we get

$$1054 \quad (\text{D.11}) \quad \mathbb{E} \left\| \frac{1}{m} \mathfrak{D}_{\Omega}^*(\epsilon) \right\| \leq \left[\mathbb{E} \left\| \frac{1}{m} \mathfrak{D}_{\Omega}^*(\epsilon) \right\|^{2 \log((n_1+n_2)n_3)} \right]^{\frac{1}{2 \log((n_1+n_2)n_3)}}.$$

1055 Combining (D.10) with (D.11), we obtain that

$$1056 \quad (\text{D.12}) \quad \begin{aligned} \mathbb{E} \left\| \frac{1}{m} \mathfrak{D}_{\Omega}^*(\epsilon) \right\| &\leq \left(\int_0^{\infty} \mathbb{P} \left(\left\| \frac{1}{m} \mathfrak{D}_{\Omega}^*(\epsilon) \right\| > \tau^{\frac{1}{2 \log((n_1+n_2)n_3)}} \right) d\tau \right)^{\frac{1}{2 \log((n_1+n_2)n_3)}} \\ &= \sqrt{e} \left[\log((n_1 + n_2)n_3) v_1^{-\log((n_1+n_2)n_3)} \Gamma(\log((n_1 + n_2)n_3)) \right. \\ &\quad \left. + 2 \log((n_1 + n_2)n_3) v_2^{-2 \log((n_1+n_2)n_3)} \Gamma(2 \log((n_1 + n_2)n_3)) \right]^{\frac{1}{2 \log((n_1+n_2)n_3)}}. \end{aligned}$$

1057 Since the Gamma-function satisfies the inequality $\Gamma(x) \leq \left(\frac{x}{2}\right)^{x-1}$, $\forall x \geq 2$. Plugging this
1058 inequality into (D.12), we obtain that

$$1059 \quad \mathbb{E} \left\| \frac{1}{m} \mathfrak{D}_{\Omega}^*(\epsilon) \right\| \leq \sqrt{e} \left[(\log((n_1 + n_2)n_3))^{\log((n_1+n_2)n_3)} v_1^{-\log((n_1+n_2)n_3)} 2^{1-\log((n_1+n_2)n_3)} \right. \\ \left. + 2(\log((n_1 + n_2)n_3))^{2\log((n_1+n_2)n_3)} v_2^{-2\log((n_1+n_2)n_3)} \right]^{\frac{1}{2\log((n_1+n_2)n_3)}}.$$

1060 Observe that $m \geq \tilde{n} \log((n_1 + n_2)n_3)(\log(\tilde{n}))^2/\mu_2$ implies that $v_1 \log((n_1 + n_2)n_3) \leq v_2^2$. Thus,
1061 we have

$$1062 \quad \mathbb{E} \left\| \frac{1}{m} \mathfrak{D}_{\Omega}^*(\epsilon) \right\| \leq \sqrt{\frac{3e \log((n_1 + n_2)n_3)}{v_1}} = C_1 \sqrt{\frac{3e\mu_2 \log((n_1 + n_2)n_3)}{\tilde{n}m}}.$$

1063 This completes the proof.

1064 **D.6. Proof of Lemma 5.8.** For any index (i, j, k) such that $1 \leq i \leq n_1$, $1 \leq j \leq n_2$,
1065 $1 \leq k \leq n_3$ and $(\Theta_{\omega_l})_{ijk} \neq 0$ for some $\omega_l \in \Omega$, let $\omega^{ijk} := ((\Theta_{\omega_l})_{ijk}, \dots, (\Theta_{\omega_l})_{ijk})^T$. Form [48,
1066 Lemma 2.4], we know that there exists a constant $C > 0$ such that for any $\tau > 0$,

$$1067 \quad \mathbb{P} \left[\left| \frac{1}{m} \sum_{l=1}^m \omega_l^{ijk} \epsilon_l \right| > \tau \right] \leq 2 \exp \left[-C \min \left(\frac{m^2 \tau^2}{M^2 \|\omega^{ijk}\|_2^2}, \frac{m\tau}{M \|\omega^{ijk}\|_{\infty}} \right) \right].$$

1068 By taking a union bound, we get that

$$1069 \quad \mathbb{P} \left[\left\| \frac{1}{m} \mathfrak{D}_{\Omega}^*(\epsilon) \right\|_{\infty} > \tau \right] \leq 2m \exp \left[-C \min \left(\frac{m^2 \tau^2}{M^2 \max \|\omega^{ijk}\|_2^2}, \frac{m\tau}{M \max \|\omega^{ijk}\|_{\infty}} \right) \right],$$

1070 where both of the maximums are taken over all such indices (i, j, k) . Evidently, $\|\omega^{ijk}\|_2^2 \leq 1$
1071 and $\|\omega^{ijk}\|_{\infty} \leq 1$. By letting

$$1072 \quad -t := -C \min \left(\frac{m^2 \tau^2}{M^2}, \frac{m\tau}{M} \right) + \log(m) \\ \geq -C \min \left(\frac{m^2 \tau^2}{M^2 \max \|\omega^{ijk}\|_2^2}, \frac{m\tau}{M \max \|\omega^{ijk}\|_{\infty}} \right) + \log(m),$$

1073 we obtain that with probability no greater than $2 \exp(-t)$,

$$1074 \quad \left\| \frac{1}{m} \mathfrak{D}_{\Omega}^*(\epsilon) \right\|_{\infty} > M \max \left\{ \sqrt{\frac{\log(m) + t}{Cm^2}}, \frac{\log(m) + t}{Cm} \right\}.$$

1075 Set $\tau^* = \max \left\{ \frac{M}{m}, \frac{M(\log(2m))}{mC} \right\}$. Then we can derive that

$$1076 \quad \mathbb{P} \left[\left\| \frac{1}{m} \mathfrak{D}_{\Omega}^*(\epsilon) \right\|_{\infty} > \tau \right] \leq \begin{cases} 1, & \tau \leq \tau^*, \\ 2m \exp \left(-\frac{Cm}{M} \tau \right), & \tau > \tau^*. \end{cases}$$

1077 Then it follows that

$$1078 \quad \mathbb{E} \left\| \frac{1}{m} \mathfrak{D}_{\Omega}^*(\epsilon) \right\|_{\infty} \leq \int_0^{\tau^*} 1 d\tau + \int_{\tau^*}^{+\infty} 2m \exp\left(-\frac{Cm}{M}\tau\right) d\tau = \frac{M(\log(2m) + 1)}{Cm},$$

1079 which completes the proof.

1080

REFERENCES

- 1081 [1] M. AHN, J.-S. PANG, AND J. XIN, *Difference-of-convex learning: directional stationarity, optimality, and*
 1082 *sparsity*, SIAM J. Optim., 27 (2017), pp. 1637–1665.
- 1083 [2] H. ATTOUCH, J. BOLTE, P. REDONT, AND A. SOUBEYRAN, *Proximal alternating minimization and*
 1084 *projection methods for nonconvex problems: An approach based on the kurdyka-tojasiewicz inequality*,
 1085 Math. Oper. Res., 35 (2010), pp. 438–457.
- 1086 [3] H. ATTOUCH, J. BOLTE, AND B. F. SVAITER, *Convergence of descent methods for semi-algebraic and*
 1087 *tame problems: proximal algorithms, forward-backward splitting, and regularized gauss-seidel meth-*
 1088 *ods*, Math. Program., 137 (2013), pp. 91–129.
- 1089 [4] M. BAI, X. ZHANG, G. NI, AND C. CUI, *An adaptive correction approach for tensor completion*, SIAM
 1090 J. Imaging Sci., 9 (2016), pp. 1298–1323.
- 1091 [5] D. BERTSEKAS, *Convex optimization theory*, Athena Sci., 2009.
- 1092 [6] J. BOLTE, S. SABACH, AND M. TEBoulLE, *Proximal alternating linearized minimization for nonconvex*
 1093 *and nonsmooth problems*, Math. Program., 146 (2014), pp. 459–494.
- 1094 [7] P. BÜHLMANN AND S. VAN DE GEER, *Statistics for high-dimensional data: methods, theory and appli-*
 1095 *cations*, Springer Science & Business Media, 2011.
- 1096 [8] E. J. CANDÈS, X. LI, Y. MA, AND J. WRIGHT, *Robust principal component analysis?*, J. ACM, 58 (2011),
 1097 pp. 1–37.
- 1098 [9] J. D. CARROLL AND J.-J. CHANG, *Analysis of individual differences in multidimensional scaling via an*
 1099 *n-way generalization of eckart-young decomposition*, Psychometrika, 35 (1970), pp. 283–319.
- 1100 [10] A. CICHOCKI, D. MANDIC, L. DE LATHAUWER, G. ZHOU, Q. ZHAO, C. CAIAFA, AND H. A. PHAN, *Ten-*
 1101 *sor decompositions for signal processing applications: From two-way to multiway component analysis*,
 1102 IEEE Signal Process. Mag., 32 (2015), pp. 145–163.
- 1103 [11] C. DING, *An introduction to a class of matrix optimization problems*, PhD thesis, Department of Mathe-
 1104 matics, National University of Singapore, 2012.
- 1105 [12] J. FAN AND R. LI, *Variable selection via nonconcave penalized likelihood and its oracle properties*, J.
 1106 Amer. Statist. Assoc., 96 (2001), pp. 1348–1360.
- 1107 [13] J. FAN, L. XUE, AND H. ZOU, *Strong oracle optimality of folded concave penalized estimation*, Ann.
 1108 Statist., 42 (2014), pp. 819–849.
- 1109 [14] G. GU, S. JIANG, AND J. YANG, *A tvscad approach for image deblurring with impulsive noise*, Inverse
 1110 Problems, 33 (2017), p. 125008.
- 1111 [15] K. GUO, D. HAN, AND T. WU, *Convergence of alternating direction method for minimizing sum of two*
 1112 *nonconvex functions with linear constraints*, Int. J. Comput. Math., 94 (2017), pp. 1653–1669.
- 1113 [16] C. J. HILLAR AND L.-H. LIM, *Most tensor problems are np-hard*, J. ACM, 60 (2013), pp. 1–39.
- 1114 [17] H. HUANG, Y. LIU, Z. LONG, AND C. ZHU, *Robust low-rank tensor ring completion*, Int. J. Comput.
 1115 Math., 6 (2020), pp. 1117–1126.
- 1116 [18] Q. JIANG AND M. K. NG, *Robust low-tubal-rank tensor completion via convex optimization.*, in Proceed-
 1117 ings of IJCAI, 2019, pp. 2649–2655.
- 1118 [19] M. E. KILMER, K. BRAMAN, N. HAO, AND R. C. HOOVER, *Third-order tensors as operators on matrices:*
 1119 *A theoretical and computational framework with applications in imaging*, SIAM J. Matrix Anal. Appl.,
 1120 34 (2013), pp. 148–172.
- 1121 [20] M. E. KILMER AND C. D. MARTIN, *Factorization strategies for third-order tensors*, Linear Algebra Appl.,
 1122 435 (2011), pp. 641–658.
- 1123 [21] O. KLOPP, *Noisy low-rank matrix completion with general sampling distribution*, Bernoulli, 20 (2014),
 1124 pp. 282–303.

- 1125 [22] O. KLOPP, K. LOUNICI, AND A. B. TSYBAKOV, *Robust matrix completion*, Probab. Theory Relat. Fields.,
1126 169 (2017), pp. 523–564.
- 1127 [23] X. Y. LAM, J. S. MARRON, D. SUN, AND K.-C. TOH, *Fast algorithms for large-scale generalized distance*
1128 *weighted discrimination*, J. Comput. Graph. Statist., 27 (2018), pp. 368–379.
- 1129 [24] K. LANGE, D. R. HUNTER, AND I. YANG, *Optimization transfer using surrogate objective functions*, J.
1130 Comput. Graph. Statist., 9 (2000), pp. 1–20.
- 1131 [25] X. LI, D. SUN, AND K.-C. TOH, *A schur complement based semi-proximal admm for convex quadratic*
1132 *conic programming and extensions*, Math. Program., 155 (2016), pp. 333–373.
- 1133 [26] Y. LI, K. SHANG, AND Z. HUANG, *Low tucker rank tensor recovery via admm based on exact and inexact*
1134 *iteratively reweighted algorithms*, J. Comput. Appl. Math., 331 (2018), pp. 64–81.
- 1135 [27] J. LIU, P. MUSIALSKI, P. WONKA, AND J. YE, *Tensor completion for estimating missing values in visual*
1136 *data*, IEEE Trans. Pattern Anal., 35 (2013), pp. 208–220.
- 1137 [28] Y. LIU, S. BI, AND S. PAN, *Equivalent lipschitz surrogates for zero-norm and rank optimization problems*,
1138 J. Global Optim., 72 (2018), pp. 679–704.
- 1139 [29] C. LU, J. FENG, Y. CHEN, W. LIU, Z. LIN, AND S. YAN, *Tensor robust principal component analysis*
1140 *with a new tensor nuclear norm*, IEEE Trans. Pattern Anal., 42 (2019), pp. 925–938.
- 1141 [30] P. MASSART, *Optimal constants for Hoeffding type inequalities*, Mathématique Université de Paris-Sud,
1142 1998.
- 1143 [31] W. MIAO, S. PAN, AND D. SUN, *A rank-corrected procedure for matrix completion with fixed basis coef-*
1144 *ficients*, Math. Program., 159 (2016), pp. 289–338.
- 1145 [32] M. MØRUP, *Applications of tensor (multiway array) factorizations and decompositions in data mining*,
1146 Data Min. Knowl. Discov., 1 (2011), pp. 24–40.
- 1147 [33] B. K. NATARAJAN, *Sparse approximate solutions to linear systems*, SIAM J. Comput., 24 (1995), pp. 227–
1148 234.
- 1149 [34] R. T. ROCKAFELLAR, *Convex analysis*, Princeton University Press, Princeton, 1970.
- 1150 [35] R. T. ROCKAFELLAR AND R. J.-B. WETS, *Variational analysis*, Springer, Berlin, 2009.
- 1151 [36] B. ROMERA-PAREDES AND M. PONTIL, *A new convex relaxation for tensor completion*, in Proceedings
1152 of NIPS, 2013, pp. 2967–2975.
- 1153 [37] O. SEMERCI, N. HAO, M. E. KILMER, AND E. L. MILLER, *Tensor-based formulation and nuclear norm*
1154 *regularization for multienergy computed tomography*, IEEE Trans. Image Process., 23 (2014), pp. 1678–
1155 1693.
- 1156 [38] F. SHANG, J. CHENG, Y. LIU, Z.-Q. LUO, AND Z. LIN, *Bilinear factor matrix norm minimization for*
1157 *robust pca: Algorithms and applications*, IEEE Trans. Pattern Anal., 40 (2017), pp. 2066–2080.
- 1158 [39] N. D. SIDIROPOULOS, L. DE LATHAUWER, X. FU, K. HUANG, E. E. PAPALEXAKIS, AND C. FALOUTSOS,
1159 *Tensor decomposition for signal processing and machine learning*, IEEE Trans. Signal Process., 65
1160 (2017), pp. 3551–3582.
- 1161 [40] T. SUN, P. YIN, L. CHENG, AND H. JIANG, *Alternating direction method of multipliers with difference*
1162 *of convex functions*, Adv. Comput. Math., 44 (2018), pp. 723–744.
- 1163 [41] P. TANG, C. WANG, D. SUN, AND K.-C. TOH, *A sparse semismooth newton based proximal majorization-*
1164 *minimization algorithm for nonconvex square-root-loss regression problems*, J. Mach. Learn. Res., 21
1165 (2020), pp. 1–38.
- 1166 [42] R. TIBSHIRANI, *Regression shrinkage and selection via the lasso*, J. R. Stat. Soc. Ser. B. Stat. Methodol.,
1167 58 (1996), pp. 267–288.
- 1168 [43] L. R. TUCKER, *Some mathematical notes on three-mode factor analysis*, Psychometrika, 31 (1966),
1169 pp. 279–311.
- 1170 [44] M. A. O. VASILESCU AND D. TERZOPOULOS, *Multilinear subspace analysis of image ensembles*, in Pro-
1171 ceedings of CVPR., 2003, pp. 93–99.
- 1172 [45] A. WANG, D. WEI, B. WANG, AND Z. JIN, *Noisy low-tubal-rank tensor completion through iterative*
1173 *singular tube thresholding*, IEEE Access, 6 (2018), pp. 35112–35128.
- 1174 [46] Y. WANG, W. YIN, AND J. ZENG, *Global convergence of admm in nonconvex nonsmooth optimization*,
1175 J. Sci. Comput., 78 (2019), pp. 29–63.
- 1176 [47] G. A. WATSON, *Characterization of the subdifferential of some matrix norms*, Linear Algebra Appl., 170
1177 (1992), pp. 33–45.
- 1178 [48] B. WU, *High-dimensional analysis on matrix decomposition with application to correlation matrix esti-*

- 1179 *mation in factor models*, PhD thesis, Department of Mathematics, National University of Singapore,
1180 2014.
- 1181 [49] W. H. XU, X. L. ZHAO, T. Y. JI, J. Q. MIAO, J. Q. MA, S. WANG, AND T. Z. HUANG, *Laplace*
1182 *function based nonconvex surrogate for low-rank tensor completion*, *Signal Process. Image*, 73 (2019),
1183 pp. 62–69.
- 1184 [50] L. YANG, T. K. PONG, AND X. CHEN, *Alternating direction method of multipliers for a class of nonconvex*
1185 *and nonsmooth problems with applications to background/foreground extraction*, *SIAM J. Imaging Sci.*,
1186 10 (2017), pp. 74–110.
- 1187 [51] Y. YANG, Y. FENG, AND J. A. SUYKENS, *Robust low-rank tensor recovery with regularized re-descending*
1188 *m-estimator*, *IEEE Trans. Neural Netw. Learn. Syst.*, 27 (2015), pp. 1933–1946.
- 1189 [52] C.-H. ZHANG, *Nearly unbiased variable selection under minimax concave penalty*, *Ann. Statist.*, 38 (2010),
1190 pp. 894–942.
- 1191 [53] H. ZHANG, P. ZHOU, Y. YANG, AND J. FENG, *Generalized majorization-minimization for non-convex*
1192 *optimization*, in *Proceedings of IJCAI*, 2019, pp. 4257–4263.
- 1193 [54] X. ZHANG, *A nonconvex relaxation approach to low-rank tensor completion*, *IEEE Trans. Neural Netw.*
1194 *Learn. Syst.*, 30 (2018), pp. 1659–1671.
- 1195 [55] X. ZHANG AND M. K. NG, *A corrected tensor nuclear norm minimization method for noisy low-rank*
1196 *tensor completion*, *SIAM J. Imaging Sci.*, 12 (2019), pp. 1231–1273.
- 1197 [56] Z. ZHANG AND S. AERON, *Exact tensor completion using t-svd*, *IEEE Trans. Signal Process.*, 65 (2016),
1198 pp. 1511–1526.
- 1199 [57] Z. ZHANG, G. ELY, S. AERON, N. HAO, AND M. KILMER, *Novel methods for multilinear data completion*
1200 *and de-noising based on tensor-svd*, in *Proceedings of CVPR*, 2014, pp. 3842–3849.
- 1201 [58] X. ZHAO, M. BAI, AND M. K. NG, *Nonconvex optimization for robust tensor completion from grossly*
1202 *sparse observations*, *J. Sci. Comput.*, 85 (2020), pp. 1–32.